

PhiBE: A PDE-based Bellman Equation for Continuous Time Policy Evaluation

Yuhua Zhu*

Abstract

In this paper, we study policy evaluation in continuous-time reinforcement learning (RL), where the state follows an unknown stochastic differential equation (SDE) but only discrete-time data are available. We first highlight that the discrete-time Bellman equation (BE) is not always a reliable approximation to the true value function because it ignores the underlying continuous-time structure. We then introduce a new bellman equation, PhiBE, which integrates the discrete-time information into a continuous-time PDE formulation. By leveraging the smooth structure of the underlying dynamics, PhiBE provides a provably more accurate approximation to the true value function, especially in scenarios where the underlying dynamics change slowly or the reward oscillates. Moreover, we extend PhiBE to higher orders, providing increasingly accurate approximations.

We further develop a model-free algorithm for PhiBE under linear function approximation and establish its convergence under model misspecification, together with finite-sample guarantees. In contrast to existing continuous-time RL analyses, where the model misspecification error diverges as the sampling interval $\Delta t \rightarrow 0$ and the sample complexity typically scales as $O(\Delta t^{-4})$, our misspecification error is independent of Δt and the resulting sample complexity improves to $O(\Delta t^{-1})$ by exploiting the smoothness of the underlying dynamics. Moreover, we identify a fundamental trade-off between discretization error and sample error that is intrinsic to continuous-time policy evaluation: finer time discretization reduces bias but amplifies variance, so excessively frequent sampling does not necessarily improve performance. This is an insight that does not arise in classical discrete-time RL analyses. Numerical experiments are provided to validate the theoretical guarantees we propose.

1 Introduction

Reinforcement learning (RL) has achieved remarkable success in *digital environments*, with applications such as AlphaGo [45], strategic gameplay [33], and fine-tuning large language models [67]. In these applications, the system state changes only after an action is taken. In contrast, many systems in the *physical world*, the state evolves continuously in time, regardless

*Department of Statistics and Data Science, University of California - Los Angeles, Los Angeles, CA 90095, USA; e-mail: yuhuaazhu@ucla.edu

of whether actions are taken in continuous or discrete time. Although these systems are fundamentally continuous in nature, the available data are typically collected at discrete time points. In addition, the time difference between data points can be irregular, sparse, and outside our control. Examples arise in the following applications:

- Health care: for instance, in diabetes treatment, a patient’s glucose level changes continuously, but measurements are recorded only when tests are performed [16, 1, 41, 14, 9, 5];
- Robotic control [26, 28, 44] and autonomous driving [43]: where the environment evolve continuously but sensor data is collected at discrete intervals;
- Financial markets [32, 34, 60, 61]: Asset prices move continuously but trades and quotes occur at discrete times;
- Plasma fusion reactors [11]: The plasma evolves in continuous time, while all experimental data are recorded as discrete-time samples via sensors.

This paper directs its focus toward addressing continuous-time RL problems [59, 13, 4, 20, 21] where the underlying dynamics follow unknown stochastic differential equations (SDEs) but only discrete-time observations are available. Since one can divide the RL problem into policy evaluation (PE) and policy update [50, 29, 53, 20], we first concentrate on the continuous-time PE problem in this paper.

Currently, there are two main approaches to addressing this challenge. One approach is to learn the continuous-time dynamics from discrete-time data and formulate the problem as an policy evaluation problem with known dynamics [23, 12, 31, 57]. The key advantage of this approach is that it preserves the continuous-time nature of the problem, enhancing the stability and interpretability of the resulting algorithms. However, identifying continuous-time dynamics from discrete-time data is often challenging, and in general, ill-posed: there are infinitely many continuous-time dynamics can yield the same discrete-time transitions. Consequently, a misspecified continuous-time model may introduce significant errors, which can propagate to the learned optimal policy and lead to suboptimal decision-making.

Another common approach to address the continuous-time PE problem involves discretizing time and treating it as a Markov reward process. This method yields an approximated value function satisfying a (discrete-time) Bellman equation (BE), thereby one can use RL algorithms such as temporal difference (TD) [48], gradient TD [40], Least square TD [7] to solve the BE. This approach is appealing for several reasons. First, it relies only on the discrete-time transition dynamics, thereby avoiding the non-identifiability issues inherent in the first approach. Second, many RL algorithms are model-free, eliminating the need to explicitly learn the transition dynamics, making these plug-and-play algorithms convenient to implement in practice. Despite these advantages, it has been observed empirically that the RL algorithms can be sensitive to time discretization [53, 35, 38, 3]. As illustrated in Figure 1, such algorithms often yield poor approximations (see Section 5.1 for the details of Figure 1). Crucially, this failure is not due to stochasticity or insufficient data; rather, it stems from a more fundamental issue: the (discrete-time) Bellman equation, is not a faithful approximation of the underlying continuous-time problem. We show in the paper that the solution to the

Bellman equation is sensitive to time discretization, the change rate of the rewards and the discount coefficient as shown in Figure 1. Fundamentally, the (discrete-time) Bellman equation is designed for discrete-time decision-making processes, where only the discrete-time transition dynamics are utilized. In contrast, the continuous-time dynamics considered in this paper are governed by a SDE, a structure that the (discrete-time) Bellman equation does not capture. To faithfully approximate the true continuous-time value function, it is therefore necessary to move beyond the standard MDP and (discrete-time) Bellman-equation frameworks.

The central question we aim to address in this paper is: if the dynamics are known to follow a standard SDE but only discrete-time data are available, can we design algorithms that exploit this structure to decisively outperform generic RL methods for policy evaluation?

First, we view the continuous-time PE problem in terms of the solution to a PDE. Then, we tackle the overall goal in two steps. The first step is to approximate the PDE operator with the discrete-time transition dynamics, and the second step is to solve the resulting equation in a model-free way. In the first step, we proposed a PDE-based Bellman equation, called PhiBE, which integrates discrete-time information into a continuous PDE. PhiBE combines the advantages of both existing frameworks while mitigating their limitations. First, PhiBE is a PDE that preserves the continuous-time differential equation structure throughout the learning process. At the same time, PhiBE relies only on discrete-time transition distributions, which is similar to the BE, making it directly compatible with discrete-time data and enabling model-free algorithm design. Moreover, our framework overcomes key drawbacks of existing methods. Unlike the continuous-time PDE approach, which requires estimating the continuous-time dynamics and may suffer from identifiability issues, PhiBE depends solely on discrete-time transitions and does not require explicit dynamic modeling. Compared with the BE, PhiBE yields a more accurate approximation of the exact solution as it utilizes the underlying differential equation structure. In addition to that, PhiBE is more robust to rapidly changing reward functions compared to BE, which allows greater flexibility in designing reward functions to effectively achieve RL objectives. Moreover, higher-order PhiBE achieves comparable error to BE with sparser data collection, enhancing the efficiency of RL algorithms. As illustrated in Figure 1, when provided with the same discrete-time information, the exact solution derived from PhiBE is closer to the true value function than BE.

In the second step, we introduce a model-free algorithm for approximating the solution to PhiBE when only discrete-time data are accessible. This algorithm can be viewed as a continuous-time counterpart to the least-squares temporal difference (LSTD) [7] by replacing the (discrete-time) Bellman equation with the PhiBE equation. Since PhiBE enjoys a smaller discretization error than the Bellman equation, the resulting algorithm achieves a significantly improved approximation accuracy for free with a slightly modification of the standard RL algorithm. As depicted in Figure 1, with exactly the same data and the same computational cost, the proposed algorithm outperforms the RL algorithms drastically.

The error analysis for continuous-time reinforcement learning differs fundamentally from that of classical discrete-time RL. For continuous-time PE under function approximation, the total error can be decomposed into three components, as illustrated in Figure 2. The first component is the discretization error, which arises from the mismatch between the underlying continuous-time dynamics and the discrete-time observations used for learning. The second

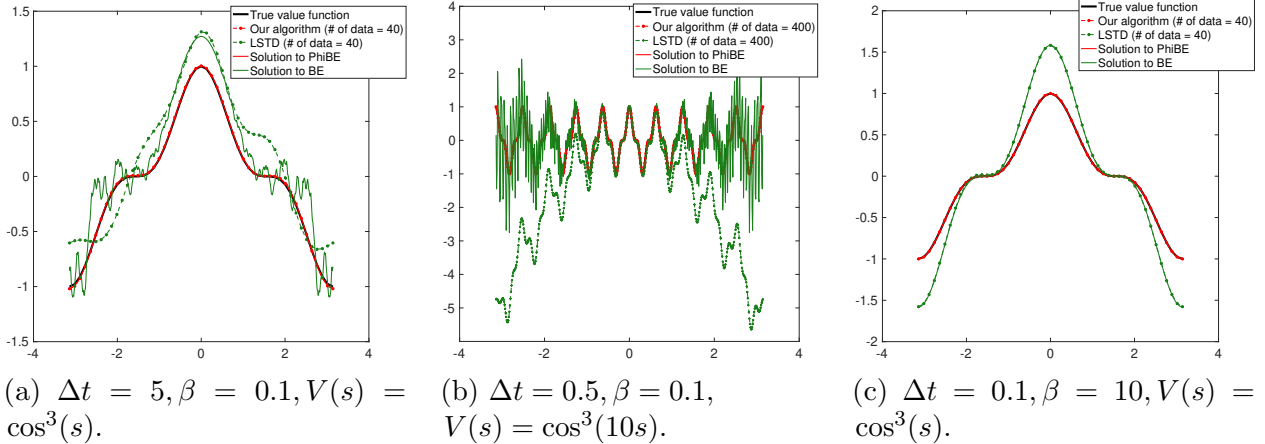


Figure 1: Here the data are collected every Δt unite of time, β is the discount coefficient, and $V(s)$ is the true value function. In our setting, a larger discount coefficient indicates that future rewards are discounted more. LSTD [7] is a popular RL algorithm for linear function approximation. The PhiBE is proposed in Section 3 and the algorithm is proposed in Section 4.

component is the algorithmic error, which may be caused by model misspecification or by finite iterations when iterative solvers are employed. In this work, we use an offline solver, and therefore the algorithmic error refers to a pure model misspecification error. The third component is the finite-sample error, which results from having only a finite number of observations. We denote by $V_{\Delta t}^{n, \Phi}$ the value function approximation obtained from n samples collected at time interval Δt using linear bases $\Phi(s)$. As $n \rightarrow \infty$, the estimator converges to $V_{\Delta t}^{\Phi}$, which still differs from the true value function V due to discretization error and the limited expressiveness of the bases. As the approximation space is enriched, i.e., the number of bases $p \rightarrow \infty$, $V_{\Delta t}^{\Phi}$ further converges to $V_{\Delta t}$, the solution of the discretized Bellman equation in the MDP framework or, the new proposed equation, PhiBE in our paper. Finally, as the data collection frequency $\Delta t \rightarrow 0$, $V_{\Delta t}$ converges to the true continuous-time value function V . Most of the existing reinforcement learning literature focuses on analyzing the finite-sample and algorithmic errors, namely the gap between $V_{\Delta t}^n$ and $V_{\Delta t}$ [36, 62, 22, 8, 63]. In contrast, comparatively little work has addressed the discretization error arising from the time discretization itself.

In this paper, we analyze all three error components within the proposed PhiBE framework and its associated algorithm. In addition, we explicitly characterize the discretization error incurred by the MDP formulation, namely the gap between the (discrete-time) Bellman equation and the true continuous-time value function. In another word, the discretization error associated with the (discrete-time) Bellman equation represents the best approximation achievable by the standard policy evaluation algorithms derived from the (discrete-time) Bellman equation, including temporal difference learning [47], least-squares temporal difference methods [7], and gradient-based temporal difference methods [49].

Our analysis leads to two notable observations. First, in terms of discretization error, PhiBE can provide a more accurate approximation than the MDP framework when the reward function exhibits high oscillation and the system dynamics evolve smoothly. This

$$V_{n,\Phi}^{\Delta t} \xrightarrow[\text{finite-sample error}]{n \rightarrow \infty} V_{\Delta t}^{\Phi} \xrightarrow[\text{algorithm error}]{p \rightarrow \infty} V_{\Delta t} \xrightarrow[\text{discretization error}]{\Delta t \rightarrow 0} V$$

Figure 2: Error decomposition for continuous-time RL

regime is common in practice because reward functions are often designed to vary sharply in order to distinguish rewards from penalties, while physical systems typically evolve smoothly over time. These properties suggest that the MDP framework may be suboptimal for certain continuous-time control problems, a limitation that has also been observed empirically [10]. Second, for continuous-time PE, we identify an inherent trade-off with respect to the time discretization Δt . More frequent data collection reduces discretization bias but increases statistical variance, requiring more samples to achieve the same accuracy. To the best of our knowledge, the only prior work reporting a similar trade-off is [64], which provides analytical results only for linear quadratic policy evaluation without function approximation. In contrast, our results apply to general controlled diffusion processes and incorporate function approximation.

Contributions

- We show that the classical Bellman equation, which does not exploit the underlying continuous-time structure, is a first-order approximation to the continuous-time PE problem, whose error deteriorates when the reward oscillates. To address this limitation, we develop the PhiBE framework that explicitly utilizes the structure of the underlying dynamics, yielding provably smaller approximation error than the Bellman equation when rewards oscillate or dynamics evolve slowly. Furthermore, we derive higher-order extensions to further enhance the approximation accuracy.
- We propose a Galerkin method to approximate the solution to the PhiBE under linear function approximation when the discrete-time transition dynamics are given. We further establish its convergence under model misspecification. In contrast to the divergent results in existing RL analyses as the data frequency $\Delta t \rightarrow 0$, we show, by exploiting the smooth structure of the underlying dynamics, that the approximation error remains well-conditioned and independent of Δt .
- We propose a model-free algorithm to approximate the Galerkin solution to the PhiBE when only data are available. We further provide a sample complexity bound guaranteeing an ϵ -accurate approximation to the Galerkin solution. In classical discrete-time RL analyses, the error scales as $O(\epsilon^{-2}\beta^{-4}\Delta t^{-4})$. By contrast, our analysis exploits the smoothness of the underlying SDE and the uniform ellipticity of the infinitesimal generator, improving the dependence on the time discretization from $O(\Delta t^{-4})$ to $O(\Delta t^{-1})$.
- Combining all the error, we identify an inherent trade-off with respect to the time discretization Δt in continuous-time PE. More frequent data collection reduces discretization bias but increases statistical variance, requiring more samples to achieve

the same accuracy. To the best of our knowledge, such an explicit trade-off, together with a nonasymptotic characterization of its dependence on $\Delta t, n$ and β , has not been systematically analyzed in prior analyses.

- The PhiBE formulation integrates discrete-time information with continuous-time PDE. By leveraging the continuous-time structure, it achieves smaller discretization error than classical RL. Moreover, due to its structural similarity to the discrete-time Bellman equation, existing RL algorithms can be seamlessly adapted to the PhiBE framework, achieving improved approximation accuracy essentially for free.

1.1 Related Work

1.1.1 Continuous-time RL

There are primarily two approaches to address continuous-time RL from the continuous-time stochastic optimal control perspective. One involves employing machine learning techniques to learn the dynamics from discrete-time data and subsequently transforming the problem into model-based continuous-time RL problem [23, 12, 31, 57]. However, the underlying continuous dynamics are often unidentifiable when only discrete-time data are available. Another approach involves developing an algorithm for the continuous-time optimal control problem and then adapts it to discrete-time data [4, 19, 20]. Typically, numerical summation in discrete time is used to approximate continuous integrals (e.g., Algorithm 2 in [4] or Equation (19) in [19]). While these methods offer valuable theoretical insights, two issues remain underexplored. First, most analyses guarantee convergence to the true value function when continuous-time data are available, but do not explicitly account for discretization error arising when only discrete samples are available. Second, although these works assume dynamics governed by a standard SDE, the resulting algorithms are not tailored to this structure and remain broadly applicable to other dynamics. By contrast, the central question of this paper is: when the dynamics follow a standard SDE but only discrete data are available, can we exploit this structure to build algorithms outperform generic RL methods? To the best of our knowledge, this is the first work to address this question systematically and establish corresponding theoretical guarantees.

The proposed method fundamentally differs from the existing literature in three key aspects. First, unlike model-based approaches, which end up solving a PDE with continuous-time information, we integrate discrete-time information into the PDE formulation. Second, unlike alternative methodologies that view it as a Markov reward process, which neglects the smoothness of the underlying dynamics, our method results in a PDE that incorporates gradients of the value function, which ensures that the solution closely approximates the true value function under smooth dynamics. Third, in contrast to most continuous-time RL algorithms that require long trajectory data, our formulation depends only on the current and next states. Consequently, algorithms derived from it require access only to transition pairs rather than full trajectories, making the approach more flexible and broadly applicable to diverse data sources.

To sum up, our work complements this line of research by bridging the gap between continuous-time algorithms and discrete-time data. We treat the discrete-time data before

the algorithm design. The PhiBE formulation offers a systematic way to approximate the continuous-time problem from discrete-time data. First, from a theoretical standpoint, because our learning algorithms retain the continuous-time PDE form, existing convergence analyses developed in the PDE [15, 27, 54, 55] can be directly applied or adapted to analyze the proposed methods. Second, from a numerical perspective, owing to the structural similarity between the PhiBE and the (discrete-time) Bellman equation, both depend only on the current and next states, most existing RL algorithms developed for solving Bellman equations can be directly applied to PhiBE.

1.1.2 Numerical schemes for HJB equation

Although the formulation of the PhiBE closely resembles the PDE associated with the continuous-time PE problem, our method is fundamentally different from traditional numerical schemes for solving PDEs in three key aspects. First, classical schemes require full knowledge of the system dynamics, whereas our model-free algorithm does not. Second, numerical schemes approximate trajectories based on known dynamics, while our approach leverages exact trajectory data to approximate the underlying dynamics. Consequently, the corresponding error analysis framework also differs. Third, the objectives of error analysis are distinct. Numerical schemes typically focus on the convergence order of the discretization, whereas one of the aims in this paper is to compare the first-order PhiBE formulation with the discrete-time MDPs formulation. Since both are first-order formulations, our analysis emphasizes the leading constant, which ultimately determines the practical performance of continuous-time PE. (See more discussion after Remark 3.)

1.1.3 Model-free algorithms for RL

Due to the structural similarity between PhiBE and (discrete-time) Bellman equation, our model-free algorithm for solving the PhiBE is closely related to model-free algorithms for the BE, particularly the LSTD method [7]. Conceptually, the proposed solver serves as the continuous-time analogue of LSTD by replacing the (discrete-time) Bellman equation with the PhiBE equation. Both approaches are model-free, employ linear function approximation, and can be derived via a Galerkin projection followed by a stochastic approximation procedure. This connection highlights an important feature of the PhiBE framework: most existing RL algorithms developed for the BE can be readily adapted to the PhiBE setting with minimal modification. Moreover, because the PhiBE formulation incurs a smaller discretization error than its BE, it achieves higher approximation accuracy given sufficient data (see Remark 8 for detailed discussion). From a theoretical perspective, our error analysis fundamentally departs from that of LSTD. The classical model-misspecification error for LSTD [30] diverges as the time discretization Δt goes to zero. In contrast, our bound remains stable by exploiting the ellipticity of the infinitesimal generator, yielding a well-conditioned characterization of model misspecification in the continuous-time limit (see more discussion after Theorem 4.1). In addition to that, we also improve the sample complexity bound from Δt^{-4} to Δt^{-1} .

Organization The setting of the problem is specified in Section 2. Section 3 introduces the PDE-based bellman equation, PhiBE, and establishes the discretization error of PhiBE and

(discrete-time) BE. In Section 4, a model-free algorithm for solving the PhiBE is proposed, algorithmic error and finite-sample error are derived. Numerical experiments are conducted in Section 5.

Notation For function $f(s) \in \mathbb{R}$, $\|f\|_{L^\infty} = \sup_s f(s)$; $\|f\|_\rho = \sqrt{\int f(s)^2 \rho(s) ds}$. For vector function $f(s) \in \mathbb{R}^d$, $\nabla f(s) \in \mathbb{R}^{d \times d}$ with $(\nabla f(s))_{ij} = \partial_{s_i} f_j$; $\|f\|_2^2 = \sum_{i=1}^d f_i^2$ represents the Euclidean Norm; $\|f\|_{L^\infty} = \sqrt{\sum_{i=1}^d \|f_i(s)\|_{L^\infty}^2}$, similar with $\|f\|_\rho$. For matrix function $f(s) \in \mathbb{R}^{d \times d}$, $\nabla \cdot f = \sum_{l=1}^d \partial_{s_l} f_{i,l}$.

2 Setting

Consider the following continuous-time policy evaluation (PE) problem, where the value function $V(s) \in \mathbb{R}$, defined as follows, is the expected discounted cumulative reward starting from s ,

$$V(s) = \mathbb{E} \left[\int_0^\infty e^{-\beta t} r(s_t) dt | s_0 = s \right]. \quad (1)$$

Here $\beta > 0$ is a discounted coefficient, $r(s) \in \mathbb{R}$ is a reward function, and the state $s_t \in \mathbb{S} = \mathbb{R}^d$ is driven by the stochastic differential equation (SDE),

$$ds_t = \mu(s_t) dt + \sigma(s_t) dB_t, \quad (2)$$

with unknown drift function $\mu(s) \in \mathbb{R}^d$ and unknown diffusion function $\sigma(s) \in \mathbb{R}^{d \times d}$. In this paper, we assume that $\mu(s), \sigma(s)$ are Lipschitz continuous and the reward function $\|r\|_{L^\infty}$ is bounded. This ensures that (2) has a unique strong solution [37] and the infinite horizon integral is bounded.

Remark 1. *Continuous-time reinforcement learning [59] can be formulated as follows:*

$$\begin{aligned} \max_{a_t = \pi(s_t)} \quad & V^\pi(s) = \mathbb{E} \left[\int_0^\infty e^{-\beta t} r(s_t, a_t) dt | s_0 = s \right] \\ \text{s.t.} \quad & ds_t = \mu(s_t, a_t) + \sigma(s_t, a_t) dB_t, \quad a_t = \pi(s_t). \end{aligned}$$

where the goal is to find the optimal policy $\pi(s)$ that maximizes the value function under unknown drift and diffusion. In this paper, we focus on the unregularized optimal control problem and therefore restrict attention to deterministic feedback policies $a_t = \pi(s_t)$. For stochastic policies (see, e.g., [19, 59]), additional challenges may arise (see, e.g., [18, 52]), which we leave for future study.

The policy evaluation problem is a fundamental step in reinforcement learning algorithms, such as actor-critic and PPO [29, 42]. Its goal is to assess the quality of a fixed policy π by evaluating the value function under that policy. The continuous-time PE problem (1)–(2) considered in this paper arises by denoting $r^\pi(s) = r(s, \pi(s))$, $\mu^\pi(s) = \mu(s, \pi(s))$, $\sigma^\pi(s) = \sigma(s, \pi(s))$. For simplicity, we omit the subscript π throughout, as the policy is fixed in the entire paper.

We aim to approximate the continuous-time value function $V(s)$ when only discrete-time information is available. To be more specific, we consider the following two cases:

- Case 1. The transition distribution $\rho(s', \Delta t | s)$ in discrete time Δt , driven by the continuous dynamics (2), is given. Here $\rho(s', \Delta t | s)$ represents the probability density function of $s_{\Delta t}$ given $s_0 = s$.
- Case 2. Trajectory data generated by the continuous dynamics (2) and collected at discrete time $j\Delta t$ is given. Here the trajectory data $s = \{s_0^l, s_{\Delta t}^l, \dots, s_{m\Delta t}^l\}_{l=1}^I$ contains I independent trajectories, and the initial state s_0^l of each trajectory are sampled from a distribution $\rho_0(s)$.

The error analysis in Section 3 is conducted under Case 1. We demonstrate that the (discrete-time) Bellman equation is not always the optimal equation to solve continuous-time PE problems even when the discrete-time transition dynamics are known, and consequently, all the RL algorithms derived from it are not optimal either. To address this, we introduce a Physics-informed Bellman equation (PhiBE) and establish that its exact solution serves as a superior approximation to the true value function compared to the classical Bellman equation. When only trajectory data is available (Case 2), one can also use the data to solve the PhiBE, referred to as model-free RL, which will be discussed in Section 4.

3 A PDE-based Bellman Equation (PhiBE)

In Section 3.1, we first introduce the (discrete-time) Bellman equation, followed by an error analysis to demonstrate why it is not always a good approximation. Then, in Section 3.2, we propose the PhiBE, a PDE-based Bellman equation, considering both the deterministic case (Section 3.2.1) and the stochastic case (Section 3.2.2). The error analysis provides guidance on when PhiBE is a better approximation than the BE.

3.1 (Discrete-time) Bellman equation

By approximating the definition of the value function (1) in discrete time, one obtains the approximated value function,

$$\tilde{V}(s) = \mathbb{E} \left[\sum_{j=0}^{\infty} e^{-\beta \Delta t j} r(s_{j\Delta t}) \Delta t | s_0 = s \right]. \quad (3)$$

In this way, it can be viewed as a policy evaluation problem in Markov Decision Process, where the state is $s \in \mathbb{S}$, the reward is $r(s)\Delta t$, and the discount factor is $e^{-\beta \Delta t}$ and the transition dynamics is $\rho(s', \Delta t | s)$. Therefore, the approximated value function $\tilde{V}(s)$ satisfies the following (discrete-time) Bellman equation [48]. In this paper, we will simply refer to it as the Bellman equation (abbreviated as BE).

Definition 1 (Definition of BE).

$$\tilde{V}(s) = r(s)\Delta t + e^{-\beta \Delta t} \mathbb{E}_{s_{\Delta t} \sim \rho(s', \Delta t | s)} [\tilde{V}(s_{\Delta t}) | s_0 = s]. \quad (4)$$

When the discrete-time transition distribution is not given, one can utilize various RL algorithms to solve the Bellman equation (4) using the trajectory data. Note that some continuous-time RL papers approximate the value function by $V(s) \approx \sum_{i=0}^T e^{-\beta i \Delta t} r(s_{i \Delta t})$, which in fact is also approximating the solution of the Bellman equation, owing to the equivalence between (4) and (3). However, if the exact solution to the Bellman equation is not a good approximation to the true value function, then all the RL algorithms derived from it will not effectively approximate the true value function. In the theorem below, we provide an upper bound for the distance between the solution \tilde{V} to the above BE and the true value function V defined in (1).

Theorem 3.1 (Discretization error for BE). *Assume that $\|r\|_{L^\infty}, \|\mathcal{L}_{\mu, \Sigma} r\|_{L^\infty}$ are bounded, then the solution $\tilde{V}(s)$ to the BE (4) approximates the true value function $V(s)$ defined in (1) with an error*

$$\|V(s) - \tilde{V}(s)\|_{L^\infty} \leq \frac{\frac{1}{2}(\|\mathcal{L}_{\mu, \Sigma} r\|_{L^\infty} + \beta \|r\|_{L^\infty})}{\beta} \Delta t + o(\Delta t),$$

where

$$\mathcal{L}_{\mu, \Sigma} = \mu(s) \cdot \nabla + \frac{1}{2} \Sigma : \nabla^2, \quad (5)$$

with $\Sigma = \sigma \sigma^\top$, and $\Sigma : \nabla^2 = \sum_{i,j} \Sigma_{ij} \partial_{s_i} \partial_{s_j}$.

Remark 2 (Assumptions on $\|\mathcal{L}_{\mu, \Sigma} r\|_{L^\infty}$). *One sufficient condition for the assumption to hold is that $\|\mu(s)\|_{L^\infty}, \|\Sigma(s)\|_{L^\infty}, \|\nabla^k r(s)\|_{L^\infty}$ for $k = 0, 1, 2$ are all bounded. However, $\|\mathcal{L}_{\mu, \Sigma} r\|_{L^\infty}$ is less restrictive than the above and allows, for example, linear dynamics $\mu(s) = \lambda s, \Sigma = 0$, with the derivative of the reward decreasing faster than a linear function at infinity, $\|s \cdot \nabla r(s)\|_{L^\infty} \leq C$.*

The proof of the theorem is given in Section 6.1. In fact, by expressing the true value function $V(s)$ as the sum of two integrals, one can more clearly tell where the error in the BE comes from. Note that $V(s)$, as defined in (1), can be equivalently written as,

$$\begin{aligned} V(s) &= \mathbb{E} \left[\int_0^{\Delta t} e^{-\beta t} r(s) dt + \int_{\Delta t}^{\infty} e^{-\beta t} r(s_t) dt | s_0 = s \right] \\ &= \mathbb{E} \left[\int_0^{\Delta t} e^{-\beta t} r(s) dt | s_0 = s \right] + e^{-\beta \Delta t} \mathbb{E} [V(s_{t+\Delta t}) | s_0 = s] \end{aligned} \quad (6)$$

One can interpret the Bellman equation defined in (4) as an equation resulting from approximating $\mathbb{E} \left[\frac{1}{\Delta t} \int_0^{\Delta t} e^{-\beta t} r(s_t) dt | s_0 = s \right]$ in (6) by $r(s)$. The error between these two terms can be bounded by:

$$\left| \mathbb{E} \left[\left(\frac{1}{\Delta t} \int_0^{\Delta t} e^{-\beta t} r(s_t) dt \right) - r(s_0) \middle| s_0 = s \right] \right| \leq \frac{1}{2} (\beta \|r\|_{L^\infty} + \|\mathcal{L}_{\mu, \Sigma} r\|_{L^\infty}) \Delta t + o(\Delta t), \quad (7)$$

characterizes the error of $\|V - \tilde{V}\|_{L^\infty}$ in Theorem 3.1.

Theorem 3.1 indicates that the solution \tilde{V} to the Bellman equation (4) approximates the true value function with a first-order error of $O(\Delta t)$. Moreover, the coefficient before Δt suggests that for the same time discretization Δt , when β is small, the error is dominated by the term $\|\mathcal{L}_{\mu, \Sigma} r(s)\|_{L^\infty}$, indicating that the error increases when the reward changes rapidly. Conversely, when β is large, the error is mainly affected by $\|r\|_{L^\infty}$, implying that the error increases when the magnitude of the reward is large.

Fundamentally, the Bellman equation is designed for discrete-time decision-making processes and depends only on the discrete-time transition kernel $\rho(s', \Delta t | s)$. This kernel may arise from any underlying mechanism. As a result, the Bellman equation does not utilize or encode any assumption about how $\rho(s', \Delta t | s)$ is generated. In particular, it does not exploit the assumption made in this paper that the discrete-time dynamics are induced by a continuous-time SDE. To incorporate this continuous-time structure into the approximation, one must go beyond the standard MDP framework. The question that the rest of this section seeks to address is whether, given the same discrete-time information, i.e., the transition distribution $\rho(s', \Delta t | s)$, time discretization Δt , and discount coefficient β , one can combine the differential equation structure with the discrete-time transition dynamics and achieve a more accurate estimation of the value function?

3.2 A PDE-based Bellman equation

In this section, we introduce a PDE-based Bellman equation, referred to as PhiBE. We begin by discussing the case of deterministic dynamics in Section 3.2.1 to illustrate the idea clearly. Subsequently, we extend our discussion to the stochastic case in Section 3.2.2.

3.2.1 Deterministic Dynamics

When $\sigma(s) \equiv 0$ in (2), the dynamics become deterministic, which can be described by the following ODE,

$$\frac{ds_t}{dt} = \mu(s_t). \quad (8)$$

If the discrete-time transition dynamics $p(s', \Delta t | s) = p_{\Delta t}(s)$ is given, where $p_{\Delta t}(s)$ provides the state at time $t + \Delta t$ when the state at time t is s , then the BE in deterministic dynamics reads as follows,

$$\frac{1}{\Delta t} \tilde{V}(s) = r(s) + \frac{e^{-\beta \Delta t}}{\Delta t} \tilde{V}(p_{\Delta t}(s)).$$

The key idea of the new equation is that, instead of approximating the value function directly, one approximates the dynamics. First note that the value function defined in (1) can be equivalently written as the solution to the following PDE,

$$\beta V(s) = r(s) + \mu(s) \cdot \nabla V(s). \quad (9)$$

The above equation is known as the Hamilton–Jacobi–Bellman (HJB) equation, often referred to as the continuous-time Bellman equation. In this paper, we will consistently refer to it as the HJB equation. A detailed derivation can be found in Appendix A or in classical control

textbooks such as [46]. Applying a finite difference scheme, one can approximate $\mu(s_t)$ by

$$\mu(s_t) = \frac{d}{dt}s_t \approx \frac{1}{\Delta t}(s_{t+\Delta t} - s_t) = \frac{1}{\Delta t}(p_{\Delta t}(s_t) - s_t),$$

and substituting it back into (9) yields

$$\beta \hat{V}(s_t) = r(s_t) + \frac{1}{\Delta t}(s_{t+\Delta t} - s_t) \cdot \nabla \hat{V}(s_t).$$

Alternatively, this equation can be expressed in the form of a PDE as follows,

$$\beta \hat{V}(s) = r(s) + \frac{1}{\Delta t}(p_{\Delta t}(s) - s) \cdot \nabla \hat{V}(s), \quad (10)$$

Note that the error now arises from

$$\left| \mu(s_t) - \frac{s_{t+\Delta t} - s_t}{\Delta t} \right| \leq \frac{1}{2} \|\mu \cdot \nabla \mu\|_{L^\infty} \Delta t,$$

which only depends on the dynamics. As long as the dynamics change slowly, i.e., the acceleration of dynamics $\left\| \frac{d^2}{dt^2}s_t \right\|_{L^\infty} = \|\mu \cdot \nabla \mu\|_{L^\infty}$ is small, the error diminishes.

We refer to (10) as PhiBE for deterministic dynamics, an abbreviation for the physics-informed Bellman equation, because it incorporates both the current state and the state after Δt , similar to the Bellman equation, while also resembling the form of the PDE (9) derived from the true continuous-time physical environment. However, unlike the Bellman equation, which is blind to the underlying SDE structure, PhiBE explicitly exploits this structure by involving the gradient of the value function, thereby embedding the smoothness induced by the continuous-time dynamics. At the same time, unlike the true PDE (9), which requires direct access to the continuous-time dynamics and is therefore non-identifiable from discrete-time information, PhiBE depends only on the discrete-time transition kernel. This makes PhiBE amenable to model-free algorithm design while still leveraging continuous-time structure.

One can derive a higher-order PhiBE by employing a higher-order finite difference scheme to approximate $\mu(s_t)$. For instance, the second-order finite difference scheme

$$\mu(s_t) \approx \hat{\mu}_2(s_t) := \frac{1}{\Delta t} \left[-\frac{1}{2}(s_{t+2\Delta t} - s_t) + 2(s_{t+\Delta t} - s_t) \right],$$

resulting in the second-order PhiBE,

$$\beta \hat{V}_2(s) = r(s) + \frac{1}{\Delta t} \left[-\frac{1}{2}(p_{\Delta t}(p_{\Delta t}(s)) - s) + 2(p_{\Delta t}(s) - s) \right] \cdot \nabla \hat{V}_2(s).$$

In this approximation, $\|\mu(s) - \hat{\mu}_2(s)\|_{L^\infty}$ has a second order error $O(\Delta t^2)$. We summarize i -th order PhiBE in deterministic dynamics in the following Definition.

Definition 2 (i -th order PhiBE in deterministic dynamics). *When the underlying dynamics are deterministic, then the i -th order PhiBE is defined as,*

$$\beta \hat{V}_i(s) = r(s) + \hat{\mu}_i(s) \cdot \nabla \hat{V}_i(s), \quad (11)$$

where

$$\hat{\mu}_i(s) = \frac{1}{\Delta t} \sum_{j=1}^i a_j^{(i)} \left(\underbrace{p_{\Delta t} \circ \cdots \circ p_{\Delta t}}_j(s) - s \right), \quad (12)$$

and

$$(a_0^{(i)}, \dots, a_i^{(i)})^\top = A_i^{-1} b_i, \quad \text{with } (A_i)_{kj} = j^k, \quad (b_i)_k = \begin{cases} 0, & k \neq 1 \\ 1, & k = 1 \end{cases} \text{ for } 0 \leq j, k \leq i. \quad (13)$$

Remark 3. Note that $\hat{\mu}_i(s)$ can be equivalently written as

$$\hat{\mu}_i(s) = \frac{1}{\Delta t} \sum_{j=1}^i a_j^{(i)} [s_{j\Delta t} - s_0 | s_0 = s].$$

There is an equivalent definition of $a^{(i)}$, given by

$$\sum_{j=0}^i a_j^{(i)} j^k = \begin{cases} 0, & k \neq 1, \\ 1, & k = 1, \end{cases} \quad \text{for } 0 \leq j, k \leq i. \quad (14)$$

Discussion on the relation to numerical schemes for the HJB equation. The PhiBE formulation is fundamentally different from classical numerical schemes for the HJB equation in three key aspects.

First of all, the goal of two approaches are different. Classical numerical schemes aim to approximate the solution of the PDE $\mathcal{L}_{\mu,\sigma} V(s) = 0$, where the operator $\mathcal{L}_{\mu,\sigma}$ is explicitly given. In contrast, the goal of our paper is not only must we approximate the solution to the PDE, but we must do so without fully knowing the PDE operator. We tackle the overall goal in two steps. The first step is to approximate the PDE operator $\mathcal{L}_{\mu,\sigma}$, and the second step is to solve the resulting equation. The PhiBE formulation (11) is constructed to address the first task, namely approximating the unknown operator $\mathcal{L}_{\mu,\sigma} V(s) = 0$ by $\mathcal{L}_{\hat{\mu},\hat{\sigma}} V(s) = 0$ using only partial information in the form of the discrete-time transition kernel $\rho(s', \Delta t | s)$, with no direct access to $\mu(s), \sigma(s)$. Consequently, the “discretization error” analyzed in this section refers to the error incurred from observing $\rho(s', \Delta t | s)$ at $\Delta t > 0$ rather than the infinitesimal kernel $\lim_{\Delta t \rightarrow 0} \rho(s', \Delta t | s)$. It does not refer to the numerical error of solving the PDE.

Second, the discretization formulations differ. Classical schemes discretize the state space over a uniform mesh h , e.g., $V'(s) \approx \frac{1}{h}(V(s+h) - V(s))$, while such uniform meshing cannot be directly applied in RL because trajectory data are irregularly distributed. Consequently, numerical error in classical schemes arises from spatial discretization, whereas in PhiBE it originates from time discretization through the approximation of $\hat{\mu}$ and $\hat{\Sigma}$. Moreover, although the definition of $\hat{\mu}(s)$ superficially resembles a finite-difference expression, its meaning is fundamentally different. In classical methods, one starts from known dynamics $\mu(s)$ and uses numerical schemes to approximate the trajectory $s_{j\Delta t}$. As a result, numerical error propagates and accumulates over time. In contrast, PhiBE takes the opposite approach: the trajectories $s_{j\Delta t}$ are observed from data and used to approximate the underlying dynamics

$\mu(s)$. This inversion of roles leads to a distinct analytical treatment of convergence and convergence rates for $\hat{V}_i(s)$ that does not accumulate over time, in sharp contrast to classical numerical discretization errors.

Finally, the error analysis frameworks and emphasis are distinct. Classical analyses establish convergence by verifying that the discrete operator is monotone, stable, and consistent, then applying comparison principles and perturbation arguments to derive convergence rates. In contrast, our analysis first quantifies the discrepancy between the data-driven dynamics $(\hat{\mu}, \hat{\Sigma})$ and the true dynamics (μ, Σ) , a component never addressed in traditional numerical analyses, and then propagates this discrepancy to the value function via PDE stability. Furthermore, while classical numerical analyses focus on the order of accuracy in the mesh size h and typically omit constants, our comparison with discrete-time RL requires explicit characterization of these constants, as both standard RL and PhiBE are first-order approximations. The leading constant, which depends on the reward and dynamics, ultimately determines the practical performance of continuous-time RL algorithms.

In summary, PhiBE differs fundamentally from classical numerical schemes for HJB equations. Nevertheless, because the continuous-time RL problem is connected to a PDE through the PhiBE formulation, one could, in principle, estimate ρ_Δ from data, compute $(\hat{\mu}, \hat{\Sigma})$ explicitly, and then apply standard numerical schemes to solve the resulting PhiBE equation. The classical convergence results would then apply to this model-based approach. However, this paper will focus on developing a model-free algorithm for solving the PhiBE equation directly from data without explicitly estimating $\hat{\mu}$ or $\hat{\Sigma}$.

The error analysis of PhiBE in the deterministic dynamics is established in the following theorem.

Theorem 3.2 (Discretization error for deterministic PhiBE). *Assume that $\|\nabla r(s)\|_{L^\infty}$, $\|\mathcal{L}_\mu^i \mu(s)\|_{L^\infty}$ are bounded. Additionally, assume that $\|\nabla \mu(s)\|_{L^\infty} < \beta$, then the solution $\hat{V}_i(s)$ to the PhiBE (11) is an i th-order approximation to the true value function $V(s)$ defined in (1) with an error*

$$\left\| \hat{V}_i(s) - V(s) \right\|_{L^\infty} \leq 2C_i \frac{\|\nabla r\|_{L^\infty} \|\mathcal{L}_\mu^i \mu\|_{L^\infty}}{(\beta - \|\nabla \mu\|_{L^\infty})^2} \Delta t^i,$$

where

$$\mathcal{L}_\mu = \mu \cdot \nabla, \tag{15}$$

and C_i is a constant defined in (49) that only depends on the order i .

See Section 6.2 for the proof of Theorem 3.2. Several remarks regarding the above theorem are in order.

1st-order PhiBE v.s. BE By Theorem 3.2, the distance between the first-order PhiBE solution and the true value function can be bounded by

$$\left\| \hat{V}_1 - V \right\|_{L^\infty} \leq \frac{2 \|\nabla r\|_{L^\infty} \|\mu \cdot \nabla \mu\|_{L^\infty}}{(\beta - \|\nabla \mu\|_{L^\infty})^2} \Delta t.$$

Comparing it with the difference between the BE solution and the true value function in deterministic dynamics,

$$\left\| \tilde{V} - V \right\|_{L^\infty} \leq \frac{\|\mu \nabla r\|_{L^\infty} + \beta \|r\|_{L^\infty}}{2\beta} \Delta t,$$

one observes that when the change of the reward is rapid, i.e., $\|\nabla r\|_{L^\infty}$ is large, but the change in velocity is slow, i.e., $\left\| \frac{d^2}{dt^2} s_t \right\|_{L^\infty} = \|\mu \cdot \nabla \mu\|_{L^\infty}$ is small, even though both \hat{V}_1 and \tilde{V} are first-order approximations to the true value function, \hat{V}_1 has a smaller upper bound.

Higher-order PhiBE The advantage of the higher-order PhiBE is two-fold. Firstly, it provides a higher-order approximation, enhancing accuracy compared to the first-order PhiBE or BE. Secondly, as demonstrated in Theorem 3.2, the approximation error of the i -th order PhiBE decreases as $\|\mathcal{L}_\mu^i \mu\|_{L^\infty}$ decreases. If the “acceleration”, i.e., $\frac{d^2}{dt^2} s_t = \mathcal{L}_\mu \mu$, of the dynamics is large but the change in acceleration, i.e., $\frac{d^3}{dt^3} s_t = \mathcal{L}_\mu^2 \mu$, is slow, then the error reduction with the second-order PhiBE will be even more pronounced in addition to the higher-order error effect.

Dependence on β When β is large, PhiBE always has a smaller discretization error than BE. However, when β is small, the BE error scales as $O(\beta^{-1})$, whereas the PhiBE error scales as $O(\beta^{-2})$. Thus, when β is small, the gap in discretization error between the two methods naturally narrows. However, as shown later in Section 4, the finite-sample error of the model-free algorithms for both BE and PhiBE scales as $O(\beta^{-2})$. As a result, in data-driven settings, the potential advantage of BE for small β is dominated by finite-sample error scales as $O(\beta^{-2})$. In contrast, PhiBE retains an advantage in regimes with slowly varying dynamics and rapidly changing reward functions.

In addition to that, in standard RL settings, the discount factor is $\gamma = e^{-\beta \Delta t} \in [0.9, 0.99]$, so the resulting range of β depends on the sampling frequency. When the data are collected at $\Delta t = 0.01$, we expect an $\beta = O(1)$, i.e., $\beta \in [1, 10]$. For data collected at $\Delta t = 0.1$, one obtains a smaller $\beta \in [0.1, 1]$. In the experiments in Section 5, we therefore evaluate both methods across a broad range $\beta \in [0.1, 10]$.

When does PhiBE outperform BE? In summary, PhiBE outperforms BE in terms of discretization error whenever one of the following conditions is present: (i) the dynamics evolve slowly; (ii) the reward function varies sharply; or (iii) the discount rate is not extremely small. In summary, these features arise frequently in continuous-time RL applications. First, slow dynamics are common in physical and biomedical systems, where state variables evolve gradually and smoothly. For instance, in glucose–insulin regulation, blood glucose levels follow physiological ODE models with inherently slow drift dynamics. Second, the reward function often needs to sharply penalize excursions outside a healthy range, so that the optimal policy strongly encourages keeping the patient within a safe region. This leads to a highly varying reward landscape, i.e., a large $\|\nabla_s r(s)\|$. Third, discount coefficients used in practice are rarely associated with extremely small continuous-time rates. In OpenAI Gym environments with $\Delta t \sim 10^{-2}$, the typical choice $\gamma \in [0.9, 0.99]$ corresponds to $\beta \in [1, 10]$. In

clinical settings with larger sampling intervals, objectives often focus on maintaining stability over short or moderate horizons, so the effective discount rate is similarly not small. Taken together, the three features are common in real-world applications, making the settings where PhiBE outperforms BE not exceptional but the typical regime for continuous-time reinforcement learning.

Assumptions on $\|\mathcal{L}_\mu^i \mu(s)\|_{L^\infty}$ Note that the boundedness assumption of $\|\mathcal{L}_\mu^i \mu(s)\|_{L^\infty}$ is required in general to establish that $\hat{\mu}_i(s)$ is an i -th order approximation to $\mu(s)$. A sufficient condition for $\|\mathcal{L}_\mu^i \mu(s)\|_{L^\infty}$ being bounded is that $\|\nabla^k \mu(s)\|_{L^\infty}$ are bounded for all $0 \leq k \leq i$. Note that the linear dynamics $\mu(s) = As$ does not satisfy this condition. We lose some sharpness for the upper bound to make the theorem work for all general dynamics. However, we prove in Theorem 3.3 that PhiBE works when $\mu(s) = As$, and one can derive a sharper error estimate for this case.

Theorem 3.3. *When the underlying dynamics follows $\frac{d}{dt}s_t = As_t$, where $s_t \in \mathbb{R}^d$ and $A \in \mathbb{R}^{d \times d}$, then the solution to the i -th order PhiBE in deterministic dynamics approximates the true value function with an error*

$$\left\| \hat{V}_i - V \right\|_{L^\infty} \leq \frac{C_i}{\beta^2} \|s \cdot \nabla r(s)\|_{L^\infty} \|A\|_2 D_A^i \Delta t^i, \quad D_A = e^{\|A\|_2 \Delta t} \|A\|_2$$

where C_i is a constant defined in (49) that only depends on the order i .

The proof of the above theorem is provided in Section 6.3. According to Theorem 3.3, even when the dynamics $s_t = e^{At}s_0$ evolve exponentially fast due to positive real parts in the eigenvalues of A , the PhiBE solution remains a good approximation to the true value function provided that $D_A \Delta t$ is small. In particular, when $D_A \Delta t < 1$, higher-order PhiBE achieves a smaller approximation error than the first-order PhiBE.

3.2.2 Stochastic dynamics

When $\sigma(s) \neq 0$ is a non-degenerate matrix, then the dynamics is stochastic and driven by the SDE in (2). By Feynman–Kac theorem [46], the value function $V(s)$ satisfies the following HJB equation,

$$\beta V(s) = r(s) + \mathcal{L}_{\mu, \Sigma} V(s), \quad (16)$$

where $\mathcal{L}_{\mu, \Sigma}$ is an operator defined in (5). However, one cannot directly solve the PDE (16) as $\mu(s), \sigma(s)$ are unknown. In the case where one only has access to the discrete-time transition distribution $\rho(s', \Delta t | s)$, we propose an i -th order PhiBE in the stochastic dynamics to approximate the true value function $V(s)$.

Definition 3 (i -th order PhiBE in stochastic dynamics). *When the underlying dynamics are stochastic, then the i -th order PhiBE is defined as,*

$$\beta \hat{V}_i(s) = r(s) + \mathcal{L}_{\hat{\mu}_i, \hat{\Sigma}_i} \hat{V}_i(s), \quad (17)$$

where

$$\begin{aligned}\hat{\mu}_i(s) &= \frac{1}{\Delta t} \sum_{j=1}^i \mathbb{E}_{s_{j\Delta t} \sim \rho(\cdot, j\Delta t|s)} \left[a_j^{(i)}(s_{j\Delta t} - s_0) | s_0 = s \right] \\ \hat{\Sigma}_i(s) &= \frac{1}{\Delta t} \sum_{j=1}^i \mathbb{E}_{s_{j\Delta t} \sim \rho(\cdot, j\Delta t|s)} \left[a_j^{(i)}(s_{j\Delta t} - s_0)(s_{j\Delta t} - s_0)^\top | s_0 = s \right]\end{aligned}\tag{18}$$

where $\mathcal{L}_{\hat{\mu}_i, \hat{\Sigma}_i}$ is defined in (5), and $a^{(i)} = (a_0^{(i)}, \dots, a_i^{(i)})^\top$ is defined in (13).

Remark 4. There is another i -th order approximation for $\Sigma(s)$,

$$\tilde{\Sigma}_i(s) = \frac{1}{\Delta t} \sum_{j=0}^i a_j^{(i)} \left(\mathbb{E}[s_{j\Delta t}^\top s_{j\Delta t} | s_0 = s] - \mathbb{E}[s_{j\Delta t} | s_0 = s]^\top \mathbb{E}[s_{j\Delta t} | s_0 = s] \right).$$

However, the unbiased estimate for $\tilde{\Sigma}(s)$

$$\tilde{\Sigma}_i(s_0) \approx \frac{1}{\Delta t} \sum_{j=1}^i a_j^{(i)} (s_{j\Delta t}^\top s_{j\Delta t} - s'_{j\Delta t} s_{j\Delta t})$$

requires two independent samples $s_{j\Delta t}, s'_{j\Delta t}$ starting from s_0 , which are usually unavailable in the RL setting. This is known as the “double Sampling” problem. One could apply a similar idea in [66, 65] to alleviate the double sampling problem when the underlying dynamics are smooth, that is, approximating $s'_{j\Delta t} \approx s_{(j-1)\Delta t} + (s_{(j+1)\Delta t} - s_{j\Delta t})$. However, it will introduce additional bias into the approximation. We leave the study of this approximation $\tilde{\Sigma}_i(s)$ or the application of BFF on $\tilde{\Sigma}_i(s)$ for future research.

The first and second-order approximations are presented as follows. The first-order approximation reads,

$$\hat{\mu}_1(s) = \frac{1}{\Delta t} \mathbb{E}[(s_{\Delta t} - s_0) | s_0 = s], \quad \hat{\Sigma}_1(s) = \frac{1}{\Delta t} \mathbb{E}[(s_{\Delta t} - s_0)(s_{\Delta t} - s_0)^\top | s_0 = s];$$

and the second-order approximation reads,

$$\begin{aligned}\hat{\mu}_2(s) &= \frac{1}{\Delta t} \mathbb{E} \left[2(s_{\Delta t} - s_0) - \frac{1}{2}(s_{2\Delta t} - s_0) | s_0 = s \right], \\ \hat{\Sigma}_2(s) &= \frac{1}{\Delta t} \mathbb{E} \left[2(s_{\Delta t} - s_0)(s_{\Delta t} - s_0)^\top - \frac{1}{2}(s_{2\Delta t} - s_0)(s_{2\Delta t} - s_0)^\top | s_0 = s \right].\end{aligned}$$

Next, we show the solution $\hat{V}_i(s)$ to the i th-order PhiBE provides an i th-order approximation to the true value function $V(s)$, under the following assumptions.

Assumption 1. Assumptions on the dynamics:

- (a) $\lambda_{\min}(\Sigma(s)) > \lambda_{\min} > 0$ for $\forall s \in \mathbb{S}$, where $\lambda_{\min}(A)$ is the smallest eigenvalue of A .
- (b) $\|\nabla^k \mu(s)\|_{L^\infty}, \|\nabla^k \Sigma(s)\|_{L^\infty}$ are bounded for $0 \leq k \leq 2i$.

The first assumption ensures the coercivity of the operator $\mathcal{L}_{\mu,\Sigma}$, which is necessary to establish the regularity of $V(s)$. The second assumption is employed to demonstrate that $\hat{\mu}_i$ and $\hat{\Sigma}_i$ are i -th approximations to μ, Σ , respectively.

To establish the error analysis, we define a weighted L^2 inner product and norm under a probability density $\rho(s)$ by

$$\langle f, g \rangle_\rho = \int f(s)g(s)\rho(s)ds, \quad \|f\|_\rho^2 = \int f^2(s)\rho(s)ds. \quad (19)$$

In addition, the density ρ satisfies

$$L_\rho = \|\nabla \log \rho\|_\rho \text{ is bounded.} \quad (20)$$

One may take $\rho(s)$ to be the stationary distribution (when it exists), namely a density satisfying

$$\int \mathcal{L}_{\mu,\Sigma}\phi(s)\rho(s)ds = 0. \quad \text{for } \forall \phi(s) \in C_c^\infty. \quad (21)$$

If a stationary distribution does not exist, one may select a density ρ such that

$$\left\| -\mu + \frac{1}{2}\nabla \cdot \Sigma + \frac{1}{2}\Sigma\nabla \log \rho \right\|_{L^\infty(\Omega)}^2 \leq \frac{1}{2}\beta\lambda_{\min}, \quad (22)$$

where $\Omega = \{s : \rho(s) \neq 0\}$. If $\Omega \neq \mathbb{R}^d$, then all assumptions and results hold on Ω , rather than on the entire space \mathbb{R}^d .

Remark 5. *Several remarks are in order for the weight $\rho(s)$. First, classical results (e.g., [17]) imply that when the drift and diffusion satisfy a suitable dissipation condition, a stationary distribution exists. Furthermore, once a stationary distribution exists, Theorem 1.1 of [6] yields the bound $L_\rho \leq \frac{1}{\lambda_{\min}} \|\mu + \nabla \cdot \Sigma\|_{L^\infty}$.*

Second, if no stationary distribution exists, one can still choose a density ρ such that (22) holds. For example, in one of our numerical experiments (35), the system admits no stationary solution when $\lambda > 0$. In this case, one may take

$$\rho(s) = \begin{cases} \frac{1}{2c}, & s \in [-c, c], \\ 0, & s \notin [-c, c], \end{cases} \quad |c| \leq \frac{\beta\sigma^2}{2\lambda},$$

which ensures (22). The trade-off is that under this choice of weighted norm, one can guarantee convergence of the approximation error only on the domain $\Omega = \{s : \rho(s) \neq 0\}$, rather than on the entire space \mathbb{R}^d . At the same time, Assumption 1 on the drift and diffusion is also relaxed: instead of requiring it to hold globally, it only needs to be satisfied on the domain Ω .

Third, if one chooses to work with the Lebesgue measure on $\Omega \subset \mathbb{R}^d$, then, in addition to Assumption 1 on the drift and diffusion terms, we require

$$\left\| -\mu + \frac{1}{2}\nabla \cdot \Sigma \right\|_{L^\infty(\Omega)}^2 \leq \frac{1}{2}\beta\lambda_{\min}.$$

This ensures that the requirement (22) remains valid when the density ρ is taken to be the (unnormalized) Lebesgue measure.

The error analysis for BE in the weighted L^2 norm is presented in the following theorem.

Theorem 3.4 (Discretization error for BE in weighted L^2 norm). *Assume that $\|r\|_\rho$, $\|\mathcal{L}_{\mu,\Sigma}r\|_\rho$ are bounded, then the solution $\tilde{V}(s)$ to the BE (4) approximates the true value function $V(s)$ defined in (1) with an error*

$$\|V(s) - \tilde{V}(s)\|_\rho \leq \frac{2(\|\mathcal{L}_{\mu,\Sigma}r\|_\rho + \beta \|r\|_\rho)}{\beta} \Delta t + o(\Delta t).$$

The proof of Theorem 3.4 is given in Section 6.4. Next, the error analysis for PhiBE in stochastic dynamics is presented in the following theorem.

Theorem 3.5 (Discretization error for stochastic PhiBE). *Under Assumption 1, and $\Delta t^i \leq D_{\mu,\Sigma,\beta}$, the solution $\hat{V}_i(s)$ to the i -th order PhiBE (17) is an i -th order approximation to the true value function $V(s)$ defined in (1) with an error*

$$\|V(s) - \hat{V}_i(s)\|_\rho \leq \left(\frac{C_{r,\mu,\Sigma}}{\beta^2} + \frac{\hat{C}_{r,\mu,\Sigma}}{\beta^{3/2}} \right) \Delta t^i,$$

where $D_{\mu,\Sigma,\beta}$, $C_{r,\mu,\Sigma}$, $\hat{C}_{r,\mu,\Sigma}$ are constants defined in (55), (56) depending on μ, Σ, r .

The proof of Theorem 3.5 is given in Section 6.5.

Remark 6 (PhiBE v.s. BE). *Here we discuss two cases. The first case is when the diffusion is known, that is, $\hat{\Sigma}_i = \Sigma$, then the distance between the PhiBE and the true value function can be bounded by*

$$\|\hat{V}_i - V\|_\rho \lesssim \frac{1}{\beta^2} \|\mathcal{L}_{\mu,\Sigma}^i \mu\|_{L^\infty} \left[\left(\frac{\|\nabla \Sigma\|_{L^\infty}}{\lambda_{\min}} + \sqrt{\frac{\|\nabla \mu\|_{L^\infty}}{\lambda_{\min}}} \right) \|r\|_\rho + \|\nabla r\|_\rho \right] \Delta t^i.$$

Similar to the deterministic case, the error of the i -th order PhiBE proportional to the change rate of the dynamics $\mathbb{E}[\frac{d^{i+1}}{dt^{i+1}} s_t] = \mathcal{L}_{\mu,\Sigma}^i \mu$. One can refer to the discussion under Theorem 3.2 for the benefit of the 1st-order PhiBE and higher-order PhiBE with respect to different dynamics.

The second case is when both drift and diffusion are unknown. Then the distance between the first-order PhiBE and the true value function can be bounded by

$$\begin{aligned} & \|\hat{V}_1 - V\|_\rho \\ & \lesssim \frac{\Delta t}{\beta^2} \left[\left(L_\mu + L_{\nabla \cdot \Sigma} + \frac{L_\Sigma}{\lambda_{\min}} \|\mu + \nabla \cdot \Sigma\|_{L^\infty} \right) \left(\sqrt{\frac{C_\nabla}{\lambda_{\min}}} \|r\|_{\rho, L^\infty} + \|\nabla r\|_{\rho, L^\infty} \right) \right] \\ & \quad + \frac{\Delta t}{\beta^{3/2}} \frac{1}{\sqrt{\lambda_{\min}}} L_\Sigma \left(\sqrt{\frac{C_\nabla}{\lambda_{\min}}} \|r\|_\rho + \|\nabla r\|_\rho \right), \end{aligned}$$

where

$$\begin{aligned}
L_\mu &\lesssim \|\mathcal{L}\mu\|, \quad L_\Sigma \lesssim \|\mu\mu^\top + \Sigma\nabla\mu + \mathcal{L}\Sigma\|_{L^\infty} + \|\mu\|_{L^\infty}, \\
L_{\nabla\cdot\Sigma} &\lesssim \sqrt{\frac{C_\nabla}{\lambda_{\min}}} \|\mu\mu^\top + \Sigma\nabla\mu + \mathcal{L}\Sigma\|_{L^\infty} + \|\nabla \cdot (\mu\mu^\top + \Sigma\nabla\mu + \mathcal{L}\Sigma)\|_{L^\infty} + \sqrt{\frac{C_\nabla}{\lambda_{\min}}} \|\mu\|_{L^\infty} \\
&\quad + \|\nabla\mu\|_{L^\infty}, \\
\sqrt{\frac{C_\nabla}{\lambda_{\min}}} &\lesssim \frac{\|\nabla\mu\|_{L^\infty}}{2\lambda} + \sqrt{\frac{\|\nabla\Sigma\|_{L^\infty}}{\lambda_{\min}}}, \quad \|r\|_{\rho, L^\infty} = \|r\|_\rho + \|r\|_{L^\infty}.
\end{aligned}$$

Here the operator \mathcal{L} represents $\mathcal{L}_{\mu, \Sigma}$. This indicates that when λ_{\min} is large or $\nabla\mu, \nabla\Sigma$ are small, the difference between \hat{V}_1 and V is smaller. Comparing it with the upper bound $\|\mathcal{L}r\|_\rho + \beta \|r\|_\rho$ for the BE, which is more sensitive to large β and reward function, the PhiBE approximation is less sensitive to these factors. When the change in the dynamics is slow, or the noise is large, even the first-order PhiBE solution is a better approximation to the true value function than the BE.

4 Model-free Algorithm for PhiBE

In this section, we assume that one only has access to the discrete-time trajectory data $\{s_0^l, s_{\Delta t}^l, \dots, s_{m\Delta t}^l\}_{l=1}^I$. We first revisit the Galerkin method for solving PDEs with known dynamics in Section 4.1, and we provide the error analysis of the Galerkin method for PhiBE. Subsequently, we introduce a model-free Galerkin method in Section 4.2. Finally, we conclude this section with an end-to-end error analysis for the model-free algorithm in Section 4.3.

4.1 Galerkin Method

Given p bases $\{\phi_i(s)\}_{i=1}^p$, the objective is to find an approximation $\bar{V}(s) = \Phi(s)^\top \theta$ to the solution $V(s)$ of the PDE,

$$\beta V(s) - \mathcal{L}_{\mu, \Sigma} V(s) = r(s),$$

where $\theta \in \mathbb{R}^p$, $\Phi(s) = (\phi_1(s), \dots, \phi_p(s))^\top$, and $\mathcal{L}_{\mu, \Sigma}$ is defined in (5). The Galerkin method involves inserting the ansatz \bar{V} into the PDE and then projecting it onto the finite bases,

$$\langle \beta \bar{V}(s) - \mathcal{L}_{\mu, \Sigma} \bar{V}(s), \Phi(s) \rangle_\rho = \langle r(s), \Phi(s) \rangle_\rho,$$

where the same measure ρ defined in (19) is used here. This results in a linear system of θ ,

$$A\theta = b, \quad A = \langle \beta \Phi(s) - \mathcal{L}_{\mu, \Sigma} \Phi(s), \Phi(s) \rangle_\rho, \quad b = \langle r(s), \Phi(s) \rangle_\rho.$$

When the dynamics $\mu(s), \Sigma(s)$ are known, one can explicitly compute the matrix A and the vector b , and find the parameter $\theta = A^{-1}b$ accordingly.

In continuous-time PE problems, one does not have access to the underlying dynamics μ, Σ . However, the approximated dynamics $\hat{\mu}_i, \hat{\Sigma}_i$ is given through PhiBE. Therefore, if one

has access to the discrete-time transition distribution, then the parameter $\theta = \hat{A}_i^{-1}b$ can be solved for by approximating A with \hat{A}_i

$$\hat{A}_i = \left\langle \beta \Phi(s) - \mathcal{L}_{\hat{\mu}_i, \hat{\Sigma}_i} \Phi(s), \Phi(s) \right\rangle_{\rho}, \quad (23)$$

where $\hat{\mu}_i, \hat{\Sigma}_i$ are defined in (18). We give the error estimate of the Galerkin method for PhiBE in the following theorem.

Theorem 4.1 (Galerkin Error). *The Galerkin solution $\hat{V}_i^G(s) = \theta^\top \Phi(s)$ satisfies*

$$\left\langle (\beta - \mathcal{L}_{\hat{\mu}_i, \hat{\Sigma}_i}) \hat{V}_i^G(s), \Phi \right\rangle_{\rho} = \langle r(s), \Phi(s) \rangle_{\rho}. \quad (24)$$

For small $\Delta t^i \leq \min\{\eta_{\mu, \Sigma, \beta}, D_{\mu, \Sigma, \beta}\}$, the Galerkin solution $\hat{V}_i^G(s)$ approximates the solution to the i -th order PhiBE defined in (17) with an error

$$\left\| \hat{V}_i^G(s) - \hat{V}_i(s) \right\|_{\rho} \leq \frac{C_G}{\beta} \inf_{V^P = \theta^\top \Phi} \left\| \hat{V}_i - V^P \right\|_{H_{\rho}^1}.$$

where $\eta_{\mu, \Sigma, \beta}, C_G, D_{\mu, \Sigma, \beta}$ are constants depending on $\mu, \Sigma, \beta, L_{\rho}^{\infty}, L_{\Phi}^{\infty}$ defined in (59), (60), (55) respectively, and $\|f\|_{H_{\rho}^1} = \|f\|_{\rho} + \|\nabla f\|_{\rho}$.

The proof of the Theorem is given in Section 6.6.

Several remarks are in order. First, the above theorem establishes an approximation-error bound under model misspecification, that is, the error arising when the true value function cannot be exactly represented within the chosen linear bases $\Phi(s)$. More specifically, the bound in Theorem 4.1 can be interpreted as the limiting error of the data-driven algorithms (Algorithms 1 and 2) when infinite data are available.

Second, the solver (24) serves as a continuous-time counterpart to LSTD [7] by replacing the discrete-time Bellman equation with the PhiBE equation. However, our bound is much tighter than the existing RL literature in terms of Δt . In Theorem 1 of [30], the approximation-error term $(1 - \gamma^2)^{-1/2} \|v - \Pi v\|$ arises from model misspecification. However, this bound diverges as $\Delta t \rightarrow 0$ because $\gamma = e^{-\beta \Delta t} \rightarrow 1$. This divergence stems from the use of the contraction property of the Bellman operator whose contraction factor is γ . Such discrete-time arguments are sharp for general RL problems where the transition dynamics have no structural assumptions. However, such contraction-based analysis is not suitable for continuous-time RL problem considered in this paper for two reasons. First, as $\Delta t \rightarrow 0$, one would expect the approximation error to decrease; yet, since $\gamma \rightarrow 1$, the contraction property vanishes, causing the approximation error to instead worsen and eventually diverge. Second, the analysis framework fails to exploit the smoothness and structural information of the underlying SDE.

In contrast, our analysis exploits the ellipticity of the infinitesimal generator $\mathcal{L}_{\hat{\mu}, \hat{\Sigma}}$ and yields an error bound $\frac{C_G}{\beta} \|v - \Pi v\|$, where C_G is independent of Δt . This establishes a stable and well-conditioned characterization of model-misspecification error in the continuous-time limit, in sharp contrast to existing discrete-time LSTD analyses. Finally, we emphasize that the improved dependence on Δt does not stem from the PhiBE framework itself, but rather from the smoothness of the discrete-time transition dynamics induced by the SDE. We expect that a comparable model-misspecification bound can be derived for the Bellman equation when the discrete-time transitions arise from an underlying SDE, and we leave this direction for future work.

Remark 7. *The Galerkin error remains bounded even when $\|\nabla \log \rho\|_{L^\infty}$ is unbounded. However, since the sample-complexity analysis in this paper assumes boundedness of $\|\nabla \log \rho\|_{L^\infty}$, we move the Galerkin error theorem under unbounded $\|\nabla \log \rho\|_{L^\infty}$ assumption to Section 6.6 to maintain internal consistency. The corresponding result is stated in Theorem 6.7.*

4.2 Model-free Galerkin method for PhiBE

When only discrete-time trajectory data is available, we first develop an unbiased estimate $\bar{\mu}_i, \bar{\Sigma}_i$ for $\hat{\mu}_i, \hat{\Sigma}_i$ from the trajectory data,

$$\begin{aligned}\bar{\mu}_i(s_{j\Delta t}^l) &= \frac{1}{\Delta t} \sum_{k=1}^i a_k^{(i)}(s_{(j+k)\Delta t}^l - s_{j\Delta t}^l), \\ \bar{\Sigma}_i(s_{j\Delta t}^l) &= \frac{1}{\Delta t} \sum_{k=1}^i a_k^{(i)}(s_{(j+k)\Delta t}^l - s_{j\Delta t}^l)(s_{(j+k)\Delta t}^l - s_{j\Delta t}^l)^\top,\end{aligned}\tag{25}$$

with $a^{(i)}$ defined in (13). Then, using the above unbiased estimate, one can approximate the matrix \hat{A} and the vector b by

$$\begin{aligned}\bar{A}_i &= \sum_{l=1}^I \sum_{j=0}^{m-i} \Phi(s_{j\Delta t}^l) \left[\beta \Phi(s_{j\Delta t}^l) - \mathcal{L}_{\bar{\mu}_i(s_{j\Delta t}^l), \bar{\Sigma}_i(s_{j\Delta t}^l)} \Phi(s_{j\Delta t}^l) \right]^\top, \\ \bar{b}_i &= \sum_{l=1}^I \sum_{j=0}^{m-i} r(s_{j\Delta t}^l) \Phi(s_{j\Delta t}^l).\end{aligned}$$

By solving the linear system $\bar{A}_i \theta = \bar{b}_i$, one obtains the approximated value function $\bar{V}(s) = \Phi(s)^\top \theta$ in terms of the finite bases. Note that our algorithm can also be applied to stochastic rewards or even unknown rewards as only observation of rewards is required at discrete time. We summarize the model-free Galerkin method for deterministic and stochastic dynamics in Algorithm 1 and Algorithm 2, respectively.

Remark 8 (Comparison to the LSTD Algorithm). *Algorithms 1, 2 serves as a continuous-time counterpart to LSTD [7] by replacing the discrete-time Bellman equation with the PhiBE equation. Both our algorithms and LSTD are model-free and employ linear basis functions. In addition to that, both methods can be derived by applying the Galerkin method, followed by a stochastic approximation of the resulting system [51].*

This connection, however, highlights a key advantage of our formulation. Owing to the structural similarity between the PhiBE (11), (17) and the discrete-time Bellman equation, both depend only on the current and next states, most existing RL algorithms developed for solving Bellman equations can be directly applied to PhiBE. Moreover, as shown in Section 3, our method enjoys a smaller discretization error, allowing one to achieve a significantly improved approximation accuracy for free with a slightly modification of the RL algorithm.

Algorithm 1 Model-free Galerkin method for i -th order PhiBE in deterministic dynamics

Given: discrete time step Δt , discount coefficient β , discrete-time trajectory data $\{(s_{j\Delta t}^l, r_{j\Delta t}^l)_{j=0}^m\}_{l=1}^I$ generated from the underlying dynamics, and a finite bases $\Phi(s) = (\phi_1(s), \dots, \phi_p(s))^\top$.

1: Calculate \bar{A}_i :

$$\bar{A}_i = \sum_{l=1}^I \sum_{j=0}^{m-i} \Phi(s_{j\Delta t}^l) [\beta \Phi(s_{j\Delta t}^l) - \bar{\mu}_i(s_{j\Delta t}^l) \cdot \nabla \Phi(s_{j\Delta t}^l)]^\top,$$

where $\bar{\mu}_i(s_{j\Delta t}^l)$ is defined in (25).

2: Calculate \bar{b}_i :

$$\bar{b}_i = \sum_{l=1}^I \sum_{j=0}^{m-i} r_{j\Delta t}^l \Phi(s_{j\Delta t}^l).$$

3: Calculate θ :

$$\theta = \bar{A}_i^{-1} \bar{b}_i.$$

4: Output $\bar{V}(s) = \theta^\top \Phi(s)$.

Algorithm 2 Model-free Galerkin method for i -th order PhiBE in stochastic dynamics

Given: discrete time step Δt , discount coefficient β , discrete-time trajectory data $\{(s_{j\Delta t}^l, r_{j\Delta t}^l)_{j=0}^m\}_{l=1}^I$ generated from the underlying dynamics, and a finite bases $\Phi(s) = (\phi_1(s), \dots, \phi_p(s))^\top$.

1: Calculate \bar{A}_i :

$$\bar{A}_i = \sum_{l=1}^I \sum_{j=0}^{m-i} \Phi(s_{j\Delta t}^l) \left[\beta \Phi(s_{j\Delta t}^l) - \bar{\mu}_i(s_{j\Delta t}^l) \cdot \nabla \Phi(s_{j\Delta t}^l) - \frac{1}{2} \bar{\Sigma}_i(s_{j\Delta t}^l) : \nabla^2 \Phi(s_{j\Delta t}^l) \right]^\top,$$

where $\bar{\mu}_i(s_{j\Delta t}^l), \bar{\Sigma}_i(s_{j\Delta t}^l)$ are defined in (25).

2: Calculate \bar{b}_i :

$$\bar{b}_i = \sum_{l=1}^I \sum_{j=0}^{m-i} r_{j\Delta t}^l \Phi(s_{j\Delta t}^l).$$

3: Calculate θ :

$$\theta = \bar{A}_i^{-1} \bar{b}_i.$$

4: Output $\bar{V}(s) = \theta^\top \Phi(s)$.

4.3 Sample Complexity of the Model-Free Algorithm for First-Order PhiBE

We now establish the sample complexity of the model-free algorithm for solving the first-order PhiBE. A sample complexity analysis for higher-order PhiBE is deferred to future work. We assume that the data consist of n independent short trajectories $\{s_i, s'_i\}_{i=1}^n$. Each trajectory provides a single transition pair: an initial state $s_i \sim \rho(s)$ and its one-step successor $s'_i \sim \rho(s', \Delta t \mid s_i)$. Here the initial density $\rho(s)$ is the weight we defined in (19), and the discrete-time transition $\rho(s', \Delta t \mid s)$ is driven by the underlying SDE (2). The model-free algorithm approximates the value function by $\hat{V}_n(s) = \Phi(s)^\top \theta_n$, where $\theta_n \in \mathbb{R}^p$ is obtained by solving the empirical linear system

$$A_n \theta_n = b_n, \quad A_n = \frac{1}{n} \sum_{i=1}^n \Phi(s_i) \left[\beta \Phi(s_i) - \mathcal{L}_{\bar{\mu}_1^i, \bar{\Sigma}_1^i} \Phi(s_i) \right]^\top, \quad b_n = \frac{1}{n} \sum_{i=1}^n r(s_i) \Phi(s_i), \quad (26)$$

where

$$\bar{\mu}_1^i = \frac{1}{\Delta t} (s'_i - s_i), \quad \bar{\Sigma}_1^i = \frac{1}{\Delta t} (s'_i - s_i)(s'_i - s_i)^\top.$$

This estimator targets the Galerkin solution $\hat{V}_1^G(s) = \Phi(s)^\top \theta$ of the first-order PhiBE defined in (24) when the discrete-time transition dynamics are known. Here θ solves

$$A\theta = b, \quad A = \int \Phi(s) \left[\beta \Phi(s) - \mathcal{L}_{\bar{\mu}_1, \bar{\Sigma}_1} \Phi(s) \right]^\top \rho(s) ds, \quad b = \int r(s) \Phi(s) \rho(s) ds. \quad (27)$$

The theorem below establishes both consistency and finite-sample guarantees.

Theorem 4.2 (Sample Complexity). *Assume that $\|\nabla^k \Phi\| \leq L_\Phi$ ρ -a.s. for $k = 0, 1, 2$, and the Gram matrix for the bases satisfies*

$$G_\Phi = \int \Phi(s) \Phi(s)^\top \rho(s) ds \succeq \lambda_\Phi I. \quad (28)$$

Suppose further that $\Delta t \leq \eta_{\mu, \Sigma, \beta}$ (same $\eta_{\mu, \Sigma, \beta}$ in Theorem 4.1). Then, for any sufficiently small $\epsilon > 0$, if

$$n \gtrsim \frac{\log(2p/\delta) R^2 L_\Phi^8 \sigma_{\max}^2}{\beta^4 \epsilon^2 \Delta t \lambda_\Phi^4}$$

where $R = \|r\|_{L^\infty}$ and $\sigma_{\max} = \|\sigma\|_{L^\infty}$, we have, with probability at least $1 - \delta$,

$$\|\hat{V}_n - \hat{V}_1^G\|_{L^\infty} \leq \epsilon.$$

Equivalently, if $n \gtrsim \frac{L_\Phi^4 \log(2p/\delta) \sigma_{\max}^2 \lambda_\Phi^{-2}}{\beta^2 \Delta t}$, then with probability $1 - \delta$,

$$\left\| V_n - \hat{V}_1^G \right\|_{L^\infty} \leq \left(L_\Phi^4 R \sigma_{\max} \lambda_\Phi^{-2} \sqrt{\log(2p/\delta)} \right) \frac{1}{\beta^2 \sqrt{n \Delta t}}$$

The proof of the above Theorem is given in Section 6.7. Several remarks are in order. The first part of Theorem 4.2 provides an explicit sample complexity bound guaranteeing an ϵ -accurate approximation to the Galerkin solution. The second part of the Theorem provides an

finite-sample bound to the Galerkin solution, which scale as $O(\beta^{-2}\Delta t^{-1/2}n^{-1/2})$. In classical discrete-time RL analyses (e.g., Theorem 1 of [30]), the error scales as $O((1-\gamma)^{-2}n^{-1/2})$. Note that their result is stated in the form $O((1-\gamma)^{-1}V_{\max}n^{-1/2})$. Since $V_{\max} = R(1-\gamma)^{-1}$, the resulting error bound in fact scales as $(1-\gamma)^{-2}$ rather than $(1-\gamma)^{-1}$. Substituting $\gamma = e^{-\beta\Delta t}$ leads to an order of $O(\beta^{-2}\Delta t^{-2}n^{-1/2})$. By contrast, our analysis exploits the smoothness of the underlying SDE and the uniform ellipticity of the infinitesimal generator $\mathcal{L}_{\hat{\mu}_1, \hat{\Sigma}_1}$, improving the dependence on the time discretization from Δt^{-2} to $\Delta t^{-1/2}$.

Corollary 1 (Overall Error Bound). *Under the same assumption in Theorem 4.2, then with probability at least $1 - \delta$,*

$$\|V_n - V(s)\|_{\rho} \lesssim \frac{C_{r,\mu,\Sigma}}{\beta^2}\Delta t + \frac{C_G}{\beta} \inf_{V^P=\theta^\top\Phi} \|\hat{V}_i - V^P\|_{H_{\rho,\infty}^1} + \frac{C_{r,\Sigma,\Phi}}{\beta^2\sqrt{n\Delta t}}$$

where $C_{r,\Sigma,\Phi} = L_{\Phi}^4 R\sigma_{\max}\lambda_{\Phi}^{-2}\sqrt{\log(2p/\delta)}$, and $C_{r,\mu,\Sigma}, C_G$ are the same constants as in Theorems 3.5 and 4.1.

Several remarks are in order. The total error consists of three components: a discretization error, a model approximation error, and a finite-sample error. Among these terms, only the model error is independent of the time step Δt . The discretization and sample errors exhibits opposite dependencies on the data collection frequency Δt , i.e.,

$$\|\hat{V}_n - V\| = O\left(\frac{\Delta t}{\beta^2} + \frac{1}{\beta^2\sqrt{n\Delta t}}\right).$$

This bound highlights a fundamental trade-off inherent in continuous-time PE. Decreasing Δt reduces the discretization bias but increases the variance of the estimator, thereby requiring a larger sample size to maintain the same level of accuracy. As a result, excessively frequent sampling does not necessarily improve overall performance.

This phenomenon is not specific to the PhiBE framework but is intrinsic to continuous-time reinforcement learning. As illustrated in Figure 6 of our numerical experiments, the model-free RL algorithm (LSTD) exhibit a similar trade-off. Similar behavior was observed in [64], who studied Monte Carlo sampling algorithm for linear-quadratic (LQ) policy evaluation. Their theoretical analysis is restricted to the LQ setting, with nonlinear dynamics examined only through numerical experiments. In contrast, our analysis applies to general controlled diffusion processes and provides explicit non-asymptotic error bounds. Moreover, their approach evaluates the value function only at discrete states and does not involve function approximation, whereas our algorithm produces a global approximation of the value function via function approximation, leading to a substantially more involved analysis. Finally, our results explicitly characterize the dependence on the discount parameter β , which is not addressed in [64].

5 Numerical Experiments

All MATLAB code used to generate the numerical results is available.¹

¹The repository is available at <https://github.com/yuhuazhumath/phibe-matlab>.

5.1 Deterministic dynamics

We first consider deterministic dynamics, where the state space is defined as $\mathbb{S} = [-\pi, \pi]$. We consider two kinds of underlying dynamics, one is linear,

$$\frac{d}{dt}s_t = \lambda s_t, \quad (29)$$

and the other is nonlinear,

$$\frac{d}{dt}s_t = \lambda \sin^2(s_t). \quad (30)$$

The reward is set to be $r(s) = \beta \cos(ks)^3 - \lambda s(-3k \cos^3(ks) \sin(ks))$ for the linear case and $r(s) = \beta \cos^3(ks) - \lambda \sin^2(s)(-3k \cos^2(ks) \sin(ks))$ for the nonlinear case, where the value function can be exactly obtained, $V(s) = \cos^3(ks)$ in both cases. We use periodic bases $\{\phi_k(s_1)\}_{k=1}^{2M+1} = \frac{1}{\sqrt{\pi}}\{\frac{1}{\sqrt{2}}, \cos(ms_1), \sin(ms_1)\}_{m=1}^M$ with M large enough so that the solution can be accurately represented by these finite bases ($M = 4$ for the low frequency value function and $M = 30$ for the high frequency value function).

For the linear dynamics, the discrete-time transition dynamics are

$$p_{\Delta t}(s) = e^{\lambda \Delta t} s.$$

Hence, one can express the BE as

$$\tilde{V}(s) = r(s)\Delta t + e^{-\beta \Delta t} \tilde{V}(e^{\lambda \Delta t} s), \quad (31)$$

and i -th order PhiBE as

$$\beta \hat{V}_i(s) = r(s) + \frac{1}{\Delta t} \left[\sum_{k=1}^i a_k^{(i)} (e^{\lambda k \Delta t} s - s) \right] \cdot \nabla \hat{V}_i(s), \quad (32)$$

respectively for $a^{(i)}$ defined in (13). For the nonlinear dynamics, we approximate $p_{\Delta t}(s)$ and generate the trajectory data numerically,

$$s_{t+\delta} = s_t + \delta \lambda \sin^2(s_t)$$

with $\delta = 10^{-4}$ sufficiently small.

The trajectory data are generated from J different initial values $s_0 \sim \text{Unif}[-\pi, \pi]$, and each trajectory has $m = 4$ data points, $\{s_0, \dots, s_{(m-1)\Delta t}\}$. Algorithm 1 is used to solve for the PhiBE, and LSTD is used to solve for BE. LSTD is similar to Algorithm 1 except that one uses \tilde{A} derived from the BE (4),

$$\tilde{A} = \sum_{l=1}^I \sum_{j=0}^{m-2} \Phi(s_{j\Delta t}^l) [\Phi(s_{j\Delta t}^l) - e^{-\beta \Delta t} \Phi(s_{(j+1)\Delta t}^l)]^\top \quad (33)$$

instead of \bar{A}_i .

In Figure 1, the data are generated from the linear dynamics (29) with $\lambda = 0.05$ and collected at different Δt . For the low-frequency value function (Figure 1/(a), (c)), we use 40

data points with $J = 10, m = 4$, whereas for the high-frequency value function (Figure 1/(b)), we use 400 data points with $J = 100, m = 4$. We compare the solution to the second-order PhiBE with the solution to BE (when the discrete-time transition dynamics are known), and the performance of LSTD with the proposed Algorithm 1 (when only trajectory data are available) with different data collection interval Δt , discount coefficient β and oscillation of reward k . Note that the exact solution to BE is computed as $\tilde{V}(s) = \sum_{i=0}^I r(e^{\lambda \Delta t i} s)$ with $I = 500/\Delta t$ large enough, and the exact solution to PhiBE is calculated by applying the Galerkin method to (32).

In Figure 3, the data are generated from the nonlinear dynamics (30) and collected at different Δt . For the low-frequency value function (Figure 3/(a), (c)), we use 80 data points with $J = 20, m = 4$, whereas for the high-frequency value function (Figure 3/(b)), we use 400 data points with $J = 100, m = 4$. We compare the solutions to the first-order and second-order PhiBE with the solution to the BE (when the discrete-time transition dynamics are known), and the performance of LSTD with the proposed Algorithm 1 (when only trajectory data are available) with different $\Delta t, \beta, k, \lambda$.

In Figure 4, the distances of the solution from PhiBE, BE to the true value function are plotted as $\Delta t \rightarrow 0$; the distances of the approximated solution by Algorithm 1 and LSTD to the true value function are plotted as the amount of data increases. We set $J = [10, 10^2, 10^3, 10^3]$ and $m = 4$ for the data size. Here, the distance is measured using the L^2 norm

$$D(V, \hat{V}) = \sqrt{\int_{-\pi}^{\pi} (V(s) - \hat{V}(s))^2 ds}. \quad (34)$$

In Figures 1 and 3, when the discrete-time transition dynamics are known, PhiBE solution is much closer to the true value function compared to the BE solution in all the experiments. Especially, the second-order PhiBE solution is almost identical to the exact value function. Additionally, when only trajectory data is available, one can approximate the solutions to PhiBE very well with only 40 or 400 data points. Particularly, when $\Delta t = 5$ is large, the solution to PhiBE still approximates the true solution very well, which indicates that one can collect data sparsely based on PhiBE. Moreover, the solution to PhiBE is not sensitive to the oscillation of the reward function, which implies that one has more flexibility in designing the reward function in the RL problem. Besides, unlike BE, the error increases when β is too small or too large, while the error for PhiBE decays as β increases. Furthermore, it's noteworthy that in Figure 3/(b) and (c), for relatively large changes in the dynamics indicated by $\|\nabla \mu\| \leq \lambda = 5$ and 2, respectively, PhiBE still provides a good approximation.

In Figure 4/(a) and (b), one can observe that the solution for BE approximates the true solution in the first order, while the solution for i -th order PhiBE approximates the true solution in i -th order. In Figure 4/(c) and (d), one can see that as the amount of data increases, the error from the LSTD algorithm stops decreasing when it reaches 10^{-1} . This is because the error between BE and the true value function $\|\tilde{V} - V\| = O(\Delta t)$ dominates the data error. On the other hand, for higher-order PhiBE, as the amount of data increases, the performance of the algorithm improves, and the error can achieve $O(\Delta t^i)$.

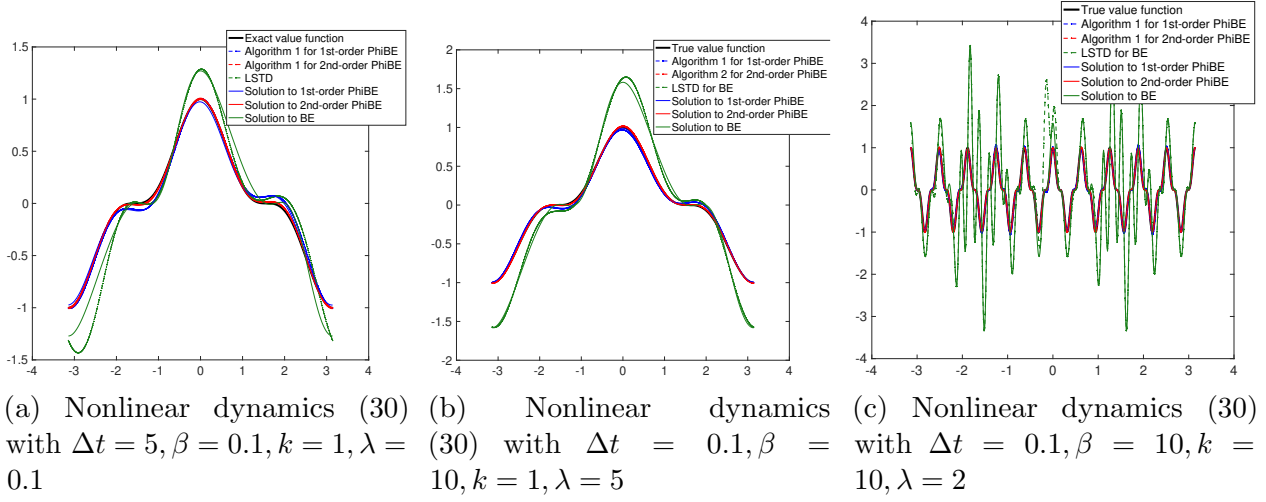


Figure 3: The PhiBE solution and the BE solution, when the discrete-time transition dynamics are given, are plotted in solid lines. The approximated PhiBE solution based on Algorithm 1 and the approximated BE solution based on LSTD, when discrete-time data are given, are plotted in dash lines. Both algorithms utilize the same data points.

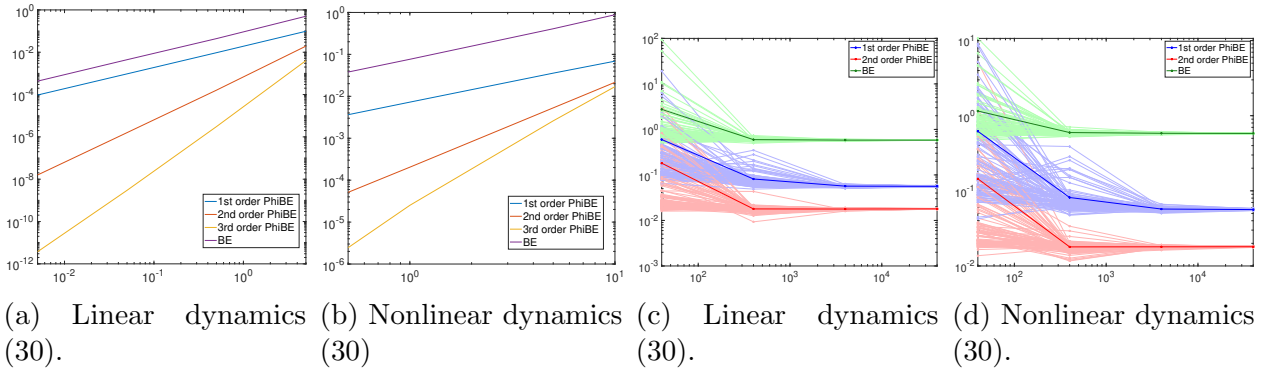


Figure 4: The L^2 error (34) of the PhiBE solutions and the BE solutions with decreasing Δt are plotted in the left two figures. The L^2 error (34) of the approximated PhiBE solutions and the approximated BE solutions with increasing amount of data collected every $\Delta t = 5$ unit of time are plotted in the right two figures. The solid lines are the average over 100 simulations for all different number of data. We set $\lambda = 0.05, \beta = 0.1, k = 1$ in both linear and nonlinear cases.

5.2 Stochastic dynamics

We consider the Ornstein–Uhlenbeck process,

$$ds(t) = \lambda s dt + \sigma dB_t, \quad (35)$$

with $\lambda = 0.05, \sigma = 1$. Here the reward is set to be $r(s) = \beta \cos^3(ks) - \lambda s(-3k \cos^2(ks) \sin(ks)) - \frac{1}{2}\sigma^2(6k^2 \cos(s) \sin^2(ks) - 3k^2 \cos^3(ks))$, where the value function can be exactly obtained, $V(s) = \cos^3(ks)$. For OU process, since the conditional density function for s_t given $s_0 = s$ follows the normal distribution with expectation $se^{\lambda t}$, variance $\frac{\sigma^2}{2\lambda}(e^{2\lambda t} - 1)$. Both PhiBE and BE have explicit forms. One can express PhiBE as,

$$\begin{aligned} \beta \hat{V}_i(s) = & r(s) + \frac{1}{\Delta t} \sum_{k=1}^i a_k^{(i)} (e^{\lambda k \Delta t} - 1) s \nabla \hat{V}(s) \\ & + \frac{1}{2\Delta t} \sum_{k=1}^i a_k^{(i)} \left[\frac{\sigma^2}{2\lambda} (e^{2\lambda k \Delta t} - 1) + (e^{\lambda k \Delta t} - 1)^2 s^2 \right] \Delta \hat{V}(s); \end{aligned} \quad (36)$$

and BE as,

$$\begin{aligned} \tilde{V}(s) = & r(s)\Delta t + e^{-\beta\Delta t} \mathbb{E} \left[\tilde{V}(s_{t+1}) | s_t = s \right] \\ = & r(s)\Delta t + e^{-\beta\Delta t} \int_{\mathbb{S}} \tilde{V}(s') \rho_{\Delta t}(s', s) ds', \end{aligned} \quad (37)$$

where

$$\rho_{\Delta t}(s', s) = \frac{1}{\sqrt{2\pi\hat{\sigma}}} \exp \left(-\frac{1}{2\hat{\sigma}^2} (s' - se^{\lambda\Delta t})^2 \right), \quad \text{with } \hat{\sigma} = \frac{\sigma^2}{2\lambda} (e^{2\lambda\Delta t} - 1).$$

In Figure 5, we compare the exact solution and approximated solution to PhiBE and BE, respectively, for different $\Delta t, \beta, k$. For the approximated solution, we set the data size $m = 4$, and $J = 10^4$ for Figure 5/(a), $J = 10^5$ for Figure 5/(b), $J = 100$ for Figure 5/(c). In Figure 6/(a), the decay of the error as $\Delta t \rightarrow 0$ for the exact solutions to PhiBE and BE are plotted. In Figure 6/(b), the decay of the approximated solution to PhiBE and BE based on Algorithm 2 and LSTD are plotted with an increasing amount of data. We set $J = [10^3, 10^4, 10^5, 10^6, 10^7]$ and $m = 4$ for the data size. In Figure 6/(c), the error of the approximated solution to PhiBE and BE based on Algorithm 2 and LSTD are plotted with a decreasing Δt . We set $J = 10^6$ and $m = 4$ for the data size.

We observe similar performance in the stochastic dynamics as in the deterministic dynamics, as shown in Figures 5 and 6. In Figure 6, the variance of the higher order PhiBE is larger than that of the first-order PhiBE because it involves more future steps. However, note that the error is plotted on a logarithmic scale. Therefore, when the error is smaller, although the variance appears to have the same width on the plot, it is actually much smaller. Particularly, when the amount of the data exceeds 10^6 , the variance is smaller than 10^{-1} . Figure 6/(c) illustrates a non-monotone dependence of the error on the time discretization Δt when the total data budget is fixed. For the data-driven RL algorithm and the first-order PhiBE method, the error initially decreases as Δt is reduced from 1 to 0.1, reflecting a regime in which discretization error dominates. As Δt is further reduced from 0.1 to 0.01, the error

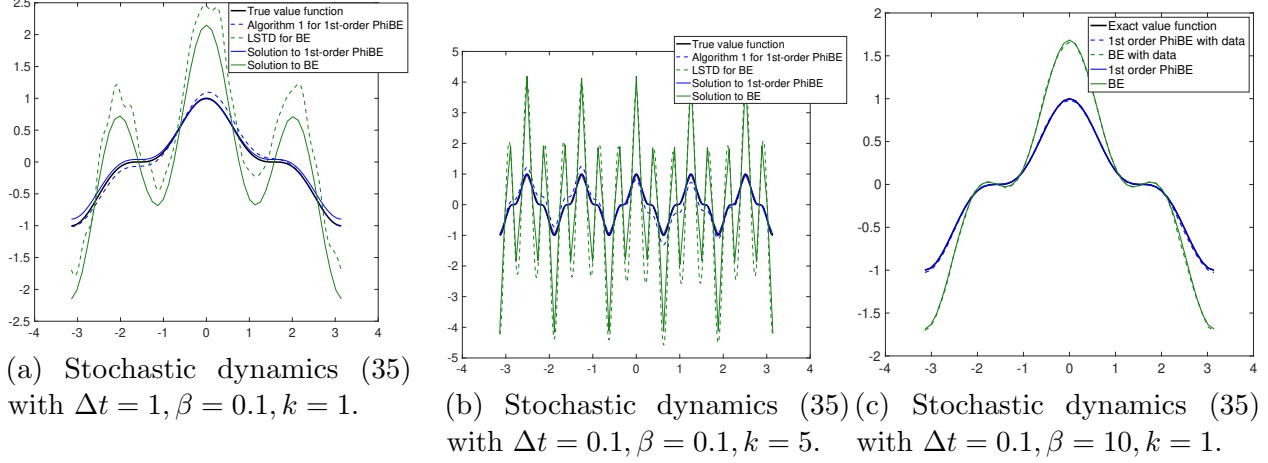


Figure 5: The PhiBE solution and the BE solution, when the discrete-time transition dynamics are given, are plotted in solid lines. The approximated PhiBE solution based on Algorithm 2 and the approximated BE solution based on LSTD, when discrete-time data are given, are plotted in dash lines. Both algorithms utilize the same data points.

increases, indicating that finite-sample error becomes dominant. The second-order PhiBE method, which exhibits higher variance, enters the variance-dominated regime earlier: its error already increases as Δt decreases from 1 to 0.1.

5.3 Stabilization problem

In the previous section, we compared the PhiBE framework with the standard RL formulation and validated our theoretical results using a synthetic example. We now examine their performance on a real control problem.

Problem setup. We consider the continuous-time PE problem

$$V(s) = \mathbb{E} \left[\int_0^\infty e^{-\beta t} (qs_t^2 + ru(s_t)^2) | s_0 = s \right] \quad (38)$$

$$dS_t = (-\kappa s_t^3 + (\alpha s_t - bu(s_t)) dt + \sigma dW_t,$$

with parameters $\kappa > 0$, $\alpha \in \mathbb{R}$, $b > 0$, and $\sigma > 0$. We focus on the linear feedback policy

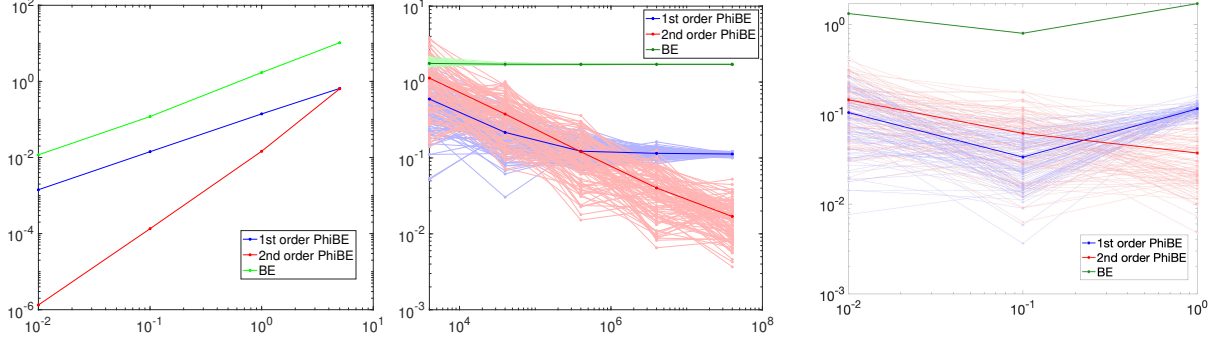
$$u(s) = Ks.$$

Under this policy, the true value function V solves the elliptic equation

$$\beta V(s) - \mathcal{L}V(s) = r(s), \quad \mathcal{L}f(s) = \left(-\kappa s^3 + (\alpha - bK)s \right) f'(s) + \frac{\sigma^2}{2} f''(s), \quad (39)$$

where $r(s) = qs^2 + rK^2s^2$.

This model represents a standard stabilization problem, where the quadratic reward balances state deviation and control effort, and the linear policy $u(s) = -Ks$ acts as a



(a) Discretization error w.r.t. (b) Approximation error w.r.t. (c) Approximation error w.r.t. data data collection frequency Δt . the amount of data. collection frequency Δt .

Figure 6: The L^2 error (34) of the PhiBE and BE solutions as a function of the time discretization Δt is shown in (a). Plot (b) reports the L^2 error of the data-driven approximations as the amount of data increases, with samples collected every $\Delta t = 1$ unit of time. Plot (c) shows the L^2 error of the data-driven approximations with a fixed budget of 4×10^6 data points as Δt decreases. Solid lines denote averages over 100 independent simulations. In all plots, we set $\beta = 0.1$ and $k = 1$.

proportional controller. When $\kappa = 0$, the dynamics reduce to a linear system, corresponding to the classical continuous-time LQR formulation widely used in robotics, aerospace, and process control. In this regime, the value function admits a closed-form solution, providing a baseline against which the approximation accuracy of RL and PhiBE can be directly evaluated. When $\kappa \neq 0$, the cubic drift introduces strong nonlinear restoring forces, modeling phenomena such as soft-spring mechanical systems or the stabilization of an inverted pendulum near its upright position.

5.3.1 Linear dynamics

In the linear-dynamics setting, the true value function admits a closed-form solution,

$$V(s) = a_1 s^2 + a_2, \quad a_1 = \frac{R}{\beta - 2\lambda}, \quad a_2 = \frac{\sigma^2}{\beta} a_1, \quad (40)$$

where $R = q + rK^2$ and $\lambda = \alpha - bK$. Moreover, for this linear system, the Bellman equation (BE) and PhiBE both admit exact analytical solutions. For the discrete-time BE, we have

$$\text{BE} : \tilde{V}(s) = Rs^2 \Delta t + \gamma \int V(s') \rho(s'|s) ds', \quad R = q + rK^2, \quad \gamma = e^{-\beta \Delta t},$$

where

$$\rho(s'|s) \sim \mathcal{N}(e^{\lambda \Delta t} s, \hat{\sigma}^2 \Delta t), \quad \hat{\sigma}^2 = \frac{\sigma^2}{2\lambda \Delta t} (e^{2\lambda \Delta t} - 1).$$

This yields the quadratic solution for BE,

$$\tilde{V}(s) = a_1^R s^2 + a_0^R, \quad a_1^R = \frac{R \Delta t}{1 - \gamma e^{2\lambda \Delta t}}, \quad a_0^R = \frac{\gamma \Delta t}{1 - \gamma} \hat{\sigma}^2 a_1^R. \quad (41)$$

Similarly, the PhiBE equation can be evaluated exactly:

$$\begin{aligned} \text{PhiBE : } \hat{V}(s) &= R s^2 + \hat{V}'(s) \int \frac{s' - s}{\Delta t} \rho(s'|s) ds' + \frac{1}{2} \hat{V}''(s) \int \frac{(s' - s)^2}{\Delta t} \rho(s'|s) ds' \\ &= R s^2 + \hat{\lambda} s \hat{V}'(s) + \frac{\hat{\sigma}^2 + \hat{\lambda}^2 s^2 \Delta t}{2} \hat{V}''(s), \quad \hat{\lambda} = \frac{e^{\lambda \Delta t} - 1}{\Delta t}. \end{aligned}$$

This yields another quadratic solution,

$$\hat{V}(s) = a_1^P s^2 + a_0^P, \quad a_1^P = \frac{R}{\beta - 2\hat{\lambda} - \eta}, \quad a_0^P = \frac{\hat{\sigma}^2}{\beta} a_1^P. \quad (42)$$

where $\eta = \frac{1}{\Delta t}(e^{2\lambda \Delta t} - 2e^{\lambda \Delta t} + 1)$.

Figure 7 compares the analytical BE and PhiBE solutions, \tilde{V} and \hat{V} , with the true value function $V(s)$ across four test cases. Throughout all experiments we set $q = 1$, $r = 0.1$, and $K = 2$. The four configurations are:

- case 1 Baseline: $\alpha = b = \frac{1}{4}, \sigma = 0.5, \beta = 1, \Delta t = 0.1$.
 - case 2 More frequent observations (smaller Δt): $\alpha = b = \frac{1}{4}, \sigma = 0.5, \beta = 1, \Delta t = 0.01$.
 - case 3 Quicker dynamics: $\alpha = b = 1, \sigma = 1, \beta = 1, \Delta t = 0.1$.
 - case 4 Less discounted (smaller β): $\alpha = b = \frac{1}{4}, \sigma = 0.5, \beta = 0.1, \Delta t = 0.1$.
- (43)

From Figure 7, we observe that reducing Δt by one order decreases the approximation error of both formulations by approximately one order, consistent with the theoretical convergence rates. Moreover, as the system dynamics become faster or the discount factor β becomes smaller, the advantage of PhiBE over BE diminishes, although PhiBE still performs better overall. This observation aligns with our theoretical analysis: (1) PhiBE achieves greater improvement when the dynamics evolve more slowly, and (2) the approximation error of PhiBE scales as $O(1/\beta^2)$, whereas that of BE scales as $O(1/\beta)$ when β is small.

We next evaluate the data-driven algorithms. To solve the PhiBE formulation, we use the first-order method in Algorithm 2; for the BE formulation, we apply LSTD as in (33). We generate $\{s_i\}_{i=1}^n$ from $[-1, 1]$ on the uniform mesh, and $s'_i \sim \mathcal{N}(e^{\lambda \Delta t} s_i, \hat{\sigma}^2 \Delta t)$ for all $1 \leq i \leq n$, consistent with the linear system dynamics. The mean and variance of the approximation error, computed over 100 Monte Carlo repetitions for all four cases, are shown in Figure 8.

Figure 8 demonstrates that the data-driven estimators concentrate around the corresponding analytic solutions in Figure 7 when the sample size is sufficiently large. However, the variability differs across scenarios. To examine this more closely, Table 1 reports the mean and variance of the approximation error. Two observations stand out from Table 1. First, across all test cases, PhiBE consistently attains smaller mean error and smaller variance compared with BE given the same amount of data. Second, for a fixed sample size, the variance increases for both methods as Δt decreases, β decreases, or the dynamics become faster.

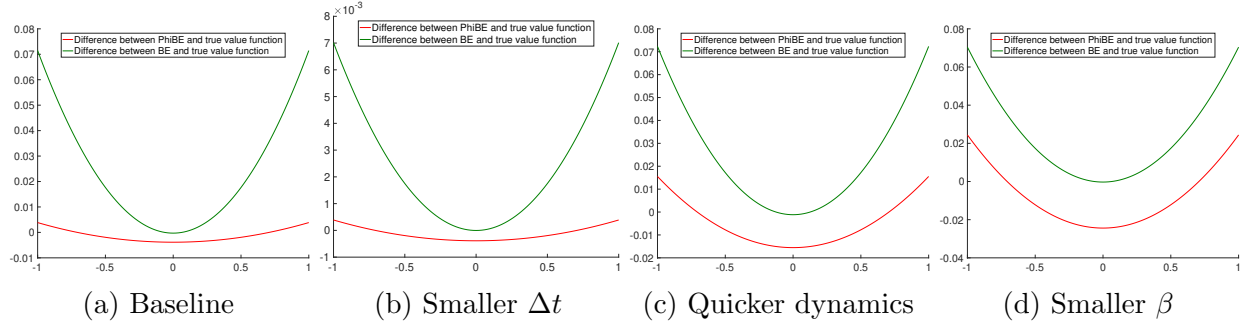


Figure 7: Stabilization control under linear dynamics. The error $\hat{V}(s) - V(s)$ from the PhiBE solution (red) and $\tilde{V}(s) - V(s)$ from the BE solution (green) are plotted, where $V(s)$, $\hat{V}(s)$, and $\tilde{V}(s)$ are given in (40), (42), and (41). Each subplot corresponds to one scenario in (43).

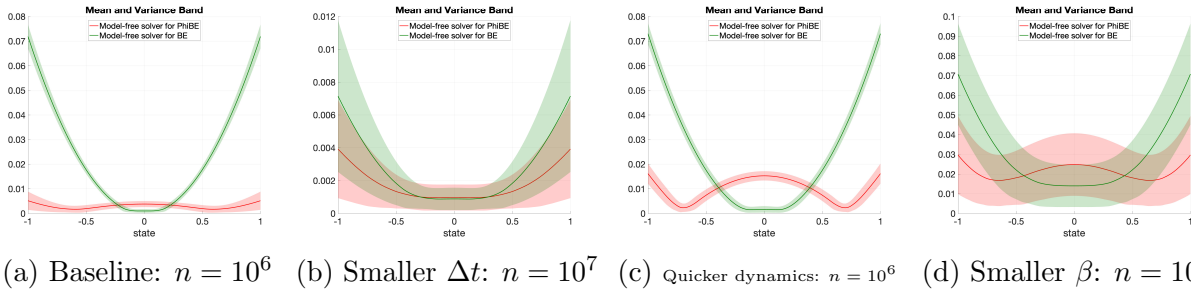


Figure 8: Stabilization control under linear dynamics. The mean and variance of the approximation error $|\hat{V}(s) - V(s)|$ from the PhiBE algorithm (Algorithm 2) are shown in red, and those of $\tilde{V}(s) - V(s)$ from the LSTD method (33) are shown in green. Each subplot corresponds to one scenario in (43), illustrating how the error behaves under different values of Δt , β , and the system dynamics.

	mean (PhiBE)	mean (BE)	variance (PhiBE)	variance (BE)
Baseline ($n = 10^6$)	4.76×10^{-3}	4.54×10^{-2}	2.7×10^{-6}	1.02×10^{-5}
Smaller Δt ($n = 10^6$)	9.64×10^{-3}	1.04×10^{-2}	3.84×10^{-5}	4.3×10^{-5}
Smaller Δt ($n = 10^7$)	2.91×10^{-3}	4.7×10^{-3}	3.6×10^{-6}	8.1×10^{-6}
Quick dynamics ($n = 10^6$)	3.45×10^{-2}	5.5×10^{-2}	3.87×10^{-4}	8.07×10^{-4}
Smaller β ($n = 10^6$)	7.48×10^{-2}	7.81×10^{-2}	2.11×10^{-3}	2.93×10^{-3}
Smaller β ($n = 10^7$)	3.41×10^{-2}	4.97×10^{-2}	1.97×10^{-4}	3.89×10^{-4}

Table 1: Comparison of the approximation error for the model-free PhiBE solver and the LSTD method under linear dynamics.

5.3.2 Nonlinear Dynamics

In this section, we demonstrate that our approach also applies to nonlinear dynamics. In this setting, the true value function is no longer available in closed form, so we approximate the ground-truth solution using a high-accuracy Galerkin method with sufficiently many polynomial basis functions. The data collection procedure follows the linear case, except that we generate each s'_i by simulating the SDE using the Euler-Maruyama scheme with step size $\delta_t = 10^{-3}$.

We consider the following four cases, setting $q = 1$, $r = 0.1$, $K = 2$, and $n = 10^6$ for all experiments:

case 1 Baseline: $\alpha = b = \kappa = 0.1, \sigma = 0.05, \beta = 1, \Delta t = 0.1$;

case 2 More frequent observations (smaller Δt): $\alpha = b = \kappa = 0.1, \sigma = 0.05, \beta = 1, \Delta t = 0.01$;

case 3 Quicker dynamics: $\alpha = b = \kappa = 1/2, \sigma = 1/4, \beta = 1, \Delta t = 0.1$;

case 4 Less discounted (smaller β): $\alpha = b = \kappa = 0.1, \sigma = 0.05, \beta = 0.1, \Delta t = 0.1$.

(44)

The resulting approximation errors are shown in Figure 9. The qualitative behavior is similar to the linear-dynamics experiments: PhiBE exhibits smaller mean error and more stable performance across all cases.

One caveat appears in Case 3, where both methods exhibit a few significant outliers. These outliers inflate the empirical variance, especially for LSTD, which in one run produced an error nearly two orders of magnitude larger than the average. This behavior is sensitive to the random sample, and a systematic analysis of such instability phenomena is left for future work.

5.4 High-Dimensional Case

We next evaluate the algorithms on a 10-dimensional linear-quadratic PE problem:

$$V(s) = \mathbb{E} \left[\int_0^\infty e^{-\beta t} (s_t^\top Q s_t) dt \mid s_0 = s \right]$$

$$ds_t = A s_t dt + \sigma dW_t,$$

where $Q \in \mathbb{R}^{10 \times 10}$ is constructed to have eigenvalues $(1, \dots, 10)$ by generating a random orthonormal matrix O and setting $Q = O^\top \text{diag}(1, \dots, 10) O$. The drift matrix $A \in \mathbb{R}^{10 \times 10}$ is

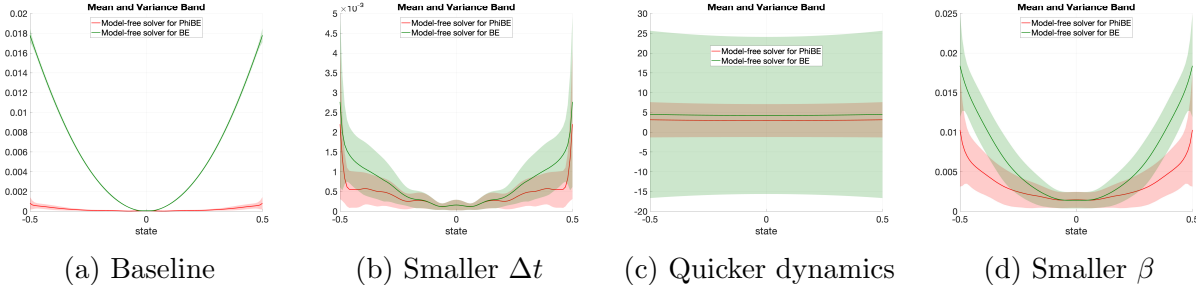


Figure 9: Stabilization control under nonlinear dynamics. The mean and variance of the approximation error $|\hat{V}(s) - V(s)|$ from the PhiBE algorithm (Algorithm 2) are shown in red, and those of $\tilde{V}(s) - V(s)$ from the LSTD method (33) are shown in green. Each subplot corresponds to one scenario in (44), illustrating how the error behaves under different values of Δt , β , and the system dynamics.

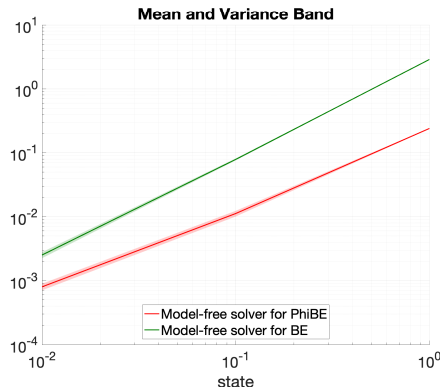


Figure 10: Stabilization control under linear dynamics with high-dimensional state space $s \in \mathbb{R}^{10}$. The mean and variance of the approximation error $\left\| \hat{V}(s) - V(s) \right\|_{\rho}$ from the PhiBE algorithm (Algorithm 2) are shown in red, and those of $\left\| \tilde{V}(s) - V(s) \right\|_{\rho}$ from the LSTD method (33) are shown in green.

generated analogously with eigenvalues $-(1, \dots, 10) \times 0.1$. The diffusion matrix $\Sigma \in \mathbb{R}^{10 \times 10}$ is diagonal matrix with all diagonal entries equal to 0.3, and we set $\beta = 1$.

We use polynomial basis functions up to second order. The dataset consists of samples $(s_i, s'_i)_{i=1}^n$, where $s_i \sim \text{Unif}([-1, 1]^{10})$, and s'_i is obtained by simulating the SDE for one step of size Δt starting from s_i . Since achieving a smaller discretization error at smaller Δt requires more samples, we choose $n = 10^5, 10^6, 10^8$ for $\Delta t = 1, 0.1, 0.01$, respectively.

Figure 10 reports the results for LSTD and the model-free PhiBE algorithm. The findings closely parallel the one-dimensional case: both error curves decay approximately at first order in Δt , confirming that the approach scales effectively to higher dimensions and that the theoretical predictions remain valid in the high-dimensional setting.

6 Proofs

6.1 Proof of Theorem 3.1.

Let $\rho(s', t|s)$ be the probability density function of s_t that starts from $s_0 = s$, then it satisfies the following PDE

$$\partial_t \rho(s', t|s) = \nabla \cdot [\mu(s') \rho(s', t|s)] + \frac{1}{2} \sum_{i,j} \partial_{s_i} \partial_{s_j} [\Sigma_{ij}(s') \rho(s', t|s)]. \quad (45)$$

with initial data $\rho(s', 0|s) = \delta_s(s')$. Let $f(t, s) = e^{-\beta t} r(s)$, then

$$\begin{aligned} V(s) - \tilde{V}(s) &= \mathbb{E} \left[\sum_{i=0}^{\infty} \int_{\Delta ti}^{\Delta t(i+1)} f(t, s_t) - f(\Delta ti, s_{\Delta ti}) dt | s_0 = s \right] \\ &= \sum_{i=0}^{\infty} \int_{\Delta ti}^{\Delta t(i+1)} \left(\int_{\mathbb{S}} f(t, s') \rho(s', t|s) - f(\Delta ti, s') \rho(\Delta ti, s') ds' \right) dt. \end{aligned} \quad (46)$$

Since

$$\begin{aligned} & \int_{\mathbb{S}} f(t, s') \rho(s', t|s) - f(\Delta ti, s') \rho(\Delta ti, s') ds' \\ &= \int_{\mathbb{S}} f(t, s') (\rho(s', t|s) - \rho(s', \Delta ti|s)) + (f(t, s') - f(\Delta ti, s')) \rho(s', \Delta ti|s) ds' \\ &= \int_{\mathbb{S}} f(t, s') \partial_t \rho(s', \xi_1|s) (t - \Delta ti) + \partial_t f(\xi_2, s') (t - \Delta ti) \rho(s', \Delta ti|s) ds' \\ & \quad \text{where } \xi_1, \xi_2 \in (\Delta ti, \Delta t(i+1)) \\ &= \int_{\mathbb{S}} \mathcal{L}_{\mu, \Sigma} f(t, s'), \rho(s', \xi_1|s) (t - \Delta ti) ds' - \int_{\mathbb{S}} \beta e^{-\beta \xi_2} r(s') \rho(s', \Delta ti|s) (t - \Delta ti) ds' \\ &= \left(e^{-\beta t} \int_{\mathbb{S}} \mathcal{L}_{\mu, \Sigma} r(s') \rho(s', \xi_1|s) ds' - \beta e^{-\beta \xi_2} \int_{\mathbb{S}} r(s') \rho(s', \Delta ti|s) ds' \right) (t - \Delta ti), \end{aligned} \quad (47)$$

where the second equality is due to the mean value theorem, and the third equality is obtained by inserting the equation (45) for $\rho(s', t|s)$ and integrating by parts. Therefore, for $t \in [\Delta ti, \Delta t(i+1)]$,

$$\begin{aligned} & \left| \int_{\mathbb{S}} f(t, s') \rho(s', t|s) - f(\Delta ti, s') \rho(\Delta ti, s') ds' \right| \\ & \leq \| \mathcal{L}_{\mu, \Sigma} r \|_{L^\infty} e^{-\beta \Delta ti} (t - \Delta ti) + \beta e^{-\beta \Delta ti} \| r \|_{L^\infty} (t - \Delta ti). \end{aligned}$$

Therefore, one has

$$\begin{aligned}
& \left\| V(s) - \tilde{V}(s) \right\|_{L^\infty} \\
& \leq \sum_{i=0}^{\infty} \int_{\Delta ti}^{\Delta t(i+1)} \left\| \mathcal{L}_{\mu, \Sigma} r \right\|_{L^\infty} e^{-\beta \Delta ti} (t - \Delta ti) + \beta e^{-\beta \Delta ti} \|r\|_{L^\infty} (t - \Delta ti) dt \\
& \leq \left(\left\| \mathcal{L}_{\mu, \Sigma} r \right\|_{L^\infty} + \beta \|r\|_{L^\infty} \right) \sum_{i=0}^{\infty} e^{-\beta \Delta ti} \int_{\Delta ti}^{\Delta t(i+1)} (t - \Delta ti) dt \\
& \leq \frac{1}{2} \left(\left\| \mathcal{L}_{\mu, \Sigma} r \right\|_{L^\infty} + \beta \|r\|_{L^\infty} \right) \sum_{i=0}^{\infty} e^{-\beta \Delta ti} \Delta t^2 = \frac{C}{1 - e^{-\beta \Delta t}} \Delta t^2 = \frac{C}{\beta} \Delta t + C \left(\frac{1}{1 - e^{-\beta \Delta t}} \Delta t^2 - \frac{\Delta t}{\beta} \right),
\end{aligned}$$

where $C = \frac{1}{2} \left(\left\| \mathcal{L}_{\mu, \Sigma} r \right\|_{L^\infty} + \beta \|r\|_{L^\infty} \right)$. Since

$$\lim_{\Delta t \rightarrow 0} C \left(\frac{1}{1 - e^{-\beta \Delta t}} \Delta t^2 - \frac{\Delta t}{\beta} \right) \frac{1}{\Delta t} = 0,$$

one has,

$$\left\| V(s) - \tilde{V}(s) \right\|_{L^\infty} = \frac{L \Delta t}{\beta} + o(\Delta t).$$

6.2 Proof of Theorem 3.2

Note that the true value function V and the i -th order PhiBE solution \hat{V} satisfies

$$\beta V(s) = r(s) + \mu(s) \cdot \nabla V(s), \quad \beta \hat{V}_i(s) = r(s) + \hat{\mu}_i(s) \cdot \nabla \hat{V}_i(s).$$

First, by the following lemma, one can bound $\left\| V - \hat{V}_i \right\|_{L^\infty}$ with $\|\mu - \hat{\mu}_i\|_{L^\infty}$.

Lemma 6.1. *For function V and \hat{V} satisfies,*

$$\beta V(s) = r(s) + \mu(s) \cdot \nabla V(s), \quad \beta \hat{V}(s) = r(s) + \hat{\mu}(s) \cdot \nabla \hat{V}(s),$$

the distance between V and \hat{V} can be bounded by

$$\left\| V - \hat{V} \right\|_{L^\infty} \leq \frac{2 \|\mu - \hat{\mu}\|_{L^\infty} \|\nabla r\|_{L^\infty}}{(\beta - \|\nabla \mu\|_{L^\infty})^2}.$$

(See Section B.1 for the proof of the above lemma.) Therefore, one has

$$\left\| V - \hat{V}_i \right\|_{L^\infty} \leq \frac{\|\mu - \hat{\mu}_i\|_{L^\infty} \|\nabla r\|_{L^\infty}}{(\beta - \|\nabla \mu\|_{L^\infty})^2}. \tag{48}$$

Then by the following lemma, one can further bound $\|\mu - \hat{\mu}_i\|_{L^\infty}$.

Lemma 6.2. *The distance between $\hat{\mu}_i(s)$ defined in (12) and the true dynamics can be bounded by*

$$\|\hat{\mu}_i(s) - \mu(s)\|_{L^\infty} \leq C_i \|\mathcal{L}_\mu^i \mu(s)\|_{L^\infty} \Delta t^i,$$

where \mathcal{L}_μ is defined in (15), and

$$C_i = \frac{\sum_{j=0}^i |a_j^{(i)}| j^{i+1}}{(i+1)!}. \quad (49)$$

(See Section B.2 for the proof of the above lemma.) Hence, one completes the proof by applying the above lemma to (48)

$$\|V - \hat{V}_i\|_{L^\infty} \leq \frac{C_i \|\mathcal{L}_\mu^i \mu\|_{L^\infty} \|\nabla r\|_{L^\infty}}{(\beta - \|\nabla \mu\|_{L^\infty})^2} \Delta t^i.$$

6.3 Proof of Theorem 3.3

For the linear dynamics $ds_t = As_t dt$, one has $s_t = e^{At} s_0$, therefore,

$$\hat{\mu}(s) = \frac{1}{\Delta t} \sum_{j=1}^i a_j^{(i)} (s_{j\Delta t} - s_0) = \frac{1}{\Delta t} \sum_{j=1}^i a_j^{(i)} (e^{Aj\Delta t} - I)s.$$

Let $\hat{A}_i = a_j^{(i)} (e^{Aj\Delta t} - I)$, then the i -th order PhiBE reads,

$$\beta \hat{V}_i(s) = r(s) + \hat{A}_i s \cdot \nabla \hat{V}_i(s),$$

which can equivalently written as

$$\beta \hat{V}_i(s) = \int_0^\infty e^{-\beta t} r(e^{\hat{A}_i t} s) dt.$$

Now define $\phi(\theta) = e^{At} e^{\theta \Delta_i t} s$, where $\Delta_i = \hat{A}_i - A$, then $e^{At} s = \phi(0)$, $e^{\hat{A}_i t} s = \phi(1)$, which implies

$$\begin{aligned} r(e^{At} s) - r(e^{\hat{A}_i t} s) &= r(\phi(0)) - r(\phi(1)) = \int_0^1 \frac{d}{d\theta} r(\phi(\theta)) d\theta = \int_0^1 \nabla(r(\phi(\theta)))^\top \phi'(\theta) d\theta \\ &= \left[\int_0^1 (\nabla r(\phi(\theta)))^\top \phi(\theta) d\theta \right] \Delta_i t. \end{aligned}$$

Therefore, one has

$$\begin{aligned} |V(s) - \hat{V}_1(s)| &= \left| \int_0^\infty e^{-\beta t} \left(r(e^{At} s) - r(e^{\hat{A}_1 t} s) \right) dt \right| \\ &= \left| \int_0^1 \left(\int_0^\infty (\nabla r(\phi(\theta)))^\top \phi(\theta) e^{-\beta t} t dt \right) d\theta \Delta_i \right| \leq \|u \cdot r(u)\|_{L^\infty} \int_0^1 \left(\int_0^\infty e^{-\beta t} t dt \right) d\theta |\Delta_A| \\ &= \frac{\|u \cdot r(u)\|_{L^\infty}}{\beta^2} \|\Delta_i\|. \end{aligned}$$

Next we estimate $\|\Delta_i\|$. First note that

$$\hat{A}_i = \frac{1}{\Delta t} \sum_{j=1}^i a_j^{(i)} (e^{Aj\Delta t} - I) = \frac{1}{\Delta t} \sum_{j=1}^i a_j^{(i)} \left(\sum_{k=1}^i \frac{1}{k!} (Aj\Delta t)^k + R_{ij} \right)$$

where

$$R_{ij} = e^{Aj\Delta t} - \sum_{k=0}^i \frac{1}{k!} (Aj\Delta t)^k = \frac{A^{i+1} (j\Delta t)^{i+1}}{(i+1)!} e^{A\xi}, \quad \text{for } \xi \in [0, j\Delta t),$$

and therefore

$$\|R_{ij}\| \leq \frac{\|A\|^{i+1} (j\Delta t)^{i+1}}{(i+1)!} e^{\|A\|j\Delta t} \leq \frac{\|A\|^{i+1} (j\Delta t)^{i+1}}{(i+1)!} e^{\|A\|i\Delta t}.$$

By the definition of $a_j^{(i)}$, one has

$$\hat{A}_i = \sum_{k=1}^i \frac{1}{k!} A^k \Delta t^{k-1} \left(\sum_{j=1}^i a_j^{(i)} j^k \right) + \frac{1}{\Delta t} \sum_{j=1}^i a_j^{(i)} R_{ij} = A + \frac{1}{\Delta t} \sum_{j=1}^i a_j^{(i)} R_{ij},$$

which leads to

$$\|\Delta_i\| = \|\hat{A}_i - A\| \leq \frac{1}{\Delta t} \sum_{j=1}^i |a_j^{(i)}| \|R_{ij}\| \leq C_i \|A\| D_A^i \Delta t^i, \quad \text{with } D_A = e^{\|A\|\Delta t} \|A\| \quad (50)$$

where C_i is defined in (49).

6.4 Proof of Theorem 3.4

We first present the property of the operator $\mathcal{L}_{\mu,\Sigma}$ that will be frequently used later in the following Proposition.

Proposition 6.3. *For the operator $\mathcal{L}_{\mu,\Sigma}$ defined in (5), under Assumption 1/(a), one has*

$$\begin{aligned} \langle \mathcal{L}_{\mu,\Sigma} V(s), V(s) \rangle_\rho &\leq -\frac{\lambda_{\min}}{2} \|\nabla V\|_\rho^2; \\ \sum_i \langle \partial_{s_i} \mathcal{L}_{\mu,\Sigma} V(s), \partial_{s_i} V(s) \rangle_\rho &\leq C_{\nabla\mu, \nabla\Sigma} \|\nabla V\|_\rho^2; \\ \langle \mathcal{L}_{\mu,\Sigma} f(s), g(s) \rangle_\rho &\leq \left[\left(\|\mu\|_{L^\infty} + \frac{1}{2} \|\nabla \cdot \Sigma\|_{L^\infty} \right) \|g\|_\rho + \frac{1}{2} \|\Sigma\|_{L^\infty} \|\nabla g\|_\rho \right] \|\nabla f\|_\rho \\ &\quad + \frac{1}{2} \|\Sigma\|_{L^\infty} \|\nabla \log \rho\|_\rho \|g\|_\rho \|\nabla f\|_{L^\infty}; \\ \langle \mathcal{L}_{\mu,\Sigma} f(s), g(s) \rangle_\rho &\leq \left[\left(\|\mu\|_{L^\infty} + \frac{1}{2} \|\nabla \cdot \Sigma\|_{L^\infty} + \frac{1}{2} \|\Sigma\|_{L^\infty} \|\nabla \log \rho\|_{L^\infty} \right) \|g\|_\rho \right. \\ &\quad \left. + \frac{1}{2} \|\Sigma\|_{L^\infty} \|\nabla g\|_\rho \right] \|\nabla f\|_\rho, \end{aligned}$$

where $C_{\nabla\mu, \nabla\Sigma}$ is defined in (52) depending on the first derivatives of μ, Σ .

Proof. Inserting the operator $\mathcal{L}_{\mu,\Sigma}$, and applying integral by parts gives,

$$\begin{aligned}
& \langle \mathcal{L}_{\mu,\Sigma} V(s), V(s) \rangle_\rho = \langle \mu \cdot \nabla V, V \rangle_\rho - \frac{1}{2} \sum_{i,j} \langle \partial_{s_j} (\Sigma_{ij} V \rho), \partial_{s_i} V \rangle \\
& = \sum_i \left\langle \mu_i \rho, \partial_{s_i} \left(\frac{1}{2} V^2 \right) \right\rangle - \frac{1}{2} \sum_{i,j} \left\langle \partial_{s_j} (\Sigma_{ij} \rho), \partial_{s_i} \left(\frac{1}{2} V^2 \right) \right\rangle - \frac{1}{2} \sum_{i,j} \langle (\partial_{s_j} V) \Sigma_{ij}, \partial_{s_i} V \rangle_\rho \\
& = - \sum_i \left\langle \partial_{s_i} (\mu_i \rho), \frac{1}{2} V^2 \right\rangle + \frac{1}{2} \sum_{i,j} \left\langle \partial_{s_i} \partial_{s_j} (\Sigma_{ij} \rho), \frac{1}{2} V^2 \right\rangle - \frac{1}{2} \int (\nabla V)^\top \Sigma (\nabla V) \rho ds \quad (51) \\
& = \left\langle \nabla \cdot \left(-\mu \rho + \frac{1}{2} \nabla \cdot (\Sigma \rho) \right), \frac{1}{2} V^2 \right\rangle - \frac{1}{2} \int (\nabla V)^\top \Sigma (\nabla V) \rho ds \\
& \leq \left\langle \nabla \cdot \left(-\mu \rho + \frac{1}{2} \nabla \cdot (\Sigma \rho) \right), \frac{1}{2} V^2 \right\rangle - \frac{\lambda_{\min}}{2} \|\nabla V\|_\rho^2,
\end{aligned}$$

where the last inequality is because of the positivity of the matrix $\Sigma(s)$ in Assumption 1.

If ρ is the stationary solution, then

$$\left\langle \nabla \cdot \left(-\mu \rho + \frac{1}{2} \nabla \cdot (\Sigma \rho) \right), \frac{1}{2} V^2 \right\rangle = 0.$$

If ρ s.t. $\frac{1}{\lambda_{\min}} \left\| -\mu + \frac{1}{2} \nabla \cdot \Sigma + \frac{1}{2} \Sigma \nabla \log \rho \right\|_{L^\infty}^2 \leq \frac{\beta}{2}$, then

$$\begin{aligned}
& \left\langle \nabla \cdot \left(-\mu \rho + \frac{1}{2} \nabla \cdot (\Sigma \rho) \right), \frac{1}{2} V^2 \right\rangle = \left\langle \left(\mu - \frac{1}{2} \nabla \cdot \Sigma - \frac{1}{2} \Sigma \nabla \log \rho \right) \rho, \nabla \left(\frac{1}{2} V^2 \right) \right\rangle \\
& \leq \left\| \mu - \frac{1}{2} \nabla \cdot \Sigma - \frac{1}{2} \Sigma \nabla \log \rho \right\|_{L^\infty} \|V\|_\rho \|\nabla V\|_\rho \\
& \leq \frac{1}{\lambda_{\min}} \left\| \mu - \frac{1}{2} \nabla \cdot \Sigma - \frac{1}{2} \Sigma \nabla \log \rho \right\|_{L^\infty}^2 \|V\|_\rho^2 + \frac{\lambda_{\min}}{4} \|\nabla V\|_\rho^2 \leq \frac{\beta}{2} \|V\|_\rho^2 + \frac{\lambda_{\min}}{4} \|\nabla V\|_\rho^2.
\end{aligned}$$

Inserting it back to (51), this completes the proof of the first inequality.

For the second part of the Lemma, first note that

$$\partial_{s_i} \mathcal{L}_{\mu,\Sigma} V = \partial_{s_i} \mu \cdot \nabla V + \frac{1}{2} \partial_{s_i} \Sigma : \nabla^2 V + \mathcal{L}_{\mu,\Sigma} \partial_{s_i} V.$$

Therefore, applying the first part of the Lemma gives

$$\begin{aligned}
& \sum_i \langle \partial_{s_i} \mathcal{L}_{\mu,\Sigma} V(s), V(s) \rangle_\rho \\
& \leq \sum_i \left(\langle \partial_{s_i} \mu \cdot \nabla V, \partial_{s_i} V \rangle_\rho + \frac{1}{2} \langle \partial_{s_i} \Sigma : \nabla^2 V, \partial_{s_i} V \rangle_\rho \right) - \frac{\lambda_{\min}}{4} \sum_i \|\nabla \partial_{s_i} V\|_\rho^2 + \frac{\beta}{2} \|\nabla V\|_\rho^2 \\
& \leq \|\nabla \mu\|_{L^\infty} \|\nabla V\|_\rho^2 + \frac{1}{2} \|\nabla \Sigma\|_{L^\infty} \|\nabla^2 V\|_\rho \|\nabla V\|_\rho - \frac{\lambda_{\min}}{4} \|\nabla^2 V\|_\rho^2 + \frac{\beta}{2} \|\nabla V\|_\rho^2 \\
& = - \frac{\lambda_{\min}}{4} \left(\|\nabla^2 V\|_\rho - \frac{\|\nabla \Sigma\|_{L^\infty}}{\lambda_{\min}} \|\nabla V\|_\rho \right)^2 + \left(\frac{\|\nabla \Sigma\|_{L^\infty}^2}{4\lambda_{\min}} + \|\nabla \mu\|_{L^\infty} + \frac{\beta}{2} \right) \|\nabla V\|_\rho^2 \\
& \leq \frac{C_{\nabla \mu, \nabla \Sigma}}{2} \|\nabla V\|_\rho^2,
\end{aligned}$$

where

$$C_{\nabla\mu, \nabla\Sigma} = \frac{\|\nabla\Sigma\|_{L^\infty}^2}{2\lambda_{\min}} + 2\|\nabla\mu\|_{L^\infty} + \beta. \quad (52)$$

For the last two inequalities, one notes

$$\begin{aligned} & \langle \mathcal{L}_{\mu, \Sigma} f, g \rangle_\rho \\ &= \langle \mu \cdot \nabla f, g \rangle_\rho - \frac{1}{2} \left[\langle \nabla f \cdot \nabla \cdot \Sigma, g \rangle_\rho + \langle \nabla f \Sigma, \nabla g \rangle_\rho + \left\langle \nabla f \Sigma, \frac{\nabla \rho}{\rho} g \right\rangle_\rho \right] \\ &\leq \left[\left(\|\mu\|_{L^\infty} + \frac{1}{2} \|\nabla \cdot \Sigma\|_{L^\infty} \right) \|g\|_\rho + \frac{\|\Sigma\|_{L^\infty}}{2} \|\nabla g\|_\rho \right] \|\nabla f\|_\rho + \left\langle \nabla f \frac{\Sigma}{2}, g \nabla \log \rho \right\rangle_\rho. \end{aligned}$$

By bounding the last term differently,

$$\frac{1}{2} \|\nabla \log \rho\|_{L^\infty} \|\Sigma\|_{L^\infty} \|g\|_\rho \|\nabla f\|_\rho \quad \text{or,} \quad \frac{1}{2} \|\nabla \log \rho\|_\rho \|\Sigma\|_{L^\infty} \|g\|_\rho \|\nabla f\|_{L^\infty},$$

one ends up with the last two inequalities of the Lemma. □

Proof of Theorem 3.4 Now we are ready to prove Theorem 3.4.

Proof. By (46), one has

$$\begin{aligned} & \left\| V(s) - \tilde{V}(s) \right\|_\rho \\ &\leq \sum_{i=0}^{\infty} \sqrt{\Delta t \int_{\Delta ti}^{\Delta t(i+1)} \left\| \int_{\mathbb{S}} f(t, s') \rho(s', t|s) - f(\Delta ti, s') \rho(\Delta ti, s') ds' \right\|_\rho^2 dt}, \end{aligned} \quad (53)$$

where the Jensen's inequality is used. By (47), one has for $t \in [\Delta ti, \Delta t(i+1)]$

$$\begin{aligned} & \left\| \int_{\mathbb{S}} f(t, s') \rho(s', t|s) - f(\Delta ti, s') \rho(\Delta ti, s') ds' \right\|_\rho \\ &\leq e^{-\beta \Delta ti} (t - \Delta ti) \left(\|p_1(\xi_1, s)\|_\rho + \beta \|p_2(\Delta ti, s)\|_\rho \right), \end{aligned}$$

where

$$p_1(s, t) = \int_{\mathbb{S}} \mathcal{L}_{\mu, \Sigma} r(s') \rho(s', t|s) ds', \quad p_2(s, t) = \int_{\mathbb{S}} r(s') \rho(s', t|s) ds'.$$

Note that both $p_1(s, t)$ and $p_2(s, t)$ satisfies

$$\partial_t p_i(s, t) = \mathcal{L}_{\mu, \Sigma} p_i(s, t), \quad \text{with initial data } p_1(0, s) = \mathcal{L}_{\mu, \Sigma} r(s), \quad p_2(0, s) = r(s).$$

By Proposition 6.3, one has

$$\partial_t \left(\frac{1}{2} \|p_i(t)\|_\rho^2 \right) \leq -\frac{\lambda_{\min}}{4} \|\nabla p_i(t)\|_\rho^2 + \frac{\beta}{2} \|p_i(t)\|_\rho^2,$$

which implies,

$$\|p_i(t)\|_\rho \leq e^{\frac{\beta}{2}t} \|p_i(0)\|_\rho.$$

Therefore, one has

$$\begin{aligned} & \left\| \int_{\mathbb{S}} f(t, s') \rho(s', t|s) - f(\Delta ti, s') \rho(\Delta ti, s') ds' \right\|_\rho \\ & \leq e^{-\beta \Delta ti} (t - \Delta ti) e^{\frac{\beta}{2} \Delta ti} \left(e^{\frac{\beta}{2} (\xi_1 - \Delta ti)} \|\mathcal{L}_{\mu, \Sigma} r(s)\|_\rho + \beta \|r(s)\|_\rho \right), \quad \xi_1 \in [\Delta ti, \Delta t(i+1)]. \end{aligned}$$

Inserting it back to (53) yields,

$$\begin{aligned} & \left\| V(s) - \tilde{V}(s) \right\|_\rho \\ & \leq \left(\|\mathcal{L}_{\mu, \Sigma} r(s)\|_\rho + \beta \|r(s)\|_\rho \right) e^{\frac{\beta}{2} \Delta t} \sum_{i=0}^{\infty} \sqrt{\Delta t e^{-\beta \Delta ti} \int_{\Delta ti}^{\Delta t(i+1)} (t - \Delta ti)^2 dt} \\ & = \left(\|\mathcal{L}_{\mu, \Sigma} r(s)\|_\rho + \beta \|r(s)\|_\rho \right) e^{\frac{\beta}{2} \Delta t} \frac{1}{\sqrt{3}} \Delta t^2 \sum_{i=0}^{\infty} e^{-\frac{\beta}{2} \Delta ti} \\ & = \frac{2}{\beta} \left(\|\mathcal{L}_{\mu, \Sigma} r(s)\|_\rho + \beta \|r(s)\|_\rho \right) \Delta t + o(\Delta t), \end{aligned}$$

where the last equality comes from

$$e^{\frac{\beta}{2} \Delta t} \Delta t^2 \sum_{i=0}^{\infty} e^{-\frac{\beta}{2} \Delta ti} = \frac{2 \Delta t}{\beta} + o(\Delta t),$$

which completes the proof. \square

6.5 Proof of Theorem 3.5

First note that V, \hat{V}_i satisfies,

$$\mathcal{L}_{\mu, \Sigma} V = \beta V - r, \quad \mathcal{L}_{\hat{\mu}_i, \hat{\Sigma}_i} \hat{V}_i = \beta \hat{V}_i - r.$$

By the following Lemma, one can bound $\|V - \hat{V}_i\|_\rho$ by the distance between μ, Σ and $\hat{\mu}_i, \hat{\Sigma}_i$.

Lemma 6.4. *For V, \hat{V} satisfying*

$$\mathcal{L}_{\mu, \Sigma} V = \beta V - r, \quad \mathcal{L}_{\hat{\mu}, \hat{\Sigma}} \hat{V} = \beta \hat{V} - r,$$

under Assumption 1/(a), if $\|\hat{\mu} - \mu\|_{L^\infty} \leq C_\mu$, $\|\hat{\Sigma} - \Sigma\|_{L^\infty} \leq C_\Sigma$, $\|\nabla \cdot (\hat{\Sigma} - \Sigma)\|_{L^\infty} \leq C_{\nabla \cdot \Sigma}$, $\|\nabla \log \rho\|_\rho \leq L_\rho$, and $C_\mu + \frac{1}{2} C_\Sigma \leq \sqrt{\frac{\beta \lambda_{\min}}{8}}$, $C_\Sigma \leq \frac{\lambda_{\min}}{4}$, one has

$$\left\| V - \hat{V} \right\|_\rho \leq \left[\frac{4C_\mu + 2C_{\nabla \cdot \Sigma}}{\beta} \left(1 + \frac{2C_\Sigma}{\lambda_{\min}} \right) + \frac{2C_\Sigma}{\sqrt{\beta \lambda_{\min}}} \right] \|\nabla V\|_\rho + \frac{2C_\Sigma L_\rho}{\beta} \|\nabla \hat{V}\|_{L^\infty}.$$

(See Section B.3 for the proof of the above lemma) Then we further apply the following lemma regarding the distance between μ, Σ and $\hat{\mu}_i, \hat{\Sigma}_i$.

Lemma 6.5. *Under Assumption 1, for $\hat{\mu}(s), \hat{\Sigma}(s)$ defined in (18), one has*

$$\|\hat{\mu}_i(s) - \mu(s)\|_{L^\infty} \leq L_\mu \Delta t^i, \quad \left\| \hat{\Sigma}_i(s)_{kl} - \Sigma(s)_{kl} \right\|_{L^\infty} \leq L_\Sigma \Delta t^i + o(\Delta t^i),$$

and

$$\left\| \nabla \cdot (\hat{\Sigma} - \Sigma) \right\|_{L^\infty}^2 \leq L_{\nabla \cdot \Sigma} \Delta t^i + o(\Delta t^i), \quad (54)$$

where $L_\mu, L_\Sigma, L_{\nabla \cdot \Sigma}$ are constants depending on μ, Σ, i defined in (75), (78), (80), respectively.

(See Section B.4 for the proof of the above lemma) Combine the above two lemmas, one can bound

$$\|V - \hat{V}_i\| \leq \left[\left(\frac{3L_\mu + 2L_{\nabla \cdot \Sigma}}{\beta} \left(1 + \frac{L_\Sigma \Delta t^i}{\lambda_{\min}} \right) + \frac{L_\Sigma}{\sqrt{\beta \lambda_{\min}}} \right) \|\nabla V\|_\rho + \frac{2L_\Sigma L_\rho}{\beta} \|\nabla \hat{V}\|_{L^\infty} \right] \Delta t^i + o(\Delta t^i)$$

for

$$\Delta t^i \leq D_{\mu, \Sigma, \beta}, \quad D_{\mu, \Sigma, \beta} = \min \left\{ \frac{\lambda_{\min}}{2L_\Sigma}, \frac{\sqrt{2\beta \lambda_{\min}}}{2L_\mu + L_{\nabla \cdot \Sigma}} \right\}, \quad (55)$$

with $L_\mu, L_\Sigma, L_{\nabla \cdot \Sigma}$ defined in (75), (78), (93). Furthermore, by the following lemma on the upper bound for $\|\nabla V\|_\rho, \|\nabla \hat{V}\|_{L^\infty}$, one completes the proof for Theorem 3.5.

Lemma 6.6. *Under Assumption 1/(a), for $V(s)$ satisfying (16), one has*

$$\begin{aligned} \|\nabla V(s)\|_\rho &\leq \frac{2}{\beta} \left(\sqrt{\frac{C_{\nabla \mu, \nabla \Sigma}}{\lambda_{\min}}} \|r\|_\rho + \|\nabla r\|_\rho \right) \\ \|\nabla V(s)\|_{L^\infty} &\leq \frac{1}{\beta} \left(\sqrt{\frac{2C_{\nabla \mu, \nabla \Sigma}}{\lambda_{\min}}} \|r\|_{L^\infty} + \|\nabla r\|_{L^\infty} \right) + o(\Delta t^{i/2}) \end{aligned}$$

where $C_{\nabla \mu, \nabla \Sigma}$ is a constant defined in (52) that depends on $\nabla \mu(s), \nabla \Sigma(s)$.

(See Section B.5 for the proof of the above lemma) one has,

$$\begin{aligned} \|V - \hat{V}_i\|_\rho &\leq \left[\left(\frac{3L_\mu + 2L_{\nabla \cdot \Sigma}}{\beta^2} + \frac{L_\Sigma}{\beta \sqrt{\beta \lambda_{\min}}} \right) \left(\sqrt{\frac{C_{\nabla \mu, \nabla \Sigma}}{\lambda_{\min}}} \|r\|_\rho + \|\nabla r\|_\rho \right) \right. \\ &\quad \left. + \frac{2L_\Sigma L_\rho}{\beta^2} \left(\sqrt{\frac{2C_{\nabla \mu, \nabla \Sigma}}{\lambda_{\min}}} \|r\|_{L^\infty} + \|\nabla r\|_{L^\infty} \right) \right] \Delta t^i + o(\Delta t^i) \\ &\leq \left[\frac{C_{r, \mu, \Sigma}}{\beta^2} + \frac{\hat{C}_{r, \mu, \Sigma}}{\beta^{3/2}} \right] \Delta t^i + o(\Delta t^i), \end{aligned}$$

where

$$\begin{aligned}
C_{r,\mu,\Sigma} &= (3L_\mu + 2L_{\nabla\cdot\Sigma}) \left(\sqrt{\frac{C_{\nabla\mu,\nabla\Sigma}}{\lambda_{\min}}} \|r\|_\rho + \|\nabla r\|_\rho \right) \\
&\quad + 2L_\Sigma L_\rho \left(\sqrt{\frac{2C_{\nabla\mu,\nabla\Sigma}}{\lambda_{\min}}} \|r\|_{L^\infty} + \|\nabla r\|_{L^\infty} \right), \\
\hat{C}_{r,\mu,\Sigma} &= \frac{L_\Sigma}{\sqrt{\lambda_{\min}}} \left(\sqrt{\frac{C_{\nabla\mu,\nabla\Sigma}}{\lambda_{\min}}} \|r\|_\rho + \|\nabla r\|_\rho \right),
\end{aligned} \tag{56}$$

with $L_\mu, L_\Sigma, L_{\nabla\cdot\Sigma}, L_\rho, C_{\nabla\mu,\nabla\Sigma}$ defined in (75), (78), (93), (20), (52).

6.6 Proof of Theorem 4.1 and Galerkin error with unbounded $\|\nabla \log \rho\|_{L^\infty}$

The i -th approximation $\hat{V}_i(s)$ can be divided into two parts,

$$\hat{V}_i(s) = \hat{V}_i^P(s) + e_i^P(s) \quad \text{with} \quad \hat{V}_i^P(s) = \sum_{k=1}^p \hat{v}_k \phi_k(s), e_i^P(s) = \hat{V}_i(s) - \hat{V}_i^P(s),$$

where $\hat{V}_i^P(s)$ could be any functions in the linear space spanned by $\Phi(s)$. Note that $\hat{V}_i(s)$ satisfies

$$\left\langle (\beta - \mathcal{L}_{\hat{\mu}_i, \hat{\Sigma}_i}) \hat{V}_i(s), \Phi \right\rangle_\rho = \langle r(s), \Phi(s) \rangle_\rho,$$

which can be divided into two parts,

$$\left\langle (\beta - \mathcal{L}_{\hat{\mu}_i, \hat{\Sigma}_i}) \hat{V}_i^P(s), \Phi \right\rangle_\rho = \langle r(s), \Phi(s) \rangle_\rho - \left\langle (\beta - \mathcal{L}_{\hat{\mu}_i, \hat{\Sigma}_i}) e_i^P(s), \Phi \right\rangle_\rho,$$

subtract the above equation from the Galerkin equation (24) gives

$$\left\langle (\beta - \mathcal{L}_{\hat{\mu}_i, \hat{\Sigma}_i}) (\hat{V}_i^G(s) - \hat{V}_i^P(s)), \Phi \right\rangle_\rho = \left\langle (\beta - \mathcal{L}_{\hat{\mu}_i, \hat{\Sigma}_i}) e_i^P(s), \Phi \right\rangle_\rho.$$

Let $e_i^G(s) = \hat{V}_i^G(s) - \hat{V}_i^P(s) = \sum_{k=1}^p e_k \phi_k(s)$, then multiplying (e_1, \dots, e_p) to the above equation yields,

$$\begin{aligned}
\left\langle (\beta - \mathcal{L}_{\hat{\mu}_i, \hat{\Sigma}_i}) e_i^G, e_i^G \right\rangle_\rho &= \left\langle (\beta - \mathcal{L}_{\hat{\mu}_i, \hat{\Sigma}_i}) e_i^P, e_i^G \right\rangle_\rho \\
\left\langle (\beta - \mathcal{L}_{\mu, \Sigma}) e_i^G, e_i^G \right\rangle_\rho &= \left\langle \mathcal{L}_{\hat{\mu}_i - \mu, \hat{\Sigma}_i - \Sigma} e_i^G, e_i^G \right\rangle_\rho + \left\langle (\beta - \mathcal{L}_{\hat{\mu}_i, \hat{\Sigma}_i}) e_i^P, e_i^G \right\rangle_\rho.
\end{aligned} \tag{57}$$

When $L_\rho^\infty = \|\nabla \log \rho\|_{L^\infty}$ is bounded, by applying the last inequality of Proposition 6.3 and Lemma 6.5, one has

$$\begin{aligned}
\frac{\beta}{2} \|e_i^G\|_\rho^2 + \frac{\lambda_{\min}}{4} \|\nabla e_i^G\|_\rho^2 &\leq c_1 \|\nabla e_i^G\|_\rho^2 + c_2 \|e_i^G\|_\rho \|\nabla e_i^G\|_\rho + \beta \|e_i^P\|_\rho \|e_i^G\|_\rho \\
&\quad + c_3 \|\nabla e_i^P\|_\rho \|\nabla e_i^G\|_\rho + c_4 \|\nabla e_i^P\|_\rho \|e_i^G\|_\rho,
\end{aligned}$$

where

$$\begin{aligned}
c_1 &= \frac{L_\Sigma}{2} \Delta t^i, \quad c_2 = \left(L_\mu + \frac{L_{\nabla \cdot \Sigma}}{2} + \frac{L_\Sigma L_\rho^\infty}{2} \right) \Delta t^i, \\
c_3 &= \frac{1}{2} (\|\Sigma\|_{L^\infty} + L_\Sigma \Delta t^i), \\
c_4 &= \left(\|\mu\|_{L^\infty} + \frac{\|\nabla \cdot \Sigma\|_{L^\infty}}{2} + \frac{\|\Sigma\|_{L^\infty} L_\rho^\infty}{2} \right) + \left(L_\mu + \frac{L_{\nabla \cdot \Sigma}}{2} + \frac{L_\Sigma L_\rho^\infty}{2} \right) \Delta t^i
\end{aligned} \tag{58}$$

with $L_\mu, L_\Sigma, L_{\nabla \cdot \Sigma}$ defined in (75), (78), (93). Under the assumption that $c_1 \leq \frac{\lambda_{\min}}{16}, \frac{c_2}{2} \leq \min \left\{ \frac{\lambda_{\min}}{16}, \frac{\beta}{4} \right\}$, i.e.,

$$\Delta t^i \leq \eta_{\mu, \Sigma, \beta}, \quad \eta_{\mu, \Sigma, \beta} = \frac{\min \left\{ \frac{\lambda_{\min}}{4}, \beta \right\}}{2L_\mu + L_{\nabla \cdot \Sigma} + L_\Sigma \max \{L_\rho^\infty, 4\}} \tag{59}$$

with $L_\mu, L_\Sigma, L_{\nabla \cdot \Sigma}$ defined in (75), (78), (93), one has

$$\begin{aligned}
\frac{\beta}{4} \|e_i^G\|_\rho^2 + \frac{\lambda_{\min}}{8} \|\nabla e_i^G\|_\rho^2 &\leq \beta \|e_i^P\|_\rho \|e_i^G\|_\rho + c_3 \|\nabla e_i^P\|_\rho \|\nabla e_i^G\|_\rho, \\
&\quad + c_4 \|\nabla e_i^P\|_\rho \|e_i^G\|_\rho \\
\|e_i^G\|_\rho &\leq 4 \|e_i^P\|_\rho + \sqrt{\frac{8}{\beta} \left(\frac{2c_3^2}{\lambda_{\min}} + \frac{4c_4^2}{\beta} \right)} \|\nabla e_i^P\|_\rho,
\end{aligned}$$

which implies that

$$\|\hat{V}_i - \hat{V}_i^G\|_\rho \leq \|e_i^P\|_\rho + \|e_i^G\|_\rho \leq 5 \|e_i^P\|_\rho + \sqrt{\frac{8}{\beta} \left(\frac{2c_3^2}{\lambda_{\min}} + \frac{4c_4^2}{\beta} \right)} \|\nabla e_i^P\|_\rho.$$

Since the above inequality holds for all V_i^P in the linear space spanned by $\{\Phi\}$, therefore,

$$\|\hat{V}_i - \hat{V}_i^G\|_\rho \leq \frac{1}{\beta} C_G \inf_{V = \theta^\top \Phi} \|\hat{V}_i - V\|_{H_\rho^1}$$

where

$$C_G = \max \left\{ 5\beta, \frac{4c_3\sqrt{\beta}}{\sqrt{\lambda_{\min}}} + 6c_4 \right\}, \quad \|f\|_{H_\rho^1} = \|f\|_\rho + \|\nabla f\|_\rho. \tag{60}$$

with c_3, c_4 defined in (58).

Theorem 6.7 (Galerkin Error with unbounded $\|\nabla \log \rho\|_{L^\infty}$). *The Galerkin solution $\hat{V}_i^G(s) = \theta^\top \Phi(s)$ satisfies*

$$\left\langle (\beta - \mathcal{L}_{\hat{\mu}_i, \hat{\Sigma}_i}) \hat{V}_i^G(s), \Phi \right\rangle_\rho = \langle r(s), \Phi(s) \rangle_\rho. \tag{61}$$

When $\|\nabla \log \rho\|_{L^\infty}$ is unbounded, assume that the bases $L_\Phi^\infty = \|\Phi\|_{L^\infty}$ is bounded, then as long as $\Delta t^i \leq \min \{\hat{\eta}_{\mu, \Sigma, \beta}, D_{\mu, \Sigma, \beta}\}$, the Galerkin solution $\hat{V}_i^G(s)$ approximates the solution to the i -th order PhiBE defined in (17) with an error

$$\|\hat{V}_i^G(s) - \hat{V}_i(s)\|_\rho \leq \frac{\hat{C}_G}{\beta} \inf_{V^P = \theta^\top \Phi} \|\hat{V}_i - V^P\|_{H_{\rho, \infty}^1}.$$

where $\hat{\eta}_{\mu,\Sigma,\beta}, \hat{C}_G, D_{\mu,\Sigma,\beta}$ are constants depending on $\mu, \Sigma, \beta, L_\rho, L_\Phi^\infty$ defined in (64), (65), (55) respectively, and $\|f\|_{H_{\rho,\infty}^1} = \|f\|_{H_\rho^1} + \|\nabla f\|_{L^\infty}$.

Proof. When $L_\rho^\infty = \|\nabla \log \rho\|_{L^\infty}$ is not bounded, by applying the last second inequality of Proposition 6.3 and Lemma 6.5 to (57), one has

$$\begin{aligned} \frac{\beta}{2} \|e_i^G\|_\rho^2 + \frac{\lambda_{\min}}{4} \|\nabla e_i^G\|_\rho^2 &\leq c_1 \|\nabla e_i^G\|_\rho^2 + c_5 \|e_i^G\|_\rho \|\nabla e_i^G\|_\rho + c_6 \|e_i^G\|_{L^\infty} \|\nabla e_i^G\|_\rho \\ &+ \beta \|e_i^P\|_\rho \|e_i^G\|_\rho + c_3 \|\nabla e_i^P\|_\rho \|\nabla e_i^G\|_\rho + c_7 \|\nabla e_i^P\|_\rho \|e_i^G\|_\rho + c_8 \|\nabla e_i^P\|_{L^\infty} \|e_i^G\|_\rho, \end{aligned} \quad (62)$$

where

$$\begin{aligned} c_5 &= \left(L_\mu + \frac{L_{\nabla \cdot \Sigma}}{2} \right) \Delta t^i, \quad c_8 = \frac{\|\Sigma\|_{L^\infty} L_\rho}{2} + \frac{L_\Sigma L_\rho}{2} \Delta t^i, \\ c_6 &= \frac{L_\Sigma L_\rho}{2} \Delta t^i, \quad c_7 = \left(\|\mu\|_{L^\infty} + \frac{\|\nabla \cdot \Sigma\|_{L^\infty}}{2} \right) + \left(L_\mu + \frac{L_{\nabla \cdot \Sigma}}{2} \right) \Delta t^i, \end{aligned} \quad (63)$$

with $L_\mu, L_\Sigma, L_{\nabla \cdot \Sigma}, L_\rho$ defined in (75), (78), (93), (20). Since

$$\|e_i^G\|_{L^\infty} = \|e^\top \Phi\|_{L^\infty} \leq \|e\|_2 \|\Phi\|_{L^\infty} \leq \frac{1}{\sqrt{\hat{\lambda}}} \|e_i^G\|_\rho \|\Phi\|_{L^\infty},$$

where $\hat{\lambda}$ is the smallest eigenvalue of the matrix B , where $B_{ij} = \int \phi_i(s) \phi_j(s) \rho(s) ds$. Note that the matrix B is always positive definite when $\{\phi_i(s)\}$ are linear independent bases w.r.t. the weighted L^2 norm. let $L_\Phi^\infty = \|\Phi\|_{L^\infty}$, then (62) can be rewritten as

$$\begin{aligned} \frac{\beta}{2} \|e_i^G\|_\rho^2 + \frac{\lambda_{\min}}{4} \|\nabla e_i^G\|_\rho^2 &\leq c_1 \|\nabla e_i^G\|_\rho^2 + c_9 \|e_i^G\|_\rho \|\nabla e_i^G\|_\rho + \beta \|e_i^P\|_\rho \|e_i^G\|_\rho \\ &+ c_3 \|\nabla e_i^P\|_\rho \|\nabla e_i^G\|_\rho + c_7 \|\nabla e_i^P\|_\rho \|e_i^G\|_\rho + c_8 \|\nabla e_i^P\|_{L^\infty} \|e_i^G\|_\rho, \end{aligned}$$

where

$$c_9 = \left(L_\mu + \frac{L_{\nabla \cdot \Sigma}}{2} + \frac{L_\Sigma L_\rho L_\Phi^\infty}{2\sqrt{\hat{\lambda}}} \right) \Delta t^i.$$

When $c_1 \leq \frac{\lambda_{\min}}{16}$, $\frac{c_9}{2} \leq \min\{\frac{\lambda_{\min}}{16}, \frac{\beta}{4}\}$, i.e.,

$$\Delta t^i \leq \hat{\eta}_{\mu,\Sigma,\beta}, \quad \hat{\eta}_{\mu,\Sigma,\beta} = \frac{\min\{\frac{\lambda_{\min}}{4}, \beta\}}{2L_\mu + L_{\nabla \cdot \Sigma} + L_\Sigma \max\left\{\frac{L_\rho L_\Phi^\infty}{\sqrt{\hat{\lambda}}}, 4\right\}}, \quad (64)$$

with $L_\mu, L_\Sigma, L_{\nabla \cdot \Sigma}$ defined in (75), (78), (93), then one has

$$\begin{aligned} \frac{\beta}{4} \|e_i^G\|_\rho^2 + \frac{\lambda_{\min}}{8} \|\nabla e_i^G\|_\rho^2 &\leq \beta \|e_i^P\|_\rho \|e_i^G\|_\rho + c_3 \|\nabla e_i^P\|_\rho \|\nabla e_i^G\|_\rho \\ &+ c_7 \|\nabla e_i^P\|_\rho \|e_i^G\|_\rho + c_8 \|\nabla e_i^P\|_{L^\infty} \|e_i^G\|_\rho, \\ \|e_i^G\|_\rho &\leq 7 \|e_i^P\|_\rho + \sqrt{\frac{16c_3^2}{\beta\lambda_{\min}} + \frac{48c_7^2}{\beta^2}} \|\nabla e_i^P\|_\rho + \frac{7c_8}{\beta} \|\nabla e_i^P\|_{L^\infty}, \end{aligned}$$

which implies that

$$\left\| \hat{V}_i - \hat{V}_i^G \right\|_\rho \leq 8 \|e_i^P\|_\rho + \sqrt{\frac{16c_3^2}{\beta\lambda_{\min}} + \frac{48c_7^2}{\beta^2}} \|\nabla e_i^P\|_\rho + \frac{7c_8}{\beta} \|\nabla e_i^P\|_{L^\infty}.$$

Since the above inequality holds for all V_i^P in the linear space spanned by $\{\Phi\}$, therefore,

$$\left\| \hat{V}_i - \hat{V}_i^G \right\|_\rho \leq \frac{1}{\beta} \hat{C}_G \inf_{V=\theta^\top \Phi} \left\| \hat{V}_i - V \right\|_{H_{\rho,\infty}^1},$$

where

$$\hat{C}_G = \max \left\{ 8\beta, \frac{4c_3\sqrt{\beta}}{\sqrt{\lambda_{\min}}} + 7c_7, 7c_8 \right\}, \quad \|f\|_{H_{\rho,\infty}^1} = \|f\|_{H_\rho^1} + \|\nabla f\|_{L^\infty}. \quad (65)$$

with c_3, c_7, c_8 defined in (58), (63). \square

6.7 Proof of Theorem 4.2

Note that in the proof, we refer the vector norm $\|b\|$ as the Euclidean norm, and the matrix norm $\|A\|$ as the operator norm.

We first prove that the matrix A defined in (26) is positive definite. By applying the first and last inequalities of Proposition 6.3, one has for $\forall \theta \in \mathbb{R}^p$,

$$\begin{aligned} \theta^\top A \theta &= \left\langle \beta V(s) - \mathcal{L}_{\hat{\mu}_1, \hat{\Sigma}_1} V(s), V(s) \right\rangle_\rho, \quad \text{with } V = \Phi(s)^\top \theta \\ &= \beta \|V(s)\|_\rho^2 - \langle \mathcal{L}_{\mu, \Sigma} V(s), V(s) \rangle_\rho - \left\langle \mathcal{L}_{\hat{\mu}_1 - \mu, \hat{\Sigma}_1 - \Sigma} V(s), V(s) \right\rangle_\rho \\ &\geq \beta \|V\|_\rho^2 + \frac{\lambda_{\min}}{2} \|\nabla V\|_\rho^2 \\ &\quad - \left[\left(\|\epsilon_\mu\|_\infty + \frac{1}{2} \|\nabla \cdot \epsilon_\Sigma\|_\infty + \frac{1}{2} \|\epsilon_\Sigma\|_\infty \|\nabla \log \rho\|_\infty \right) \|V(s)\|_\rho \|\nabla V\|_\rho + \frac{1}{2} \|\epsilon_\Sigma\|_\infty \|\nabla V\|_\rho^2 \right] \end{aligned}$$

where $\epsilon_\mu = \hat{\mu}_1 - \mu, \epsilon_\Sigma = \hat{\Sigma}_1 - \Sigma$. By Lemma 6.5, one has

$$\|\epsilon_\mu\|_\infty + \frac{1}{2} \|\nabla \cdot \epsilon_\Sigma\|_\infty + \frac{1}{2} \|\epsilon_\Sigma\|_\infty \|\nabla \log \rho\|_\infty \lesssim (L_\mu + L_\Sigma L_\rho^\infty + L_{\nabla \cdot \Sigma}) \Delta t, \quad \|\epsilon_\Sigma\|_\infty \leq L_\Sigma \Delta t.$$

Under the assumption that $\Delta t \leq \eta_{\mu, \Sigma, \beta}$ defined in (59) is small enough, one can further bound

$$\theta^\top A \theta \geq \frac{\beta}{2} \|V\|_\rho^2 = \frac{\beta}{2} \theta^\top G_\Phi \theta \geq \frac{\beta \lambda_\Phi}{2} \|\theta\|^2,$$

where the last inequality comes from Assumption (28) on Φ .

In addition, one also has boundedness on $\|b\|$,

$$\|b\| = \left\| \int r(s) \Phi(s) \rho(s) ds \right\| \leq R L_\Phi, \quad R = \|r\|_{L^\infty}.$$

Next, one can divided the error $\|\theta_n - \theta\|$ by

$$\begin{aligned} \|\theta_n - \theta\| &= \|A_n^{-1}b_n - A^{-1}b\| = \|A_n^{-1}(b_n - b) - (A_n^{-1} - A^{-1})b\| \\ &\leq \|A_n^{-1}\| \|b_n - b\| + \|A_n^{-1}\| \|A_n - A\| \|A^{-1}\| \|b\|. \end{aligned}$$

If one has,

$$\|A_n - A\| \lesssim \min \left\{ \frac{\beta\lambda_\Phi}{4}, \frac{(\beta\lambda_\Phi)^2\epsilon}{16RL_\Phi^2} \right\}, \quad \|b_n - b\| \leq \frac{\epsilon\beta\lambda_\Phi}{8L_\Phi}$$

then by the positive definite of A and boundedness of b , one has

$$\|V_n - V\| \leq \|\theta_n - \theta\| L_\Phi \leq \left(\frac{4}{\beta\lambda_\Phi} \|b_n - b\| + \frac{8L_\Phi R}{(\beta\lambda_\Phi)^2} \|A_n - A\| \right) L_\Phi \leq \epsilon$$

Since we assume ϵ small enough, so the goal becomes the sample complexity to bound

$$\|b_n - b\| \leq \frac{\epsilon\beta\lambda_\Phi}{8L_\Phi}, \quad \|A_n - A\| \lesssim \frac{(\beta\lambda_\Phi)^2\epsilon}{16RL_\Phi^2} \quad (66)$$

Next, we bound the first term. Let $b_i = r(s_i)\Phi(s_i)$ with $s_i \sim \rho$. By the boundedness of $\|r\|_\infty$ and the almost-sure boundedness of $\Phi(s)$, the random vectors b_i are uniformly bounded. Applying Bernstein's inequality for sums of bounded random vectors [58], we obtain that for $n \geq \log(1/\delta)$, with probability at least $1 - \delta$,

$$\|b_n - b\| = \left\| \frac{1}{n} \sum_{i=1}^n b_i - E[b_i] \right\| \lesssim L_\Phi R \sqrt{\frac{\log(1/\delta)}{n}}$$

Therefore, the sample complexity to achieve the first error in (66) is

$$n \gtrsim \frac{\log(1/\delta)L_\Phi^2 R^2}{\epsilon^2 \beta^2 \lambda_\Phi^2}$$

Now we bound the second term. Let $w_i = s'_i - s_i$. Under Assumption 1, the transition density $\rho(\Delta t, w | s_i)$ admits two-sided Gaussian bounds of Aronson type [2]. Specifically, there exist positive constants c_1, c_2, c_3, c_4 , depending only on the dimension d , the ellipticity constants λ, Λ of $\sigma\sigma^\top$, and $\|b\|_\infty$, such that for all sufficiently small Δt ,

$$c_1 \Delta t^{-d/2} \exp\left(-\frac{|w|^2}{c_2 \Delta t}\right) \leq \rho(\Delta t, w | s_i) \leq c_3 \Delta t^{-d/2} \exp\left(-\frac{|w|^2}{c_4 \Delta t}\right).$$

Define the norm $\|\cdot\|_{\psi_1}$ for scalar random variable X as

$$\|X\|_{\psi_1} = \inf \left\{ C > 0 : \mathbb{E} \left[e^{\frac{|X|}{C}} \right] \leq 2 \right\},$$

and for vector or matrix X , it refers to

$$\|X\|_{\psi_1} = \sup_{\|u\|_2=1} \|u^\top X\|_{\psi_1}, \quad \|X\|_{\psi_1} = \sup_{\|u\|_2=\|v\|_2=1} \|u^\top X v\|_{\psi_1}.$$

then one has,

$$\|w_i\|_{\psi_1|s_i} \lesssim \sigma_{\max} \sqrt{\Delta t}.$$

It is well known that sub-Gaussian random variables are sub-exponential and that

$$\|X\|_{\psi_1} \lesssim \|X\|_{\psi_2},$$

where the implicit constant is universal [58].

Let $M_i(t) := \int_0^t u^\top \sigma(s_\tau) dB_\tau$ with some $\|u\| = 1$, Since the quadratic variant of $M_i(t)$ can be bounded by [24]

$$\langle M_i \rangle_t = \int_0^t u^\top \sigma(s_\tau) \sigma(s_\tau)^\top u d\tau \leq \sigma_{\max}^2 t,$$

$\lambda M_i(t)$ is a continuous local martingale with $M_i(0) = 0$ and $\mathbb{E}[\exp(\frac{\lambda^2}{2} \langle M \rangle_t)] < \infty$ for any finite t . By Doléans–Dade exponential martingale theorem [25, Chapter 3]

$$Z_t := \exp\left(\lambda M_t - \frac{\lambda^2}{2} \langle M \rangle_t\right)$$

is a martingale, and therefore

$$\mathbb{E}[Z_t | s_i(0) = s_i] = Z_0 = 1.$$

It follows that

$$\mathbb{E}[\exp(\lambda M_{\Delta t}) | s_i(0) = s_i] \leq \exp\left(\frac{\lambda^2}{2} \langle M \rangle_{\Delta t}\right) \leq \exp\left(\frac{\lambda^2}{2} \sigma_{\max}^2 \Delta t\right).$$

This implies [58]

$$\|M_i(\Delta t)\|_{\psi_2|s_i} \leq C \sigma_{\max} \sqrt{\Delta t}, \quad (67)$$

for universal constants C . In addition, because the upper bound is independent of s_i , and the relation between $\|\cdot\|_{\psi_1}$ and $\|\cdot\|_{\psi_2}$ [58], one has,

$$\|M_i(\Delta t)\|_{\psi_1} \lesssim \sigma_{\max} \sqrt{\Delta t}. \quad (68)$$

Let $Y_i = \int_0^{\Delta t} \mu(s_i(t)) dt$, then $|Y_i| \leq \|\mu\|_{L^\infty} \Delta t$. Because of (68) and $u^\top w_i = M_i(\Delta t) + u^\top Y_i$, one has

$$\|w_i - \mathbb{E}[w_i]\|_{\psi_1} \leq 2\|w_i\|_{\psi_1} \lesssim \sigma_{\max} \sqrt{\Delta t} + \|\mu\|_{L^\infty} \Delta t.$$

Therefore,

$$\left\| \frac{w_i}{\Delta t} \cdot \nabla \Phi(s_i) - \mathbb{E} \left[\frac{w_i}{\Delta t} \cdot \nabla \Phi(s_i) \right] \right\|_{\psi_1} \lesssim L_\Phi \left(\frac{\sigma_{\max}}{\sqrt{\Delta t}} + \|\mu\|_{L^\infty} \right).$$

By (67) and the boundedness of $\|\nabla^2 \Phi(s)\| \leq L_\Phi$, one has $M_i^\top \nabla^2 \Phi(s_i) M_i$ is sub-exponential, therefore, one has

$$\begin{aligned} & \|w_i^\top \nabla^2 \Phi(s_i) w_i\|_{\psi_1|s_i} \leq \|M_i^\top \nabla^2 \Phi(s_i) M_i\|_{\psi_1|s_i} + 2 \|M_i^\top \nabla^2 \Phi(s_i) Y_i\|_{\psi_1|s_i} + \|Y_i^\top \nabla^2 \Phi(s_i) Y_i\|_{\psi_1|s_i} \\ & \lesssim L_\Phi \left(\sigma_{\max}^2 \Delta t + \|\mu\|_{L^\infty} \sigma_{\max} \Delta t \sqrt{\Delta t} + \|\mu\|_{L^\infty}^2 \Delta t^2 \right) \end{aligned}$$

Hence, one has

$$\begin{aligned} & \left\| \frac{1}{\Delta t} w_i^\top \nabla^2 \Phi(s_i) w_i - \mathbb{E} \left[\frac{1}{\Delta t} w_i^\top \nabla^2 \Phi(s_i) w_i \right] \right\|_{\psi_1} \leq 2 \left\| \frac{1}{\Delta t} w_i^\top \nabla^2 \Phi(s_i) w_i \right\|_{\psi_1} \\ & \lesssim L_\Phi (\sigma_{\max}^2 + \sigma_{\max} \|\mu\|_{L^\infty} \sqrt{\Delta t} + \|\mu\|_{L^\infty}^2 \Delta t). \end{aligned}$$

Therefore, for $A_i = \Phi(s_i) \left(\beta \Phi(s_i) - \frac{w_i}{\Delta t} \cdot \nabla \Phi(s_i) - \frac{1}{2\Delta t} w_i^\top \nabla^2 \Phi(s_i) w_i \right)^\top$

$$\|A_i - \mathbb{E}[A_i]\|_{\psi_1} \lesssim L_\Phi^2 \left(\beta + \frac{\sigma_{\max}}{\sqrt{\Delta t}} + \|\mu\|_{L^\infty} + \sigma_{\max}^2 + \sigma_{\max} \|\mu\|_{L^\infty} \sqrt{\Delta t} + \|\mu\|_{L^\infty}^2 \Delta t \right).$$

Finally, by applying Bernstein inequality [56], one obtains that with probability $1 - \delta$, one has

$$\|A_n - A\| \lesssim \|A_i - \mathbb{E}[A_i]\|_{\psi_1} \left(\sqrt{\frac{\log(2p/\delta)}{n}} + \frac{\log(2p/\delta)}{n} \right)$$

In addition, for $n \geq \log(2p/\delta)$ large enough, and Δt small enough, one can further simplify the above inequality

$$\|A_n - A\| \lesssim \frac{L_\Phi^2 \sigma_{\max}}{\sqrt{\Delta t}} \sqrt{\frac{\log(2p/\delta)}{n}}$$

Therefore, the sample complexity to achieve the error in (66) is

$$n \gtrsim \frac{\log(2p/\delta) R^2 L_\Phi^8 \sigma_{\max}^2}{\beta^4 \epsilon^2 \Delta t \lambda_\Phi^4}.$$

To summarize, with probability $1 - \delta$, if

$$n \gtrsim \max \left\{ \frac{\log(2p/\delta) R^2 L_\Phi^8 \sigma_{\max}^2}{\beta^4 \epsilon^2 \Delta t \lambda_\Phi^4}, \frac{\log(1/\delta) L_\Phi^2 R^2}{\epsilon^2 \beta^2 \lambda_\Phi^2} \right\}$$

one has

$$\left\| V_n - \hat{V}_1^G \right\|_\rho \leq \epsilon$$

This gives the first inequality.

On the other hand, if

$$n \gtrsim n_1 = \frac{16 L_\Phi^4 \log(2p/\delta) \left(\frac{\sigma_{\max}}{\sqrt{\Delta t}} \right)^2}{\beta^2 \lambda_\Phi^2} \approx \frac{L_\Phi^4 \log(2p/\delta) \sigma_{\max}^2 \lambda_\Phi^{-2}}{\beta^2 \Delta t}$$

then w.p. $1 - \delta$, one has

$$\|A_n - A\| \leq \frac{\beta \lambda_\Phi}{4}.$$

Therefore, for $\forall n \geq n_1$, w.p. $1 - \delta$, one has,

$$\begin{aligned} \|V_n - V\| & \leq \left(\frac{4}{\beta \lambda_\Phi} \|b_n - b\| + \frac{8 L_\Phi R}{(\beta \lambda_\Phi)^2} \|A_n - A\| \right) L_\Phi \\ & \lesssim \left(\frac{4}{\beta \lambda_\Phi} L_\Phi R \sqrt{\frac{\log(p/\delta)}{n}} + \frac{8 L_\Phi R}{(\beta \lambda_\Phi)^2} L_\Phi^2 \sigma_{\max} \sqrt{\frac{\log(2p/\delta)}{n \Delta t}} \right) L_\Phi \\ & \lesssim \left(L_\Phi^4 R \sigma_{\max} \lambda_\Phi^{-2} \sqrt{\log(2p/\delta)} \right) \frac{1}{\beta^2 \sqrt{n \Delta t}} \end{aligned}$$

7 Conclusion

In this paper, we introduce PhiBE, a PDE-based Bellman equation that integrates discrete-time information into a continuous-time PDE. PhiBE outperforms the classical Bellman equation in approximating the continuous-time PE problem, particularly in scenarios where underlying dynamics evolve slowly. Importantly, the approximation error of PhiBE depends on the dynamics, making it more robust against changes in reward structures. This property allows greater flexibility in designing reward functions to effectively achieve RL objectives. We further proposed higher-order PhiBE, which yields improved approximations of the true value function and achieves the same accuracy with sparser data, thereby improving sample efficiency. In addition, we developed a model-free algorithm for solving PhiBE under linear function approximation and established theoretical guarantees that sharpen classical RL convergence results, particularly in their dependence on the discretization step size Δt .

This work serves as the first step toward a systematic PDE-based approach to continuous-time reinforcement learning. We expect the PhiBE framework to extend naturally to more general RL settings, including richer function classes and control problems beyond policy evaluation.

Appendix

A Derivation of the HJB equation under deterministic dynamics

By the definition of $V(s)$ in (1), one has

$$V(s_t) = \int_t^\infty e^{-\beta(\tilde{t}-t)} r(s_{\tilde{t}}) d\tilde{t},$$

which implies that,

$$\frac{d}{dt}V(s_t) = \beta \int_t^\infty e^{-\beta(\tilde{t}-t)} r(s_{\tilde{t}}) d\tilde{t} - r(s_t).$$

Using the chain rule on the LHS of the above equation yields $\frac{d}{dt}V(s_t) = \frac{d}{dt}s_t \cdot \nabla V(s_t)$, and the RHS can be written as $\beta V(s_t) - r(s_t)$, resulting in a PDE for the true value function

$$\beta V(s_t) = r(s_t) + \frac{d}{dt}s_t \cdot \nabla V(s_t). \tag{69}$$

or equivalently,

$$\beta V(s) = r(s) + \mu(s) \cdot \nabla V(s). \tag{70}$$

B Proof of Lemmas

B.1 Proof of Lemma 6.1

By Feynman–Kac theorem, it is equivalently to write \hat{V} as,

$$\hat{V} = \int_0^\infty e^{-\beta t} r(\hat{s}_t) dt \quad \text{with} \quad \frac{d}{dt} \hat{s}_t = \hat{\mu}(s_t).$$

Hence,

$$\begin{aligned} |V(s) - \hat{V}(s)| &= \left| \int_0^\infty e^{-\beta t} (r(s_t) - r(\hat{s}_t)) dt \right| = \left| \int_0^\infty e^{-\beta t} \left(\int_{s_t}^{\hat{s}_t} \nabla r(s) ds \right) dt \right| \\ &\leq \|\nabla r\|_{L^\infty} \int_0^\infty e^{-\beta t} |\hat{s}_t - s_t| dt, \end{aligned} \quad (71)$$

where

$$\frac{d}{dt} s_t = \mu(s_t), \quad \frac{d}{dt} \hat{s}_t = \hat{\mu}(\hat{s}_t), \quad s_0 = \hat{s}_0 = s. \quad (72)$$

Subtracting the two equations in (72) and multiplying it with $(\hat{s}_t - s_t)^\top$ gives

$$\begin{aligned} \frac{1}{2} \frac{d}{dt} \|\hat{s}_t - s_t\|^2 &= (\hat{\mu}(\hat{s}_t) - \mu(s_t))(\hat{s}_t - s_t) \\ &= ((\hat{\mu}(\hat{s}_t) - \mu(\hat{s}_t)) + (\mu(\hat{s}_t) - \mu(s_t))) (\hat{s}_t - s_t) \\ &\leq \|\mu - \hat{\mu}\|_{L^\infty} \|\hat{s}_t - s_t\| + \|\nabla \mu(s)\|_{L^\infty} \|\hat{s}_t - s_t\|^2 \\ &\leq \frac{1}{2\epsilon} \|\mu - \hat{\mu}\|_{L^\infty}^2 + \left(\frac{\epsilon}{2} + \|\nabla \mu(s)\|_{L^\infty} \right) \|\hat{s}_t - s_t\|^2, \quad \text{for } \forall \epsilon > 0, \end{aligned}$$

where the mean value theorem is used in the first inequality. This implies

$$\|\hat{s}_t - s_t\|_2 \leq \frac{1}{\sqrt{\epsilon}} \|\mu - \hat{\mu}\|_{L^\infty} t^{1/2} e^{(\epsilon/2 + \|\nabla \mu\|_{L^\infty})t}.$$

Inserting the above inequality back to (71) gives

$$\begin{aligned} \|V(s) - \hat{V}(s)\|_{L^\infty} &\leq \frac{1}{\sqrt{\epsilon}} \|\nabla r\|_{L^\infty} \|\mu - \hat{\mu}\|_{L^\infty} \int_0^\infty e^{-(\beta - \epsilon/2 - \|\nabla \mu\|_{L^\infty})t} t^{1/2} dt \\ &= \frac{\sqrt{\pi} \|\mu - \hat{\mu}\|_{L^\infty} \|\nabla r\|_{L^\infty}}{2\sqrt{\epsilon}(\beta - \epsilon/2 - \|\nabla \mu(s)\|_{L^\infty})^{3/2}}. \end{aligned}$$

Assigning $\epsilon = \frac{1}{2}(\beta - \|\nabla \mu(s)\|_{L^\infty})$ to the above inequality completes the proof.

B.2 Proof of Lemma 6.2

By Taylor expansion, one has

$$s_{j\Delta t} = \sum_{k=0}^i \frac{(j\Delta t)^k}{k!} \left(\frac{d^k}{dt^k} s_t \Big|_{t=0} \right) + \frac{(j\Delta t)^{i+1}}{(i+1)!} \left(\frac{d^{i+1}}{dt^{i+1}} s_t \Big|_{t=\xi_j} \right)$$

with $\xi_j \in (0, j\Delta t)$. Inserting it into $\hat{\mu}_i(s)$ gives,

$$\begin{aligned}
\hat{\mu}_i(s) &= \frac{1}{\Delta t} \sum_{j=0}^i a_j^{(i)} [s_{j\Delta t} | s_0 = s] \\
&= \frac{1}{\Delta t} \sum_{j=0}^i a_j^{(i)} \left[\sum_{k=0}^i \left(\frac{d^k}{dt^k} s_t \Big|_{t=0} \right) \frac{(\Delta t j)^k}{k!} + \left(\frac{d^{i+1}}{dt^{i+1}} s_t \Big|_{t=\xi_j} \right) \frac{(\Delta t j)^{i+1}}{(i+1)!} \right] \\
&= \frac{1}{\Delta t} \sum_{k=0}^i \left(\frac{d^k}{dt^k} s_t \Big|_{t=0} \right) \frac{(\Delta t)^k}{k!} \sum_{j=0}^i a_j^{(i)} j^k + \frac{1}{\Delta t} \sum_{j=0}^i a_j^{(i)} \left(\frac{d^{i+1}}{dt^{i+1}} s_t \Big|_{t=\xi_j} \right) \frac{(\Delta t j)^{i+1}}{(i+1)!} \\
&= \left(\frac{d}{dt} s_t \Big|_{t=0} \right) + \frac{\Delta t^i}{(i+1)!} \sum_{j=0}^i a_j^{(i)} j^{i+1} \left(\frac{d^{i+1}}{dt^{i+1}} s_t \Big|_{t=\xi_j} \right),
\end{aligned}$$

where the last equality is due to the definition of $a^{(i)}$ in (14). Since

$$\frac{d}{dt} s_t \Big|_{t=0} = \mu(s_0) = \mu(s),$$

one has

$$|\hat{\mu}_i(s) - \mu(s)| = \frac{\Delta t^i}{(i+1)!} \left| \sum_{j=0}^i a_j^{(i)} j^{i+1} \left(\frac{d^{i+1}}{dt^{i+1}} s_t \Big|_{t=\xi_j} \right) \right|.$$

Since

$$\frac{d^{i+1}}{dt^{i+1}} s_t = \frac{d^i}{dt^i} (\mu(s_t)) = \mathcal{L}_\mu^i \mu(s_t),$$

then as long as $\|\mathcal{L}_\mu^i \mu(s_t)\|_{L^\infty}$ is bounded, one has

$$\|\hat{\mu}_i(s) - \mu(s)\|_{L^\infty} \leq \frac{\|\mathcal{L}_\mu^i \mu(s)\|_{L^\infty}}{(i+1)!} \sum_{j=0}^i |a_j^{(i)}| j^{i+1} \Delta t^i = C_i \|\mathcal{L}_\mu^i \mu(s)\|_{L^\infty} \Delta t^i.$$

B.3 Proof of Lemma 6.4

Subtracting the second equation from the first one and let $e(s) = V(s) - \hat{V}(s)$ gives,

$$\beta e = \mathcal{L}_{\mu, \Sigma} e + (\mathcal{L}_{\mu, \Sigma} - \mathcal{L}_{\hat{\mu}, \hat{\Sigma}}) \hat{V}.$$

Multiply the above equation with $e(s)\rho(s)$ and integrate it over $s \in \mathbb{S}$, one has,

$$\begin{aligned}
\frac{\beta}{2} \|e\|_\rho^2 &= \langle \mathcal{L}_{\mu, \Sigma} e, e \rangle_\rho + \langle \mathcal{L}_{\hat{\mu} - \mu, \hat{\Sigma} - \Sigma} \hat{V}, e \rangle_\rho \\
&\leq -\frac{\lambda_{\min}}{4} \|\nabla e\|_\rho^2 + \left(C_\mu + \frac{1}{2} C_{\nabla \cdot \Sigma} \right) \|e\|_\rho \|\nabla \hat{V}\|_\rho + \frac{1}{2} C_\Sigma \|\nabla e\|_\rho \|\nabla \hat{V}\|_\rho \\
&\quad + \frac{1}{2} C_\Sigma L_\rho \|e\|_\rho \|\nabla \hat{V}\|_{L^\infty} \\
&\leq -\left(\frac{\lambda_{\min}}{4} - c_2 \right) \|\nabla e\|_\rho^2 + \left(c_1 \|e\|_\rho + c_2 \|\nabla V\|_\rho \right) \|\nabla e\|_\rho + \left(c_1 \|\nabla V\|_\rho + c_3 \|\nabla \hat{V}\|_{L^\infty} \right) \|e\|_\rho,
\end{aligned} \tag{73}$$

where the first and third equations in Proposition 6.3 are used for the first inequality, $\|\nabla\hat{V}\|_\rho \leq \|\nabla V\|_\rho + \|\nabla e\|_\rho$ are used for the second inequality, and $c_1 = C_\mu + \frac{1}{2}C_{\nabla\Sigma}$, $c_2 = \frac{1}{2}C_\Sigma$, $c_3 = \frac{1}{2}C_\Sigma L_\rho$. Under the assumption that $c_2 \leq \frac{\lambda_{\min}}{4}$, one has

$$\begin{aligned} \frac{\beta}{2} \|e\|_\rho^2 &\leq -\frac{\lambda_{\min}}{8} \left(\|\nabla e\|_\rho - \frac{4}{\lambda_{\min}}(c_1 \|e\|_\rho + c_2 \|\nabla V\|_\rho) \right)^2 \\ &\quad + \frac{2}{\lambda_{\min}}(c_1 \|e\|_\rho + c_2 \|\nabla V\|_\rho)^2 + \left(c_1 \|\nabla V\|_\rho + c_3 \|\nabla\hat{V}\|_{L^\infty} \right) \|e\|_\rho \\ &\leq \frac{2c_1^2}{\lambda_{\min}} \|e\|_\rho^2 + \left[\left(\frac{4c_1c_2}{\lambda_{\min}} + c_1 \right) \|\nabla V\|_\rho + c_3 \|\nabla\hat{V}\|_{L^\infty} \right] \|e\|_\rho + \frac{2c_2^2}{\lambda_{\min}} \|\nabla V\|_\rho^2. \end{aligned}$$

Under the assumption that $2c_1^2 \leq \frac{1}{8}\beta\lambda_{\min}$, one has

$$\frac{\beta}{4} \|e\|_\rho^2 \leq \left[\frac{4}{\beta} \left(\frac{4c_1c_2}{\lambda_{\min}} + c_1 \right)^2 + \frac{2c_2^2}{\lambda_{\min}} \right] \|\nabla V\|_\rho^2 + \frac{4c_3^2}{\beta} \|\nabla\hat{V}\|_{L^\infty}^2 + \frac{\beta}{8} \|e\|_\rho^2,$$

which yields,

$$\|e\|_\rho \leq \left[\frac{4c_1}{\beta} \left(\frac{4c_2}{\lambda_{\min}} + 1 \right) + \frac{3c_2}{\sqrt{\beta\lambda_{\min}}} \right] \|\nabla V\|_\rho + \frac{4c_3}{\beta} \|\nabla\hat{V}\|_{L^\infty}.$$

B.4 Proof of Lemma 6.5

The proof of Lemma 6.5 relies on the following two lemmas, which we will prove later.

Lemma B.1. Define operator $\Pi_{i,\Delta t}f(s) = \frac{1}{\Delta t} \mathbb{E}[\sum_{j=1}^i a_j^{(i)} f(s_j\Delta t - s_0) | s_0 = s]$ with $a_j^{(i)}$ defined in (14) and $f(0) = 0$, then

$$\Pi_{i,\Delta t}f(s) = [\mathcal{L}_{\mu,\Sigma}f](0) + \frac{1}{\Delta t i!} \sum_{j=1}^i a_j^{(i)} \int_0^{j\Delta t} \mathbb{E}[\mathcal{L}_{\mu,\Sigma}^{i+1}f(s_t - s_0) | s_0 = s] t^i dt.$$

Lemma B.2. For $p(s, t) = \mathbb{E}[f(s_t) | s_0 = s]$ with s_t driven by the SDE (2), then under Assumption 1/(a), one has

$$\|\nabla p(s, t)\|_{L^\infty} \leq \sqrt{\frac{C_{\nabla\mu, \nabla\Sigma}}{\lambda_{\min}}} \|f\|_{L^\infty} + \|\nabla f\|_{L^\infty}, \quad \text{with } C_{\nabla\mu, \nabla\Sigma} \text{ defined in (52).}$$

For $p(s, t) = \mathbb{E}[f(s_t)(s_t - s_0) | s_0 = s]$ with s_t driven by the SDE (2), then under Assumption 1/(a), one has

$$\begin{aligned} \|p(s, t)\|_{L^\infty} &\leq C_1(\|\mu\|_{C^1}, \|\Sigma\|_{C^1}, \|f\|_{C^1}) \sqrt{e^t - 1}. \\ \|\nabla p(s, t)\|_{L^\infty} &\leq C_2(\|\mu\|_{C^2}, \|\Sigma\|_{C^2}, \|f\|_{C^2}) \sqrt{e^t - 1}. \end{aligned}$$

where $C_1(\|\mu\|_{C^1}, \|\Sigma\|_{C^1}, \|f\|_{C^1})$ and $C_2(\|\mu\|_{C^2}, \|\Sigma\|_{C^2}, \|f\|_{C^2})$ are defined in (86) and (91).

Now we are ready to prove Lemma 6.5. By Lemma B.1, one has

$$\hat{\mu}_i(s) = \mu(s) + \frac{1}{\Delta t i!} \sum_{j=1}^i a_j^{(i)} \left(\int_0^{j\Delta t} \mathbb{E}[\mathcal{L}_{\mu, \Sigma}^i \mu(s_t) | s_0 = s] t^i dt \right), \quad (74)$$

which implies that

$$\|\hat{\mu}_i(s) - \mu(s)\|_{L^\infty} \leq \frac{\|\mathcal{L}_{\mu, \Sigma}^i \mu(s)\|_{L^\infty}}{\Delta t i!} \sum_{j=1}^i |a_j^{(i)}| \int_0^{j\Delta t} t^i dt \leq L_\mu \Delta t^i,$$

where

$$L_\mu = \hat{C}_i \|\mathcal{L}_{\mu, \Sigma}^i \mu(s)\|_{L^\infty} \quad \text{with } \hat{C}_i = \sum_{j=1}^i \frac{|a_j^{(i)}| j^{i+1}}{(i+1)!} \text{ defined in (49)}. \quad (75)$$

To prove the second inequality in the lemma, first apply Lemma B.1, one has

$$\begin{aligned} \hat{\Sigma}_i(s) &= \Sigma(s) \\ &+ \frac{1}{\Delta t i!} \sum_{j=1}^i a_j^{(i)} \int_0^{j\Delta t} \mathbb{E}[\mathcal{L}_{\mu, \Sigma}^i (\mu(s_t)(s_t - s_0)^\top + (s_t - s_0)\mu^\top(s_t) + \Sigma(s_t)) | s_0 = s] t^i dt. \end{aligned} \quad (76)$$

Note that

$$\begin{aligned} h(s_t) &:= \mathcal{L}_{\mu, \Sigma}^i (\mu(s_t)(s_t - s_0)^\top + (s_t - s_0)\mu^\top(s_t) + \Sigma(s_t)) \\ &\quad - [\mathcal{L}_{\mu, \Sigma}^i \mu(s_t)(s_t - s_0)^\top + (s_t - s_0)(\mathcal{L}_{\mu, \Sigma}^i \mu(s_t))^\top] \end{aligned} \quad (77)$$

is a function that only depends on the derivative $\nabla^j \Sigma, \nabla^j \mu$ up to $2i$ -th order, which can be bounded under Assumption 1/(b). Thus applying the second inequality of Lemma B.2 yields

$$\begin{aligned} &\|\mathbb{E}[\mathcal{L}_{\mu, \Sigma}^i (\mu(s_t)(s_t - s_0)^\top + (s_t - s_0)\mu^\top(s_t) + \Sigma(s_t)) | s_0 = s]\|_{L^\infty} \\ &\leq \|h(s)\|_{L^\infty} + 2C_1 e^{t/2}, \end{aligned}$$

where $C_1 = C_1(\|\mu\|_{C^1}, \|\Sigma\|_{C^1}, \|\mathcal{L}_{\mu, \Sigma}^i \mu\|_{C^1})$ defined in (86). Hence, one has,

$$\begin{aligned} &\left\| \int_0^{j\Delta t} \mathbb{E}[\mathcal{L}_{\mu, \Sigma}^i (\mu(s_t)(s_t - s_0)^\top + (s_t - s_0)\mu^\top(s_t) + \Sigma(s_t)) | s_0 = s] t^i dt \right\|_{L^\infty} \\ &\leq \frac{1}{i+1} \|h\|_{L^\infty} (j\Delta t)^{i+1} + 2C_1 \int_0^{j\Delta t} (2+t)t^i dt, \quad \text{for } j\Delta t \leq 3 \\ &= \frac{1}{i+1} (\|h\|_{L^\infty} + 4C_1) (j\Delta t)^{i+1} + 2C_1 \frac{1}{i+2} (j\Delta t)^{i+2}, \end{aligned}$$

where $e^{t/2} \leq 2+t$ for $t \leq 3$ are used in the first inequality. Plugging the above inequality back to (76) implies

$$\left\| \hat{\Sigma}_i(s) - \Sigma(s) \right\|_{L^\infty} \leq L_\Sigma \Delta t^i + o(\Delta t^i),$$

where

$$L_\Sigma = \hat{C}_i (\|h(s)\|_{L^\infty} + 4C_1 (\|\mu\|_{C^1}, \|\Sigma\|_{C^1}, \|\mathcal{L}_{\mu, \Sigma}^i \mu\|_{C^1})) \quad (78)$$

with $\hat{C}_i, h(s), C_1(p, q, g)$ defined in (75), (77), (86).

To prove the third inequality, one first takes $\nabla \cdot$ to (76),

$$\nabla \cdot \hat{\Sigma}_i(s) = \nabla \cdot \Sigma(s) + \frac{1}{\Delta t i!} \sum_{j=1}^i a_j^{(i)} \int_0^{j\Delta t} \nabla \cdot p(s, t) t^i dt,$$

where

$$p(s, t) = \mathbb{E}[h(s_t) | s_0 = s] + \mathbb{E}[\mathcal{L}_{\mu, \Sigma}^i \mu(s_t) (s_t - s_0)^\top + (s_t - s_0) (\mathcal{L}_{\mu, \Sigma}^i \mu(s_t))^\top | s_0 = s],$$

with h defined in (77). Therefore, by the first and third inequalities in Lemma B.2, and denoting $c_1 = \sqrt{C_{\nabla \mu, \nabla \Sigma} / \lambda_{\min}} \|h\|_{L^\infty} + \|\nabla \cdot h\|_{L^\infty}$, $c_2 = C_2(\|\mu\|_{C^2}, \|\Sigma\|_{C^2}, \|\mathcal{L}_{\mu, \Sigma}^i \mu\|_{C^2})$, one has

$$\begin{aligned} \left\| \nabla \cdot \hat{\Sigma}_i(s) - \nabla \cdot \Sigma(s) \right\|_{L^\infty} &\leq \frac{1}{\Delta t i!} \sum_{j=1}^i |a_j^{(i)}| \left(\int_0^{j\Delta t} c_1 t^i + 2c_2 e^{t/2} t^i dt \right) \\ &\leq \frac{1}{\Delta t i!} \sum_{j=1}^i |a_j^{(i)}| \left(\int_0^{j\Delta t} (c_1 + 4c_2) t^i + 2c_2 t^{i+1} dt \right) = L_{\nabla \cdot \Sigma} \Delta t^i + o(\Delta t^i), \end{aligned} \quad (79)$$

where

$$\begin{aligned} L_{\nabla \cdot \Sigma} &= \hat{C}_i \left[\sqrt{C_{\nabla \mu, \nabla \Sigma} / \lambda_{\min}} \|h\|_{L^\infty} + \|\nabla \cdot h\|_{L^\infty} \right. \\ &\quad \left. + 4C_2(\|\mu\|_{C^2}, \|\Sigma\|_{C^2}, \|\mathcal{L}_{\mu, \Sigma}^i \mu\|_{C^2}) \right], \end{aligned} \quad (80)$$

with $\hat{C}_i, h(s), C_{\nabla \mu, \nabla \Sigma}, C_2(p, q, g)$ defined in (75), (77), (52), (91).

Proof of Lemma B.1

Proof. First note that

$$\Pi_{i, \Delta t} f(s) = \frac{1}{\Delta t} \sum_{j=1}^i a_j^{(i)} \int_{\mathbb{S}} f(s' - s) \rho(s', j\Delta t | s) ds', \quad (81)$$

where $\rho(s', t | s)$ is defined in (45). By Taylor's expansion, one has

$$\rho(s', j\Delta t | s) = \sum_{k=0}^i \partial_t^k \rho(s', 0 | s) \frac{(j\Delta t)^k}{k!} + \frac{1}{i!} \int_0^{j\Delta t} \partial_t^{i+1} \rho(s', t | s) t^i dt.$$

Inserting the above equation into (81) yields,

$$\begin{aligned} \Pi_{i, \Delta t} f(s) &= \underbrace{\frac{1}{\Delta t} \sum_{k=0}^i \left(\sum_{j=1}^i a_j^{(i)} j^k \right) \frac{(\Delta t)^k}{k!} \int_{\mathbb{S}} f(s' - s) \partial_t^k \rho(s', 0 | s) ds'}_I \\ &\quad + \underbrace{\frac{1}{\Delta t i!} \sum_{j=1}^i a_j^{(i)} \left(\int_{\mathbb{S}} \int_0^{j\Delta t} f(s' - s) \partial_t^{i+1} \rho(s', t | s) t^i dt ds' \right)}_{II}. \end{aligned}$$

By the definition of $a_j^{(i)}$, the first part can be simplified to

$$\begin{aligned} I &= \frac{1}{\Delta t} \left(\sum_{j=1}^i a_j^{(i)} \right) \int_{\mathbb{S}} f(s' - s) \rho(s', 0|s) ds' + \int_{\mathbb{S}} f(s' - s) \partial_t \rho(s', 0|s) ds' \\ &= \frac{\sum_{j=1}^i a_j^{(i)}}{\Delta t} f(0) + \int_{\mathbb{S}} \mathcal{L}_{\mu, \Sigma} f(s' - s) \rho(s', 0|s) ds' = \mathcal{L}_{\mu, \Sigma} f(0). \end{aligned}$$

Apply integration by parts, the second part can be written as

$$II = \frac{1}{\Delta t i!} \sum_{j=1}^i a_j^{(i)} \int_0^{j\Delta t} \mathbb{E}[\mathcal{L}_{\mu, \Sigma}^{i+1} f(s_t - s_0) | s_0 = s] t^i dt,$$

which completes the proof. \square

Proof of Lemma B.2

Proof. Note that $p(s, t)$ satisfies the following forward Kolmogorov equation [39],

$$\partial_t p(s, t) = \mathcal{L}_{\mu, \Sigma} p(s, t), \quad \text{with } p(s, 0) = f(s).$$

Multiplying p to the above equation and let $q_l = \partial_{s_l} p$, with Assumption 1/(a), one has

$$\partial_t \left(\frac{1}{2} p^2 \right) = \mathcal{L}_{\mu, \Sigma} \left(\frac{1}{2} p^2 \right) - \frac{1}{2} q^\top \Sigma q, \quad \partial_t \left(\frac{1}{2} p^2 \right) \leq \mathcal{L}_{\mu, \Sigma} \left(\frac{1}{2} p^2 \right) - \frac{\lambda_{\min}}{2} \|q\|_2^2. \quad (82)$$

On the other hand, q_l satisfies

$$\partial_t q_l = \mathcal{L}_{\mu, \Sigma} q_l + \mathcal{L}_{\partial_{s_l} \mu, \partial_{s_l} \Sigma} p, \quad \text{with } q(s, 0) = \partial_{s_l} f(s). \quad (83)$$

Multiplying q_l to the above equation and then summing it over l gives,

$$\begin{aligned} \partial_t \left(\frac{1}{2} \|q\|_2^2 \right) &= \mathcal{L}_{\mu, \Sigma} \left(\frac{1}{2} \|q\|_2^2 \right) - \frac{1}{2} \sum_l (\nabla q_l)^\top \Sigma (\nabla q_l) + q^\top \nabla \mu \cdot q + \sum_l \frac{1}{2} (\partial_{s_l} \Sigma : \nabla q) q_l, \\ \partial_t \left(\frac{1}{2} \|q\|_2^2 \right) &\leq \mathcal{L}_{\mu, \Sigma} \left(\frac{1}{2} \|q\|_2^2 \right) - \frac{\lambda_{\min}}{2} \|\nabla q\|_2^2 + \|\nabla \mu\|_2 \|q\|_2^2 + \frac{1}{2} \|\nabla \Sigma\|_2 \|\nabla q\|_2 \|q\|_2 \\ &\leq \mathcal{L}_{\mu, \Sigma} \left(\frac{1}{2} \|q\|_2^2 \right) + \underbrace{\left(\|\nabla \mu\|_{L^\infty} + \frac{\|\nabla \Sigma\|_{L^\infty}^2}{8\lambda_{\min}} \right)}_{\frac{\lambda_{\min} c}{2}} \|q\|_2^2. \end{aligned}$$

Adding the above inequality to $c \times (82)$ with $c = \frac{C_{\nabla \mu, \nabla \Sigma}}{\lambda_{\min}}$ and $C_{\nabla \mu, \nabla \Sigma}$ defined in (52), one has

$$\partial_t \left(\frac{c}{2} p^2 + \frac{1}{2} \|q\|_2^2 \right) \leq \mathcal{L}_{\mu, \Sigma} \left(\frac{c}{2} p^2 + \frac{1}{2} \|q\|_2^2 \right).$$

Let $g(s, t) = \frac{c}{2}p^2 + \frac{1}{2}\|q\|_2^2$, then $\partial_t g \leq \mathcal{L}_{\mu, \Sigma} g$. Let $g_1(s, t) = \mathbb{E}[cf(s_t)^2/2 + \|\nabla f(s_t)\|_2^2/2 | s_0 = s]$, then $g_1(s, t)$ satisfying $\partial_t g_1 = \mathcal{L}_{\mu, \Sigma} g_1$, with $g_1(0, s) = g(0, s)$. Since $\|g_1(t, s)\|_{L^\infty} \leq \frac{c}{2}\|f\|_{L^\infty}^2 + \frac{1}{2}\|\nabla f\|_{L^\infty}^2$, by comparison theorem, one has for $\forall s \in \mathbb{S}$

$$g(t, s) \leq g_1(t, s) \leq \frac{1}{2}(c\|f\|_{L^\infty}^2 + \|\nabla f\|_{L^\infty}^2),$$

which completes the proof for the first inequality.

For the second $p(t, s) = \mathbb{E}[f(s_t)(s_t - s_0) | s_0 = s]$, Let $p_1(t, s) = \mathbb{E}[f(s_t)s_t | s_0 = s]$, $p_2(t, s) = \mathbb{E}[f(s_t) | s_0 = s]$, then note that it satisfies the following PDE,

$$\partial_t p = \partial_t(p_1 - p_2 s) = \mathcal{L}_{\mu, \Sigma} p_1 - (\mathcal{L}_{\mu, \Sigma} p_2) s = \mathcal{L}_{\mu, \Sigma} p + \mu p_2 + \Sigma \nabla p_2, \quad \text{with } p(0, s) = 0.$$

Multiplying it with p^\top and letting $q = \nabla p$ gives,

$$\partial_t \left(\frac{1}{2} \|p\|_2^2 \right) \leq \mathcal{L}_{\mu, \Sigma} \left(\frac{1}{2} \|p\|_2^2 \right) - \frac{\lambda_{\min}}{2} \|q\|_2^2 + \frac{1}{2a} \|\mu p_2 + \Sigma \nabla p_2\|_{L^\infty}^2 + \frac{a}{2} \|p\|_2^2, \quad \text{for } \forall a > 0.$$

Let $c_2 = \|\mu p_2 + \Sigma \nabla p_2\|_{L^\infty}^2$, one has

$$\partial_t \left(\frac{1}{2} \|p\|_2^2 \right) \leq \mathcal{L}_{\mu, \Sigma} \left(\frac{1}{2} \|p\|_2^2 \right) - \frac{\lambda_{\min}}{2} \|q\|_2^2 + \frac{c_2}{2a} + \frac{a}{2} \|p\|_2^2, \quad \text{for } \forall a > 0. \quad (84)$$

Let $g(t, s) = \frac{1}{2} \|p\|_2^2 e^{-at} + \frac{c_2}{2a^2} e^{-at}$, then,

$$\partial_t g \leq \mathcal{L}_{\mu, \Sigma} g, \quad \text{with } g(0, s) = \frac{c_2}{2a^2}. \quad (85)$$

Similarly, by comparison theorem, $\|g(t, s)\|_{L^\infty} \leq \|g(0, s)\|_{L^\infty} = \frac{c_2}{2a^2}$, which implies,

$$\|p(t, \cdot)\|_{L^\infty} \leq \frac{\sqrt{c_2}}{a} \sqrt{e^{at} - 1} = \sqrt{c_2} \sqrt{e^t - 1} \leq C_1 (\|\mu\|_{C^1}, \|\Sigma\|_{C^1}, \|f\|_{C^1}) \sqrt{e^t - 1}$$

with

$$C_1 (\|\mu\|_{C^1}, \|\Sigma\|_{C^1}, \|f\|_{C^1}) = \|\mu\|_{L^\infty} \|f\|_{L^\infty} + \|\Sigma\|_{L^\infty} \left(\sqrt{\frac{C_{\nabla \mu, \nabla \Sigma}}{\lambda_{\min}}} \|f\|_{L^\infty} + \|\nabla f\|_{L^\infty} \right) \quad (86)$$

where the first equality is obtained by selecting $a = 1$. One obtains the last inequality by applying the first inequality in this Lemma to $\|\nabla p_2\|_{L^\infty}$ and $\|p_2\|_{L^\infty} \leq \|f\|_{L^\infty}$.

On the other hand, letting $h(t, s) = \mu p_2 + \Sigma \nabla p_2$, taking ∇ to (85) and multiplying q^\top to it gives,

$$\partial_t \left(\frac{1}{2} \|q\|_2^2 \right) = \mathcal{L}_{\mu, \Sigma} \left(\frac{1}{2} \|q\|_2^2 \right) - \frac{1}{2} \sum_l (\nabla q_l)^\top \Sigma (\nabla q_l) + q^\top \nabla \mu \cdot q + \sum_l \frac{1}{2} (\partial_{s_l} \Sigma : \nabla q) q_l + q \cdot \nabla h, \quad (87)$$

$$\begin{aligned} \partial_t \left(\frac{1}{2} \|q\|_2^2 \right) &\leq \mathcal{L}_{\mu, \Sigma} \left(\frac{1}{2} \|q\|_2^2 \right) - \frac{\lambda_{\min}}{2} \|\nabla q\|_2^2 + \|\nabla \mu\|_2 \|q\|_2^2 + \frac{1}{2} \|\nabla \Sigma\|_2 \|\nabla q\|_2 \|q\|_2 + \frac{1}{2a} \|\nabla h\|_{L^\infty}^2 \\ &\quad + \frac{a}{2} \|q\|_2^2 \\ &\leq \mathcal{L}_{\mu, \Sigma} \left(\frac{1}{2} \|q\|_2^2 \right) + \left(\|\nabla \mu\|_{L^\infty} + \frac{\|\nabla \Sigma\|_{L^\infty}^2}{8\lambda_{\min}} \right) \|q\|_2^2 + \frac{1}{2a} \|\nabla h\|_{L^\infty}^2 + \frac{a}{2} \|q\|_2^2. \end{aligned}$$

Adding the above inequality to $c \times (84)$ with $c = \frac{C_{\nabla\mu, \nabla\Sigma}}{\lambda_{\min}}$ and $C_{\nabla\mu, \nabla\Sigma}$ defined in (52), one has

$$\partial_t \left(\frac{1}{2} p^2 + \frac{c}{2} \|q\|_2^2 \right) \leq \mathcal{L}_{\mu, \Sigma} \left(\frac{1}{2} p^2 + \frac{c}{2} \|q\|_2^2 \right) + \frac{1}{2a} (\|\nabla h\|_{L^\infty}^2 + c \|\mu\|_{L^\infty}^2) + a \left(\frac{1}{2} \|p\|_2^2 + \frac{c}{2} \|q\|_2^2 \right).$$

Let $g(s, t) = \left(\frac{c}{2} p^2 + \frac{1}{2} \|q\|_2^2 \right) e^{-at} + \frac{1}{2a^2} (c \|\mu\|_{L^\infty}^2 + \|\nabla h\|_{L^\infty}^2) e^{-at}$, then

$$\partial_t g \leq \mathcal{L}_{\mu, \Sigma} g, \quad \text{with } g(s, 0) = \frac{1}{2a^2} (c \|\mu\|_{L^\infty}^2 + \|\nabla h\|_{L^\infty}^2).$$

By the comparison theorem, one has $g(s, t) \leq 0$, which implies

$$\frac{c}{2} \|p\|_{L^\infty}^2 + \frac{1}{2} \|q\|_{L^\infty}^2 \leq \frac{1}{2a^2} (c \|\mu\|_{L^\infty}^2 + \|\nabla h\|_{L^\infty}^2) (e^{at} - 1)$$

$$\|q\|_{L^\infty} \leq (\sqrt{c} \|\mu\|_{L^\infty} + \|\nabla h\|_{L^\infty}) \sqrt{e^t - 1}$$

Since one needs to bound $\nabla^2 p_2$, we will estimate it first. Taking ∂_{s_k} to (83), and letting $q_{lk} = \partial_{s_k} \partial_{s_l} p$, one has,

$$\partial_t q_{lk} = \mathcal{L}_{\mu, \Sigma} q_{lk} + \mathcal{L}_{\partial_{s_l} \mu, \partial_{s_l} \Sigma} q_{lk} + \mathcal{L}_{\partial_{s_k} \mu, \partial_{s_k} \Sigma} q_{lk} + \mathcal{L}_{\partial_{s_l} \partial_{s_k} \mu, \partial_{s_l} \partial_{s_k} \Sigma} P$$

Multiplying q_{lk} to both sides of the above equation, and summing it over l, m gives,

$$\begin{aligned} & \partial_t \left(\frac{1}{2} \|\nabla^2 p\|_2^2 \right) \\ & \leq \mathcal{L}_{\mu, \Sigma} \left(\frac{1}{2} \|\nabla^2 p\|_2^2 \right) + \underbrace{\left(\|\nabla \mu\|_{L^\infty}^2 + \frac{\|\nabla \Sigma\|_{L^\infty}^2}{2\lambda_{\min}} + \frac{1}{2} \|\nabla^2 \Sigma\|_{L^\infty}^2 \right)}_{c_3} \|\nabla^2 p\|_2^2 + \frac{1}{2} \|\nabla^2 \mu\|_2^2 \|q\|_2^2 \end{aligned} \quad (88)$$

The equation (87) gives

$$\partial_t \left(\frac{1}{2} \|\nabla p\|_2^2 \right) \leq \mathcal{L}_{\mu, \Sigma} \left(\frac{1}{2} \|\nabla p\|_2^2 \right) - \frac{\lambda_{\min}}{4} \|\nabla^2 p\|_2^2 + \lambda_{\min} c \|q\|_2^2. \quad (89)$$

Now combining (82), (89) and (88) leads to,

$$\begin{aligned} & (82) \times \frac{2}{\lambda_{\min}} \left(\frac{1}{2} \|\nabla^2 \mu\|_2^2 + 4cc_3 \right) + (89) \times \frac{4c_3}{\lambda_{\min}} + (88) \\ & = \frac{1}{2} \partial_t \left[\frac{2}{\lambda_{\min}} \left(\frac{1}{2} \|\nabla^2 \mu\|_2^2 + 4cc_3 \right) \|p\|_2^2 + \frac{4c_3}{\lambda_{\min}} \|\nabla p\|_2^2 + \|\nabla^2 p\|_2^2 \right] \\ & \leq \frac{1}{2} \mathcal{L}_{\mu, \Sigma} \left[\frac{2}{\lambda_{\min}} \left(\frac{1}{2} \|\nabla^2 \mu\|_2^2 + 4cc_3 \right) \|p\|_2^2 + \frac{4c_3}{\lambda_{\min}} \|\nabla p\|_2^2 + \|\nabla^2 p\|_2^2 \right] \end{aligned} \quad (90)$$

By comparison theorem, one has

$$\|\nabla^2 p\|_2 \leq \frac{1}{\sqrt{\lambda_{\min}}} (\|\nabla^2 \mu\|_2 + 2\sqrt{cc_3}) \|f\|_2 + \frac{2\sqrt{c_3}}{\sqrt{\lambda_{\min}}} \|\nabla f\|_2 + \|\nabla^2 f\|_2$$

By the first inequality of this Lemma and the above inequality, one has,

$$\sqrt{c} \|\mu\|_{L^\infty} + \|\nabla h\|_{L^\infty} \leq C_2(\|\mu\|_{C^2}, \|\Sigma\|_{C^2}, \|f\|_{C^2})$$

where

$$\begin{aligned} & C_2(\|\mu\|_{C^2}, \|\Sigma\|_{C^2}, \|f\|_{C^2}) \\ &= \sqrt{c} \|\mu\|_{L^\infty} + \|\nabla \mu\|_{L^\infty} \|f\|_{L^\infty} \\ & \quad + (\|\mu\|_{L^\infty} + \|\nabla \Sigma\|_{L^\infty}) (\sqrt{c} \|f\|_{L^\infty} + \|\nabla f\|_{L^\infty}) \\ & \quad + \|\Sigma\|_{L^\infty} \left[\frac{1}{\sqrt{\lambda_{\min}}} (\|\nabla^2 \mu\|_2 + 2\sqrt{cc_3}) \|f\|_2^2 + \frac{2\sqrt{c_3}}{\sqrt{\lambda_{\min}}} \|\nabla f\|_2 + \|\nabla^2 f\|_2 \right] \end{aligned} \tag{91}$$

which completes the proof. \square

B.5 Proof of Lemma 6.6

Based on Proposition 6.3, one has

$$\begin{aligned} \frac{\beta}{2} \|V\|_\rho^2 - \langle r(s), V(s) \rangle_\rho &\leq -\frac{\lambda_{\min}}{4} \|\nabla V(s)\|_\rho^2; \\ \beta \|\nabla V\|_\rho^2 - \langle \nabla r(s), \nabla V(s) \rangle_\rho &\leq \frac{C_{\nabla \mu, \nabla \Sigma}}{2} \|\nabla V\|_\rho^2. \end{aligned}$$

Multiplying $\frac{2C_{\nabla \mu, \nabla \Sigma}}{\lambda_{\min}}$ to the first inequality and adding it to the second one gives

$$\begin{aligned} & \beta \left(\frac{C_{\nabla \mu, \nabla \Sigma}}{\lambda_{\min}} \|V\|^2 + \|\nabla V(s)\|_\rho^2 \right) \\ & \leq \frac{1}{2\beta} \left(\frac{C_{\nabla \mu, \nabla \Sigma}}{\lambda_{\min}} \|r\|_\rho^2 + \|\nabla r\|_\rho^2 \right) + \frac{\beta}{2} \left(\frac{2C_{\nabla \mu, \nabla \Sigma}}{\lambda_{\min}} \|V\|_\rho^2 + \|\nabla V\|_\rho^2 \right), \end{aligned} \tag{92}$$

which implies

$$\|\nabla V(s)\|_\rho \leq \frac{2}{\beta} \left(\sqrt{\frac{C_{\nabla \mu, \nabla \Sigma}}{\lambda_{\min}}} \|r\|_\rho + \|\nabla r\|_\rho \right).$$

For the second inequality, Let $p(s, t) = \mathbb{E}[r(s_t) | s_0 = s]$, then by Lemma B.2, one has

$$\begin{aligned} & \left\| \nabla \hat{V}(s) \right\|_{L^\infty} = \left\| \int_0^\infty e^{-\beta t} \nabla p(s, t) dt \right\|_{L^\infty} \leq \int_0^\infty e^{-\beta t} \|\nabla p(s, t)\|_{L^\infty} dt \\ & \leq \int_0^\infty e^{-\beta t} \left(\sqrt{\frac{C_{\nabla \hat{\mu}, \nabla \hat{\Sigma}}}{\lambda_{\min}}} \|r\|_{L^\infty} + \|\nabla r\|_{L^\infty} \right) dt \\ & \leq \frac{1}{\beta} \left(\frac{1}{\sqrt{\lambda_{\min}}} \sqrt{2C_{\nabla \mu, \nabla \Sigma} + \frac{1}{2\lambda_{\min}} \left\| \nabla(\Sigma - \hat{\Sigma}) \right\|_{L^\infty}^2} + 2\|\nabla(\mu - \hat{\mu})\|_{L^\infty} \|r\|_{L^\infty} + \|\nabla r\|_{L^\infty} \right). \end{aligned}$$

Similar to the estimate of the $\left\| \nabla \cdot (\Sigma - \hat{\Sigma}) \right\|_{L^\infty}$ in Lemma 6.2, one has,

$$\left\| \nabla(\Sigma - \hat{\Sigma}_i) \right\|_{L^\infty} \leq L_{\nabla \Sigma} \Delta t^i + o(\Delta t^i),$$

where

$$L_{\nabla\Sigma} = \hat{C}_i \left[\sqrt{C_{\nabla\mu, \nabla\Sigma} / \lambda_{\min}} \|h\|_{L^\infty} + \|\nabla h\|_{L^\infty} + 4 \left(\sqrt{C_{\nabla\mu, \nabla\Sigma} / \lambda_{\min}} \|\mu\|_{L^\infty} + \|\nabla\mu\|_{L^\infty} \right) \right], \quad (93)$$

with $\hat{C}_i, h(s), C_{\nabla\mu, \nabla\Sigma}$ defined in (75), (77), (52). Taking ∇ to (74) gives,

$$\|\nabla(\mu - \hat{\mu}_i)\|_{L^\infty} \leq \frac{1}{\Delta t^i} \sum_{j=1}^i |a_j^{(i)}| \int_0^{j\Delta t} \|\nabla p(s, t)\| t^i dt$$

with

$$p(s, t) = \mathbb{E}[\mathcal{L}_{\mu, \Sigma}^i \mu(s_t) | s_0 = s].$$

By Lemma B.2, one has,

$$\|\nabla(\mu - \hat{\mu}_i)\|_{L^\infty} \leq L_{\nabla\mu} \Delta t^i$$

with

$$L_{\nabla\mu} = C_i \left(\sqrt{\frac{C_{\nabla\mu, \nabla\Sigma}}{\lambda_{\min}}} \|\mathcal{L}_{\mu, \Sigma}^i \mu(s)\|_{L^\infty} + \|\nabla \mathcal{L}_{\mu, \Sigma}^i \mu(s)\|_{L^\infty} \right). \quad (94)$$

Therefore,

$$\|\nabla \hat{V}(s)\|_{L^\infty} \leq \frac{1}{\beta} \left[\left(\sqrt{\frac{2C_{\nabla\mu, \nabla\Sigma}}{\lambda_{\min}}} + \frac{L_{\nabla\Sigma}}{\sqrt{2\lambda_{\min}}} \Delta t^i + \sqrt{\frac{2L_{\nabla\mu}}{\lambda_{\min}}} \Delta t^{i/2} \right) \|r\|_{L^\infty} + \|\nabla r\|_{L^\infty} \right] + o(\Delta t^i).$$

References

- [1] Brandon Amos, Ivan Jimenez, Jacob Sacks, Byron Boots, and J Zico Kolter. Differentiable mpc for end-to-end planning and control. Advances in neural information processing systems, 31, 2018.
- [2] Donald G. Aronson. Bounds for the fundamental solution of a parabolic equation. Bulletin of the American Mathematical Society, 73, 1967.
- [3] Leemon C Baird. Reinforcement learning in continuous time: Advantage updating. In Proceedings of 1994 IEEE International Conference on Neural Networks (ICNN'94), volume 4, pages 2448–2453. IEEE, 1994.
- [4] Matteo Basei, Xin Guo, Anran Hu, and Yufei Zhang. Logarithmic regret for episodic continuous-time linear-quadratic reinforcement learning over a finite-time horizon. The Journal of Machine Learning Research, 23(1):8015–8048, 2022.
- [5] Tadej Battelino, Thomas Danne, Richard M Bergenstal, Stephanie A Amiel, Roy Beck, Torben Biester, Emanuele Bosi, Bruce A Buckingham, William T Cefalu, Kelly L Close, et al. Clinical targets for continuous glucose monitoring data interpretation: recommendations from the international consensus on time in range. Diabetes care, 42(8):1593–1603, 2019.

- [6] Vladimir I Bogachev, N Krylov, and Michael Röckner. Regularity of invariant measures: the case of non-constant diffusion part. journal of functional analysis, 138(1):223–242, 1996.
- [7] Steven J Bradtke and Andrew G Barto. Linear least-squares algorithms for temporal difference learning. Machine learning, 22:33–57, 1996.
- [8] Qi Cai, Zhuoran Yang, Chi Jin, and Zhaoran Wang. Provably efficient exploration in policy optimization. In International Conference on Machine Learning, pages 1283–1294. PMLR, 2020.
- [9] Claudio Cobelli, Chiara Dalla Man, Giovanni Sparacino, Lalo Magni, Giuseppe De Nicolao, and Boris P Kovatchev. Diabetes: models, signals, and control. IEEE reviews in biomedical engineering, 2:54–96, 2009.
- [10] Kris De Asis and Richard S Sutton. An idiosyncrasy of time-discretization in reinforcement learning. arXiv preprint arXiv:2406.14951, 2024.
- [11] Jonas Degraeve, Federico Felici, Jonas Buchli, Michael Neunert, Brendan Tracey, Francesco Carpanese, Timo Ewalds, Roland Hafner, Abbas Abdolmaleki, Diego de Las Casas, et al. Magnetic control of tokamak plasmas through deep reinforcement learning. Nature, 602(7897):414–419, 2022.
- [12] Cosimo Della Santina, Christian Duriez, and Daniela Rus. Model-based control of soft robots: A survey of the state of the art and open challenges. IEEE Control Systems Magazine, 43(3):30–65, 2023.
- [13] Kenji Doya. Reinforcement learning in continuous time and space. Neural computation, 12(1):219–245, 2000.
- [14] Harry Emerson, Matthew Guy, and Ryan McConville. Offline reinforcement learning for safer blood glucose control in people with type 1 diabetes. Journal of Biomedical Informatics, 142:104376, 2023.
- [15] Xiaoqin Guo, Hung Vinh Tran, and Yuming Paul Zhang. Policy iteration for nonconvex viscous hamilton–jacobi equations. arXiv preprint arXiv:2503.02159, 2025.
- [16] Xin Guo, Anran Hu, Renyuan Xu, and Junzi Zhang. A general framework for learning mean-field games. Mathematics of Operations Research, 48(2):656–686, 2023.
- [17] Wen Huang, Min Ji, Zhenxin Liu, and Yingfei Yi. Steady states of fokker–planck equations: I. existence. Journal of Dynamics and Differential Equations, 27:721–742, 2015.
- [18] Yanwei Jia, Du Ouyang, and Yufei Zhang. Accuracy of discretely sampled stochastic policies in continuous-time reinforcement learning. arXiv preprint arXiv:2503.09981, 2025.

- [19] Yanwei Jia and Xun Yu Zhou. Policy evaluation and temporal-difference learning in continuous time and space: A martingale approach. The Journal of Machine Learning Research, 23(1):6918–6972, 2022.
- [20] Yanwei Jia and Xun Yu Zhou. Policy gradient and actor-critic learning in continuous time and space: Theory and algorithms. The Journal of Machine Learning Research, 23(1):12603–12652, 2022.
- [21] Yanwei Jia and Xun Yu Zhou. q-learning in continuous time. Journal of Machine Learning Research, 24(161):1–61, 2023.
- [22] Chi Jin, Zhuoran Yang, Zhaoran Wang, and Michael I Jordan. Provably efficient reinforcement learning with linear function approximation. In Conference on learning theory, pages 2137–2143. PMLR, 2020.
- [23] Rushikesh Kamalapurkar, Patrick Walters, and Warren E Dixon. Model-based reinforcement learning for approximate optimal regulation. Automatica, 64:94–104, 2016.
- [24] Ioannis Karatzas and Steven Shreve. Brownian motion and stochastic calculus. springer, 2014.
- [25] Ioannis Karatzas and Steven E. Shreve. Brownian Motion and Stochastic Calculus. Springer, 2nd edition, 1998.
- [26] Amirmohammad Karimi, Jun Jin, Jun Luo, A Rupam Mahmood, Martin Jagersand, and Samuele Tosatto. Dynamic decision frequency with continuous options. In 2023 IEEE/RSJ International Conference on Intelligent Robots and Systems (IROS), pages 7545–7552. IEEE, 2023.
- [27] Bekzhan Kerimkulov, David Siska, and Lukasz Szpruch. Exponential convergence and stability of Howard’s policy improvement algorithm for controlled diffusions. SIAM J. Control Optim., 58(3):1314–1340, 2020.
- [28] Jens Kober, J. Andrew Bagnell, and Jan Peters. Reinforcement learning in robotics: A survey. The International Journal of Robotics Research, 32(11):1238–1274, 2013.
- [29] Vijay Konda and John Tsitsiklis. Actor-critic algorithms. Advances in neural information processing systems, 12, 1999.
- [30] Alessandro Lazaric, Mohammad Ghavamzadeh, and Rémi Munos. Finite-sample analysis of least-squares policy iteration. The Journal of Machine Learning Research, 13(1):3041–3074, 2012.
- [31] Jaeyoung Lee and Richard S Sutton. Policy iterations for reinforcement learning problems in continuous time and space—fundamental theory and methods. Automatica, 126:109421, 2021.
- [32] Robert C Merton. Optimum consumption and portfolio rules in a continuous-time model. In Stochastic optimization models in finance, pages 621–661. Elsevier, 1975.

- [33] Volodymyr Mnih, Koray Kavukcuoglu, David Silver, Andrei A. Rusu, Joel Veness, Marc G. Bellemare, Alex Graves, Martin Riedmiller, Andreas K. Fidjeland, Georg Ostrovski, Stig Petersen, Charles Beattie, Amir Sadik, Ioannis Antonoglou, Helen King, Dharshan Kumaran, Daan Wierstra, Shane Legg, and Demis Hassabis. Human-level control through deep reinforcement learning. Nature, 518(7540):529–533, 2015.
- [34] John Moody and Matthew Saffell. Learning to trade via direct reinforcement. IEEE Transactions on Neural Networks, 12(4):875–889, 2001.
- [35] Rémi Munos. Policy gradient in continuous time. Journal of Machine Learning Research, 7:771–791, 2006.
- [36] Rémi Munos and Csaba Szepesvári. Finite-time bounds for fitted value iteration. Journal of Machine Learning Research, 9:815–857, 2008.
- [37] Bernt Oksendal. Stochastic differential equations: an introduction with applications. Springer Science & Business Media, 2013.
- [38] Seohong Park, Jaekyeom Kim, and Gunhee Kim. Time discretization-invariant safe action repetition for policy gradient methods. Advances in Neural Information Processing Systems, 34:267–279, 2021.
- [39] Grigorios A Pavliotis. Stochastic processes and applications. Springer, 2016.
- [40] Doina Precup, Richard S Sutton, and Sanjoy Dasgupta. Off-policy temporal-difference learning with function approximation. In ICML, pages 417–424, 2001.
- [41] Angel Romero, Yunlong Song, and Davide Scaramuzza. Actor-critic model predictive control. In 2024 IEEE International Conference on Robotics and Automation (ICRA), pages 14777–14784. IEEE, 2024.
- [42] John Schulman, Filip Wolski, Prafulla Dhariwal, Alec Radford, and Oleg Klimov. Proximal policy optimization algorithms. arXiv preprint arXiv:1707.06347, 2017.
- [43] Antonio Sciarretta, Michael Back, and Lino Guzzella. Optimal control of parallel hybrid electric vehicles. IEEE Transactions on control systems technology, 12(3):352–363, 2004.
- [44] Bruno Siciliano and Luigi Villani. Robot force control. Springer Science & Business Media, 1999.
- [45] David Silver, Aja Huang, Chris J. Maddison, Arthur Guez, Laurent Sifre, George Van Den Driessche, Julian Schrittwieser, Ioannis Antonoglou, Veda Panneershelvam, Marc Lanctot, Sander Dieleman, Dominik Grewe, John Nham, Nal Kalchbrenner, Ilya Sutskever, Timothy Lillicrap, Madeleine Leach, Koray Kavukcuoglu, Thore Graepel, and Demis Hassabis. Mastering the game of go with deep neural networks and tree search. Nature, 529(7587):484–489, 2016.
- [46] Daniel W Stroock and SR Srinivasa Varadhan. Multidimensional diffusion processes, volume 233. Springer Science & Business Media, 1997.

- [47] Richard S Sutton. Learning to predict by the methods of temporal differences. Machine learning, 3(1):9–44, 1988.
- [48] Richard S Sutton and Andrew G Barto. Reinforcement learning: An introduction. MIT press, 2018.
- [49] Richard S Sutton, Hamid Reza Maei, Doina Precup, Shalabh Bhatnagar, David Silver, Csaba Szepesvári, and Eric Wiewiora. Fast gradient-descent methods for temporal-difference learning with linear function approximation. In Proceedings of the 26th annual international conference on machine learning, pages 993–1000, 2009.
- [50] Richard S Sutton, David McAllester, Satinder Singh, and Yishay Mansour. Policy gradient methods for reinforcement learning with function approximation. Advances in neural information processing systems, 12, 1999.
- [51] Csaba Szepesvári. Least squares temporal difference learning and galerkin’s method. In Mini-Workshop: Mathematics of Machine Learning, Oberwolfach Reports, European Mathematical Society, Oberwolfach, pages 2385–2388, 2011.
- [52] Lukasz Szpruch, Tanut Treetanthiploet, and Yufei Zhang. Optimal scheduling of entropy regularizer for continuous-time linear-quadratic reinforcement learning. SIAM Journal on Control and Optimization, 62(1):135–166, 2024.
- [53] Corentin Tallec, Léonard Blier, and Yann Ollivier. Making deep q-learning methods robust to time discretization. In International Conference on Machine Learning, pages 6096–6104. PMLR, 2019.
- [54] Wenpin Tang, Hung Vinh Tran, and Yuming Paul Zhang. Policy iteration for the deterministic control problems—a viscosity approach. SIAM Journal on Control and Optimization, 63(1):375–401, 2025.
- [55] Wenpin Tang, Yuming Paul Zhang, and Xun Yu Zhou. Exploratory hjb equations and their convergence. SIAM Journal on Control and Optimization, 60(6):3191–3216, 2022.
- [56] Joel A. Tropp. User-friendly tail bounds for sums of random matrices. Foundations of Computational Mathematics, 12(4):389–434, 2012.
- [57] Kyriakos G Vamvoudakis and Frank L Lewis. Online actor–critic algorithm to solve the continuous-time infinite horizon optimal control problem. Automatica, 46(5):878–888, 2010.
- [58] Roman Vershynin. High-dimensional probability: An introduction with applications in data science, volume 47. Cambridge university press, 2018.
- [59] Haoran Wang, Thaleia Zariphopoulou, and Xun Yu Zhou. Reinforcement learning in continuous time and space: A stochastic control approach. The Journal of Machine Learning Research, 21(1):8145–8178, 2020.

- [60] Haoran Wang and Xun Yu Zhou. Continuous-time mean–variance portfolio selection: A reinforcement learning framework. Mathematical Finance, 30(4):1273–1308, 2020.
- [61] Peter Whittle. Risk-sensitive linear/quadratic/gaussian control. Advances in Applied Probability, 13(4):764–777, 1981.
- [62] Lin Yang and Mengdi Wang. Sample-optimal parametric q-learning using linearly additive features. In International conference on machine learning, pages 6995–7004. PMLR, 2019.
- [63] Junyu Zhang, Chengzhuo Ni, Csaba Szepesvari, Mengdi Wang, et al. On the convergence and sample efficiency of variance-reduced policy gradient method. Advances in Neural Information Processing Systems, 34:2228–2240, 2021.
- [64] Zichen Vincent Zhang, Johannes Kirschner, Junxi Zhang, Francesco Zanini, Alex Ayoub, Masood Dehghan, and Dale Schuurmans. Managing temporal resolution in continuous value estimation: a fundamental trade-off. Advances in Neural Information Processing Systems, 36:62519–62548, 2023.
- [65] Yuhua Zhu, Zachary Izzo, and Lexing Ying. Borrowing from the future: Addressing double sampling in model-free control. In Mathematical and Scientific Machine Learning, pages 1099–1136. PMLR, 2022.
- [66] Yuhua Zhu and Lexing Ying. Borrowing from the future: An attempt to address double sampling. In Mathematical and scientific machine learning, pages 246–268. PMLR, 2020.
- [67] Daniel M. Ziegler, Nisan Stiennon, Jeffrey Wu, Tom Brown, Alec Radford, Dario Amodei, and Paul F. Christiano. Fine-tuning language models from human preferences. arXiv preprint arXiv:1909.08593, 2019.